Targeting acid ceramidase in acute myeloid leukemia

Jennifer M. Pearson

Shelby, NC

BS, Biochemistry, High Point University, 2014

MS, Biological & Physical Sciences, University of Virginia, 2016

A Dissertation presented to the Graduate Faculty

of the University of Virginia in Candidacy for the Degree of

Doctor of Philosophy

Department of Biochemistry and Molecular Genetics

University of Virginia

November 2019

ABSTRACT

Acute myeloid leukemia (AML) is a hematologic malignancy characterized by expansion of myeloid blasts. These immature cells overpopulate the blood and bone marrow leading to anemia, neutropenia and thrombocytopenia associated with increased risk of infection. AML progresses rapidly and many patients relapse after treatment. Only about 25% of patients survive five years past diagnosis. Although our understanding of the disease has evolved significantly, many of the latest therapeutics do not dramatically improve survival. One major challenge in treating AML is genetic heterogeneity among patients. For this reason, we aim to characterize and target a common biochemical dependence in AML cells. Dysregulation of sphingolipid metabolism is an emerging area of study in several cancers including AML. Generally, patients have increased levels of enzymes that form pro-survival sphingosine 1-phosphate and decreased levels of enzymes that form pro-death ceramides. These enzymes are crucial for regulating cell fate, and identifying compounds that target these enzymes creates an opportunity to restore this balance. In these studies, we identify and characterize SACLAC an inhibitor of one of these enzymes, acid ceramidase (AC). AC detoxifies pro-death ceramides, and blocking AC causes accumulation of these pro-death signals. AC is elevated in AML patients and is associated with poor prognosis, highlighting its potential as a therapeutic target. We found that SACLAC potently inhibits AC and increases ceramide levels. SACLAC induces apoptosis through altered splicing of Mcl-1. Importantly, we demonstrate that SACLAC reduces leukemic burden at the cellular level in two mouse models of AML. However, SACLAC delivery is limited by poor solubility. To address this, we formulated a nanoliposomal SACLAC (nanoSACLAC) to improve delivery and safety *in vivo.* We found that nanoSACLAC has reduced potency due to

serum interactions, but this can be attenuated by adding cholesterol into the nanoliposome. Since SACLAC targets Mcl-1, we also explored the potential for co-treatment with therapeutics with known Mcl-1-mediated resistance. In fact, AML cells that were resistant to Bcl-2 inhibitor ABT-199—currently approved to treat older adults with AML—were sensitized when they were co-treated with SACLAC. Together, these studies highlight SACLAC as an interesting novel therapeutic with potential to inform further investigation of sphingolipid-based therapies for AML.

ACKNOWLEDGEMENTS

Thank you to my friends and family who helped me maintain my sanity during the ultimate test of character and self-discipline, especially Tiffany and Kevin who spent many maddening days with me.

Thank you to Dave and Su-Fern who helped me grow as a scientist and a person while showing me what it means to be a supportive and compassionate mentor.

Thank you to Dr. Loughran for always being my advocate and encouraging me to think bigger.

Thank you to all the Loughran Lab members of past and present for your companionship and mentorship.

Thank you to my committee (BJ, Jeff and Kevin) for investing your time in me and challenging me to reach my full potential.

Thank you to Kayla Friedman and Malcolm Morgan of the Centre for Sustainable Development, University of Cambridge, UK for producing the Microsoft Word thesis template used to produce this document.

CONTENTS

LIST OF TABLES

LIST OF FIGURES

LIST OF ABBREVIATIONS AND ACRONYMS

5-FU	5-fluorouracil
ABTR	ABT-737 resistant
AC	acid ceramidase, ASAH1
AML	acute myeloid leukemia
APL	acute promyelocytic leukemia
AraC	cytosine arabinoside, also known as cytarabine
ASAH1	N-acylsphingosine amidohydrolase 1, acid ceramidase
ASXL1	ASXL transcriptional regulator 1
ATRA	all-trans retinoic acid
BCL-2	B-cell lymphoma 2
BCR-ABL1	breakpoint cluster region/proto-oncogene tyrosine kinase fusion
BH3	Bcl-2 homology domain 3
c-KIT	mast/stem cell growth factor receptor
CEBPA	CCAAT/enhancer-binding protein alpha
CR	complete remission
DMSO	dimethylsufolxide
DNMT3a	DNA methyltransferase 3 alpha
EC_{50}	concentration for 50% effect
FAB	French-American-British [classification]
FLAG-IDA	fludarabine, cytarabine, idarubicin and G-CSF regimen
FLT3	FMS-like tyrosine kinase 3
G-CSF	granulocyte-colony stimulating factor
GM-CSF	granulocyte-macrophage colony-stimulating factor
ITD	internal tandem duplication
JAK2	Janus kinase 2
MCL-1	myeloid cell leukemia 1

MDS	myelodysplastic syndrome
MTS	[3-(4,5-dimethylthiazol-2-yl)-5-(3-carboxymethoxyphenyl)-2-(4-sulfophenyl)-2H-tetrazolium
NF-kB	nuclear factor kappa-B
NPM1	nucleophosmin 1
NT	no treatment
P-gP	P-glycoprotein
PBMC	peripheral blood mononuclear cell
PCR	polymerase chain reaction
PEG	polyethylene glycol
PML-RARa	promyelocytic leukemia/retinoic acid receptor alpha fusion
rhAC	recombinant human AC
RUNX1	runt-related transcription factor 1
RUNX1	RUNX family transcription factor 1
S1P	sphingosine 1-phosphate
S1PR	sphingosine 1-phosphate receptor
SCF	stem cell factor
SF3B1	splicing factor 3b subunit 1
SPHK	sphingosine kinase
SRSF2	serine arginine rich splicing factor 2
STAT3	signal transducer and activator of transcription 3
TET2	Tet methylcytosine dioxygenase 2
TP53	tumor protein p53
U2AF1	U2 small nuclear RNA auxiliary factor 1
VCR	vincristine resistant
WBC	white blood cell
WHO	World Health Organization
WT	wild-type

LIST OF APPENDICES

1 LITERATURE REVIEW

1.1 ACUTE MYELOID LEUKEMIA

Acute myeloid leukemia (AML) is a malignancy of the blood and bone marrow characterized by uncontrolled proliferation of immature immune cells of the myeloid lineage. These cells, called blasts, overpopulate the blood and compromise the healthy white blood cell population. As an acute disease, AML is sudden onset and progresses quickly. Only 27% of patients survive five years past diagnosis (Noone et al.). Prognosis is even worse for some groups, including those above the age of 65 and those whose disease has developed from myelodysplastic syndrome or chemotherapy (Klepin and Balducci, 2009; Leone et al., 2001; Okuyama et al., 2013).

In addition to the challenge of a quickly progressing disease, AML is also extremely genetically heterogenous. Even the most common mutations in AML are only present in about 30% of adult cases (Hatzimichael et al., 2013), presenting a unique challenge in developing new therapies.

1.1.1 DIAGNOSIS

AML patients present with symptoms such as fever, fatigue, frequent infections and unexplained weight loss. These symptoms are reflective of underlying issues like anemia and neutropenia (De Kouchkovsky and Abdul-Hay, 2016). Blood and bone marrow smears (**Figure 1.1**) are used to examine relative quantity and morphology of cells, and presence of at least 20% blasts generally constitutes diagnosis with acute leukemia. To diagnose myeloid lineage leukemia, cells are immunophenotyped using myeloid specific markers (Döhner et al., 2017). AML can further be subdivided into nine categories based

on the French-American-British (FAB) classification (**Table 1.1**). This classification type was developed in the 1970s to subcategorize AML into morphological groups. However, with several developments related to genetic changes and pathogenesis, the World Health Organization (WHO) classification (**Table 1.2**) provides more detail for classifying, predicting and treating AML (American Cancer Society; Arber et al., 2016).

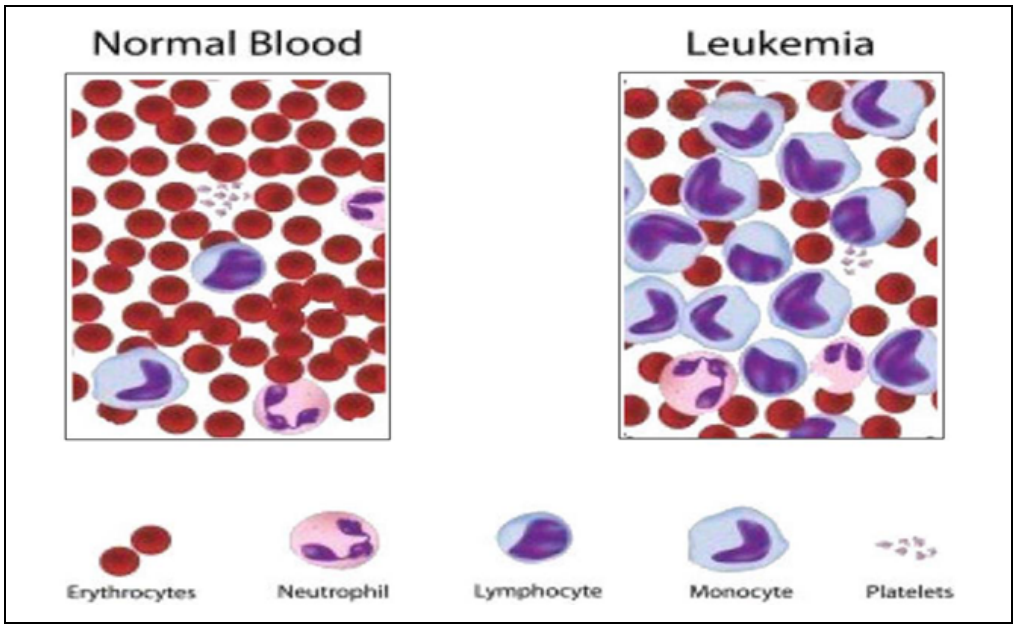

Figure 1.1: Normal and leukemic cells in the blood

Expansion of white blood cell populations within the bone marrow is characteristic of leukemia (El-Refaei and Qahtani, 2016).

FAB Subtype	Name
M0	Undifferentiated acute myeloblastic leukemia
M1	Acute myeloblastic leukemia with minimal maturation
M2	Acute myeloblastic leukemia with maturation
M3	Acute promyelocytic leukemia (APL)
M4	Acute myelomonocytic leukemia
M4 eos	Acute myelomonocytic leukemia with eosinophila
M5	Acute monocytic leukemia
M6	Acute erythroid leukemia
M7	Acute megakaryoblastic leukemia

Table 1.1: The French-American-British (FAB) classification of AML

The FAB system categorizes AML subtypes by morphology (American Cancer Society).

AML with certain genetic abnormalities (gene or chromosome changes) • **AML with a translocation between chromosomes 8 and 21 [t(8;21)]** • **AML with a translocation or inversion in chromosome 16 [t(16;16) or inv(16)]** • **APL with the *PML-RARA* fusion gene** • **AML with a translocation between chromosomes 9 and 11 [t(9;11)]** • **AML with a translocation between chromosomes 6 and 9 [t(6:9)]** • **AML with a translocation or inversion in chromosome 3 [t(3;3) or inv(3)]** • **AML (megakaryoblastic) with translocation between chromosomes 1 and 22 [t(1:22)]** • **AML with the *BCR-ABL1* (*BCR-ABL*) fusion gene** • **AML with mutated *NPM1* gene** • **AML with biallelic mutations of the *CEBPA* gene** • **AML with mutated *RUNX1* gene**
AML with myelodysplasia-related changes
AML related to previous chemotherapy or radiation
AML not otherwise specified (similar to FAB classification) • **AML with minimal differentiation (FAB M0)** • **AML without maturation (FAB M1)** • **AML with maturation (FAB M2)** • **Acute myelomonocytic leukemia (FAB M4)** • **Acute monoblastic/monocytic leukemia (FAB M5)** • **Pure erythroid leukemia (FAB M6)** • **Acute megakaryoblastic leukemia (FAB M7)** • **Acute basophilic leukemia** • **Acute panmyelosis with fibrosis**
Myeloid sarcoma
Myeloid proliferations related to Down syndrome

Table 1.2: World Health Organization (WHO) classification of AML

The WHO system categorizes subtypes based on several disease characteristics including genetic changes and pathogenesis (Arber et al., 2016).

Prognosis of AML depends on a variety of factors including classification, presence of driver mutations, age, gene expression profiling and tumor characteristics (American Cancer Society). Overall, older patients have poorer prognoses since they are usually unable to undergo intensive chemotherapy (Klepin and Balducci, 2009). Patients with mutations in FLT3, TP53, RUNX1 and ASXL1 genes also have worse prognoses (Devillier et al., 2015; Kottaridis et al., 2001; Stengel et al., 2018). Higher white blood cell (WBC) count at diagnosis generally correlates to greater disease severity and lower survival time (de Jonge et al., 2011). However, some patients have more favorable prognoses if they have acute promyelocytic leukemia (APL) or mutations in NPM1 or CEBPA (Dombret and Gardin, 2016; Heath et al., 2017; Preudhomme et al., 2002).

1.1.2 GENETICS

Many genetic abnormalities found in AML are highlighted in the WHO classification (**Table 1.2)**, but the heterogeneity of the disease is far more complex. A comprehensive study of 200 patients found 260 genes with somatic mutations in at least 2 of the 200 samples (Cancer Genome Atlas Research Network et al., 2013). The top hits were classified by functional groups: transcription factor fusions, tumor suppressors, DNA methylation, activated signaling, myeloid transcription factors, chromatic modifiers, cohesion and spliceosome. The most recurrent mutations were FLT3 (28%), NPM1 (27%) and DNMT3a (26%). Subsequent studies have expanded these findings to larger cohorts of patients to identify molecular markers for diagnosis and predict treatment response (Metzeler et al., 2016; Tyner et al., 2018).

FLT3

Fms-related tyrosine kinase 3 (FLT3) is normally expressed in early hematopoietic cells and is important for normal development and differentiation. Mutations in FLT3, either internal tandem duplications (ITD) or tyrosine kinase domain (TKD) mutations, can result in constitutive activation of the tyrosine kinase domain which is upstream of STAT, ERK and AKT pathways (Takahashi, 2011). Even patients who do not have mutations in FLT3 generally have increased expression. This activity can coordinate with another co-occurring mutations to increase expansion of AML cells (Gilliland and Griffin, 2002).

NPM1

Nucleophosmin 1 (NPM1) is a phosphoprotein that acts as a shuttle between the nucleolus to the cytoplasm. NPM1 plays a role in several important processes including ribosome biogenesis, tumor suppression and maintenance of genomic stability. Mutations in NPM1, mostly in exon 12, lead to an imbalance of nuclear import/export that results in NPM1 becoming cytoplasmic. This leads to several changes—genomic instability, activation of oncogenes, inhibition of death signals, and abherrant hematopoeisis. However, cytoplasmic NPM1 is not sufficient to cause leukemia on its own, so other events are required in order to induce leukemogenesis associated with NPM1 mutations (Heath et al., 2017).

DNMT3A

DNA methyltransferase 3 alpha (DNMT3a) is an enzyme responsible for transferring a methyl group to cytosine, creating 5-methylcytosine. DNA methylation can lead to transcriptional activation or repression, resulting in

altered gene expression. Mutations in DNMT3a are dominant-negative, dramatically reducing DNA methylation. This is an initiating event in leukemic development associated with epigenetic reprogramming and transformation of cells (Castelli et al., 2018), along with development of chemoresistance (Guryanova et al., 2016).

SPLICEOSOME

The spliceosome is an extremely intricate complex composed of small nuclear RNAs and hundreds of proteins. This complex is responsible for removing introns from pre-mRNA to produce a transcript for protein synthesis. These genes are crucial for proper assembly of splicing machinery and removal of introns from pre-mRNA (Matera and Wang, 2014). Mutations in spliceosome-complex genes including U2AF1, SF3B1 and SRSF2 are estimated to occur in around 14% of AML patients (Cancer Genome Atlas Research Network et al., 2013). These mutations result in disruption of spliceosome assembly which causes defective splicing. This was identified as a novel leukemogenic pathway by (Makishima et al., 2012). In a small patient cohort, altered splicing patterns were identified in genes otherwise associated with AML (RUNX1 and TET2). Interestingly, these mutations are even more prevalent in myelodysplastic syndrome (MDS), which sometimes precedes AML (Inoue et al., 2016).

1.1.3 PATHOGENESIS

AML can arise from a preceding hematologic disorder like MDS, treatment-related toxicities from radiation or chemotherapy, or as a *de novo* disease. Other origins may include clonal hematopoiesis of indeterminate potential (CHIP) or age-related clonal hematopoiesis (ARCH) where cells possess somatic

mutations but do not meet additional criteria for diagnosis (Heuser et al., 2016). On a cellular level, AML is an expansion of immature myeloid cells (called blasts). This expansion can occur as the result of impaired differentiation and blast transformation as a result of acquired driving molecular or genetic changes.

GENETIC CHANGES

As seen in the classification table previously (**Table 1.2**), there are several large chromosomal translocations. These changes create fusion proteins such as PML-RARα (promyelocytic leukemia and retinoic acid receptor alpha) or BCR-ABL1 (breakpoint cluster region-proto-oncogene tyrosine-protein kinase). PML-RARα fusions suppress terminal myeloid differentiation, while BCR-ABL1 fusions constitutively activate tyrosine kinase pathways to maintain proliferation and resistance to cell death (Kang et al., 2016; Tussié-Luna et al., 2006). Alternatively, genetic mutations can drive leukemogenesis. The most common model of leukemogenesis involves Class I driver mutations such as FLT3, STAT3 and c-KIT and Class II differentiation mutations like NPM1 and CEBPA. Class I mutations initiate oncogenic signaling and proliferation while Class II mutations keep new and existing cells from differentiating into healthy leukocytes (De Kouchkovsky and Abdul-Hay, 2016). AML is molecularly and genetically heterogeneous, suggesting that no one change causes AML, but rather combinations of mutations cooperate to induce leukemogenesis.

DYSREGULATION OF BCL-2 FAMILY PROTEINS

In additional to genetic and molecular changes, protein expression can also affect the pathogenesis of AML. In general, AML cells express high levels of the anti-apoptotic Bcl-2 (B-cell lymphoma 2) family proteins. These proteins

function as anti-apoptotic regulators, but when they are dysregulated, abnormal cells can proliferate unchecked. Bcl-2 family members can also act as mitochondrial channels and protect cells from cytotoxic agents. In fact, increased expression of Bcl-2 is associated with poor treatment response (Campos et al., 1993). Importantly, Mcl-1 (myeloid cell leukemia 1) stands out in the Bcl-2 family because it is the only protein (among Bcl-2, Bcl-xL, Bcl-w and Mcl-1) required for development and proliferation of AML cells (Glaser et al., 2012). These studies highlight a potential, targetable vulnerability in AML.

EPIGENETIC CHANGES

Epigenetic changes can also create vulnerabilities that facilitate AML pathogenesis. Mutations in epigenetic regulators (DNMTs, IDH1/2, TET, etc.) can be found in originating clones, suggesting a contributory role to pathogenesis (Sun et al., 2018). AML fusion proteins can also hijack chromatic modulators to control gene silencing and activation (Greenblatt and Nimer, 2014). Therefore, both the fusion proteins and the alternatively regulated genes can play important roles in pathogenesis.

1.1.4 TREATMENT

AML is typically treated using the 7+3 regimen consisting of seven days continuous infusion of cytarabine along with anthracycline for three days. Dosing and specific anthracycline prescribed are informed by cytogenetic profiling. This standard of care has been in place for decades, and many patients achieve complete remission (CR) after induction therapy. However, the rate of relapse is high, often requiring additional treatment. For older adults who cannot tolerate intensive chemotherapy, hypomethylating agents may

improve overall survival, but these patients primarily receive supportive and palliative care (De Kouchkovsky and Abdul-Hay, 2016). It is important to note that treatment for some AML cases is very straightforward, namely acute promyelocytic leukemia. These leukemias result from a PML-RARα fusion protein that can be targeted effectively with all-trans retinoic acid (ATRA) or arsenic trioxide (Quignon et al., 1997).

ALTERNATIVE STRATEGIES

Patients with incomplete remission or disease relapse can repeat 7+3 therapy or utilize other treatments such as FLAG-IDA (fludarabine, cytarabine, G-CSF and idarubicin) or combinations with mitoxantrone. As many as 50% of relapse and refractory AML cases can achieve CR temporarily. Consolidation therapies such as low dose chemotherapy or allogenic hematopoietic stem cell transplant can be used to decrease probability of recurrence (De Kouchkovsky and Abdul-Hay, 2016). Ultimately, 5-year overall survival is still around 25% (Noone et al.).

THERAPEUTICS TARGETING MUTATIONS

Many treatment advances have been made, but few show substantial survival benefit. Of the existing options, many are mutation-targeted. Sorafenib (Zhang et al., 2008), midostaurin (Stone et al., 2005), and quizartinib (Cortes et al., 2018) are FLT3 inhibitors that can be used to improve initial response, but changes in overall survival are not pronounced. However, continued investigation of FLT3-targeted therapeutics is important due to poorer prognoses in patients with mutations in FLT3 (Kottaridis et al., 2001). Fortunately, FLT3 inhibitor gilteritinib was FDA-approved in late 2018 and shows promise for improved survival and remission rates in patients with relapsed/refractory AML

(Dhillon, 2019). Other therapeutics are available to target mutations in KIT, JAK2, IDH, RAS and others, but still without significant survival benefit (Hatzimichael et al., 2013).

THERAPEUTICS TARGETING PATHWAYS

In addition to targeting gene mutations, some advances have been made that target survival pathways in AML. In late 2018, the Hedgehog pathway inhibitor glasdegib was approved for the treatment of newly diagnosed AML in combination with low dose cytarabine (LDAC) (Cortes et al., 2019). Median survival was improved with combination treatment (8.3 months) over LDAC alone (4.3 months), but several side effects limit quality of life (Norsworthy et al., 2019). The Bcl-2 inhibitor ABT-199 (venetoclax) was approved in late 2018, in combination with hypomethylating agents, for patients unable to undergo intensive chemotherapy (DiNardo et al., 2019). Median overall survival in these groups was around 15 months (Pollyea et al., 2018). Although these therapuetics are promising, there is still substantial room for improvement.

1.2 SPHINGOLIPID METABOLISM

Sphingolipids are essential for formation of the plasma membrane and maintaining structural integrity of the cell. However, sphingolipid metabolism also produces bioactive molecules important for regulating processes like cell survival and differentiation (Ryland et al., 2011). Although sphingolipid metabolism is complex, ceramide and sphingosine 1-phosphate (S1P) are the bioactive core (**Figure 1.2**).

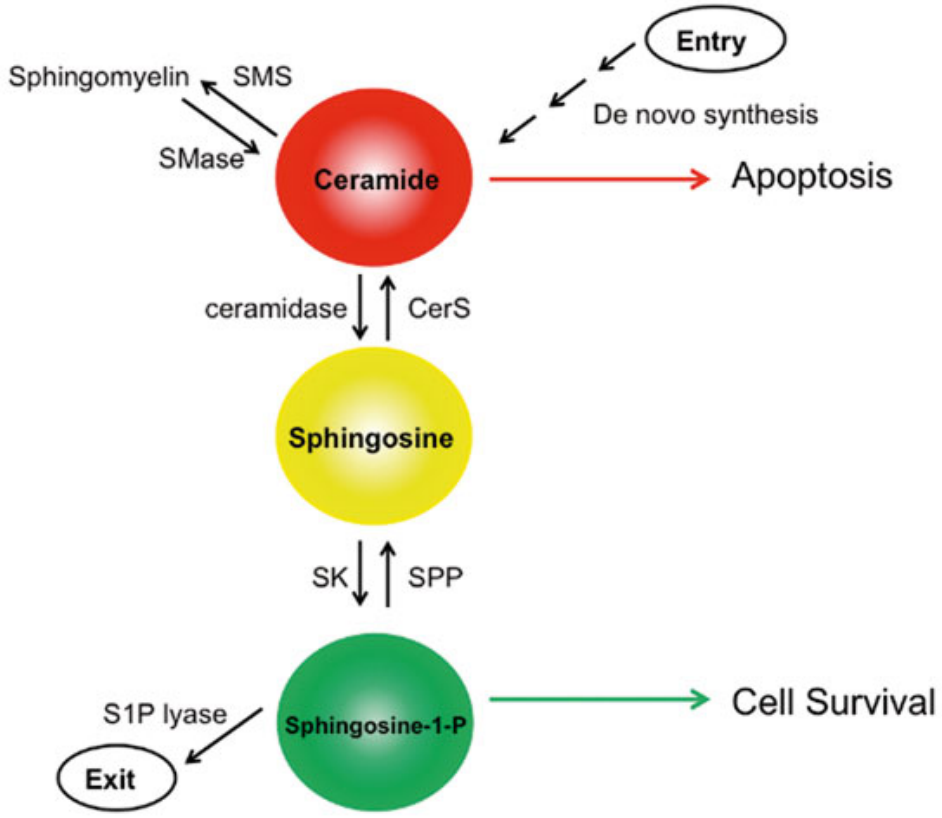

Figure 1.2: Sphingolipid metabolism and homeostasis

Ceramide is synthesized *de novo* and can also be generated through breakdown of complex sphingolipids. Ceramide can also be further metabolized to sphingosine, which is then phosphorylated to generate S1P. Degradation of S1P by S1P lyase marks the exit from sphingolipid pathway. Ceramide has been linked to anti-proliferative responses including apoptosis while S1P is important for survival. Homeostasis is maintained through interconversion of ceramide and S1P though sphingosine. Abbreviations used: SMase — sphingomyelinase, SMS — sphingomyelin synthase, CerS — ceramide synthase, SK — sphingosine kinase, SPP — sphingosine-1-phosphate phosphatase, S1P lyase — sphingosine-1-phosphate lyase (Tirodkar and Voelkel-Johnson, 2012).

1.2.1 CERAMIDE METABOLISM

Ceramides are a class of sphingolipids containing a sphingoid base and a fatty acid. The fatty acid is cleaved by a ceramidase to produce sphingosine, which is subsequently phosphorylated by sphingosine kinase to produce S1P. This reversible process is key in regulating cell survival and death. Dysregulation of metabolites and enzymes that feed into this pathway has been shown to contribute to the progression of several diseases including multiple cancers (**Table** 1.3) ranging from colon cancer to leukemia to melanoma (Hannun and Obeid, 2018; Ryland et al., 2011; Takabe and Spiegel, 2014). This is based largely upon alterations in the ratio of ceramide to S1P.

Ceramide accumulation induces apoptosis and other cell death mechanisms while formation of S1P promotes cell survival (Ryland et al., 2011). In healthy cells, the ratio of ceramide to S1P is relatively stable so that pro-survival and pro-death signals are balanced. However, if this balance is disrupted, cells normally destined for death can proliferate leading to disease. This balance is tightly regulated by the enzymes involved in formation and breakdown of ceramide. When pro-death signals are prominent, cells push towards ceramide accumulation via S1P phosphatases to generate sphingosine and ceramide synthases to generate ceramide. As in the case of cancer, pro-survival signals dominate. This leads to formation of sphingosine and pro-survival S1P through ceramidases and sphingosine kinases, respectively. Exploiting this imbalance in complex diseases like AML provides a unique and promising outlet for discovery novel therapeutic targets. Importantly, increasing ceramides can also sensitize cancer cells to chemotherapy (Li and Zhang, 2015).

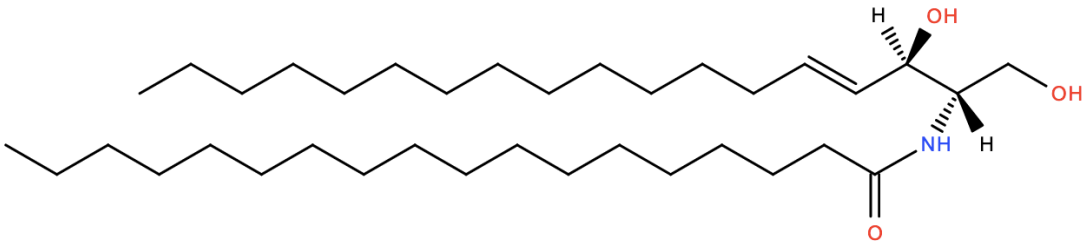

Figure 1.3: Structure of ceramide

The structure of ceramide includes sphigosine and a fatty acid chain of different lengths. C18 ceramide is presented as an example (Sud et al., 2006).

	Sphingolipid	Differential expression	Type of cancer	Reference
Enzymes	Acid Ceramidase	Increased	T-Large Granular Lymphocytic Leukemia, Prostate	85, 132, 133
	Sphingosine Kinase 1	Increased	Lung, Colon, Breast, Ovarian, Stomach, Uterine, Kidney, Glioblastoma, Non-Hodgkin Lymphoma	61, 143–148
	S1P Lyase	Decreased	Colon, Melanoma	160, 161
	S1P Phosphatase	Decreased	Colon	160
	Ceramide Kinase	Increased	Liver, Breast	162, 164
	Serine Palmitoyl-coA Transferase	Decreased	Colon	145
	Alk-Sphingomyelinase	Decreased	Colon, Liver	145, 189
	Glucosylceramide Synthase	Increased	Leukemia, Breast, Melanoma, Neuroblastoma, Ovarian, Colon	15, 90, 145, 196–201
Metabolites	Ceramide	Increased	Head and Neck, Breast, LGL, Pancreas	51, 52
		Decreased	Squamous and Non-squamous Head and Neck, Ovarian, Astrocytoma, Colon	47, 48, 50, 51
	Dihydroceramide	Increased	Endometrial	124
	Sphinganine	Increased	Endometrial	124
	Sphingosine	Increased	Endometrial	124
	Sphingosine-1-Phosphate	Increased	Glioblastoma	61
	Galactosylceramide	Increased	Ovarian	91
	Sulfatide	Increased	Colon, Lung, Ovarian, Kidney	92–96
	Gangliosides (GD3, GM2, GD2)	Increased	Melanoma, Neuroblastoma, Lymphoma, Ovarian	99, 100
	Sphingomyelin	Decreased	Colon	49

Table 1.3: Sphingolipid metabolites that are differentially expressed or generated in cancer

Many sphingolipid metabolites and sphingolipid-generating enzymes are altered in a variety of cancer types (Ryland et al., 2011).

1.2.2 SPHINGOLIPIDS IN AML

In AML, patients generally exhibit upregulation of enzymes involved in the formation of S1P and the degradation of ceramide (Tan et al., 2016), suggesting a dependence on this pathway for AML blast survival. Manipulation of ceramide levels, both directly and through the enzymes regulating its formation and breakdown, is at the forefront of current AML sphingolipid research. Blocking intracellular ceramide modifications, along with treating with exogenous ceramide using nanoliposomes has been shown to induce apoptosis in AML (Brown et al., 2013). Treatment with ceramide analog LCL-461 leads to death of AML cells, including those that are drug resistant (Dany et al., 2016). Further, acid ceramidase inhibition with LCL-204 induces apoptosis of AML cells by ceramide accumulation (Tan et al., 2016).

1.2.3 ACID CERAMIDASE

There are five ceramidases whose enzymatic activity depends upon pH. Acid ceramidase (ASAH1), neutral ceramidase (ASAH2) and alkaline ceramidases (ACER1-3). Generally, ceramides function to regulate differentiation, growth and proliferation of cells. ASAH1, referred to as AC, dominates the literature as a therapeutic target, while other ceramidases have not been studies as extensively in this context. AC is a lipid hydrolase that cleaves ceramide to produce sphingosine. The recently published crystal structure (**Figure 1.4**) illustrates the alpha and beta subunits as well as key residues (Gebai et al., 2018). AC is distinct from other ceramidases because it functions optimally in acidic environments like the lysosome. pH and proximity mediate the

interaction between Cys-143 and Asp-162 which initiates an autocleavage event to produce the active beta subunit (Shtraizent et al., 2008).

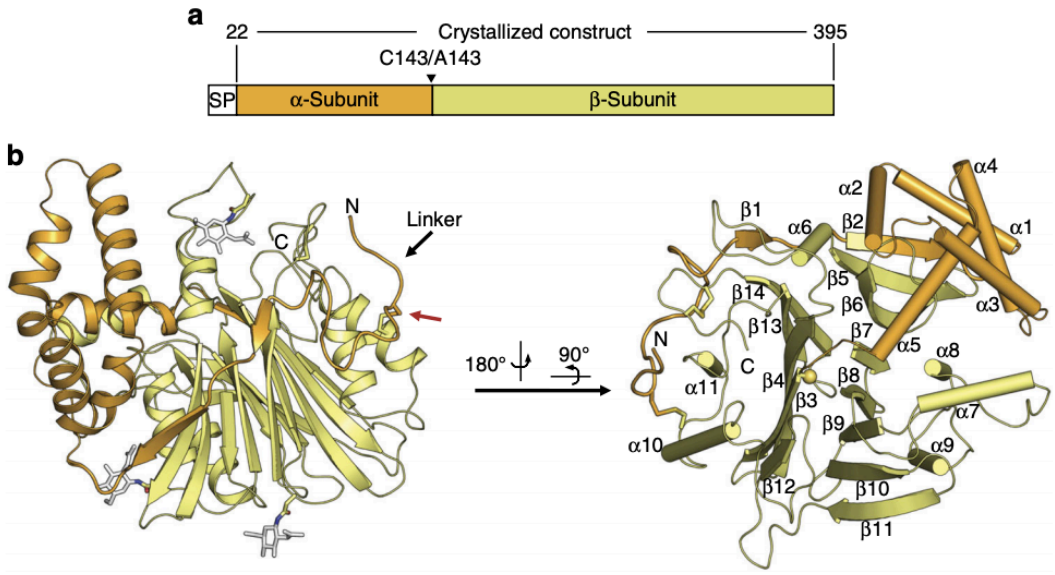

Figure 1.4: Crystal structure of acid ceramidase

Acid ceramidase consists of an alpha and a beta subunit with a critical Cys-143 residue in between (Gebai et al., 2018).

AC IN HUMAN DISEASE

AC is globally expressed in tissue, with the highest expression in the heart. At the cellular level, AC functions optimally at acidic pH and is predominantly located in the lysosome. Localization occurs as a result of glycosylation and mannose-6-phosphorylation after synthesis (Ferlinz et al., 2001). Homozygous mutant mice are embryonic lethal, while heterozygous mutants experience lipid storage disease (Li et al., 2002). AC deficient mice also experience disrupted hematopoiesis (Dworski et al., 2015). Humans with AC deficiency develop Farber Disease (Dulaney et al., 1976), a lysosomal storage disorder. Farber Disease is extremely rare and heritable, with only about 200 cases

reported worldwide. Many cases manifest within a few months of birth while milder cases may become problematic in childhood. Patients with Farber Disease experience severe pain in the joints and extremities due to nodules filled with lipids and an excess of ceramide in lysosomes. At best, patients only survive through mid to late childhood (Ehlert et al., 2007). Fortunately, enzyme replacement therapy with recombinant human AC (rhAC) normalizes many inflamed tissues in mice (He et al., 2017). Subsequently, the rhAC therapeutic RVT-801 received Fast Track and Rare Pediatric Disease designations by the FDA to expedite evaluation of clinical potential (Enzyvant, 2019).

AC IN CANCER

AC is upregulated in multiple cancers including prostate, melanoma and head and neck cancers (Musumarra et al., 2003). Multiple studies have shown that blocking AC activity induces ceramide accumulation leading to cell death (Vethakanraj et al., 2015; Roh et al., 2016; Lai et al., 2017). Further, increased AC leads to proliferation and increased growth rate of oncogenic cells (Zeidan et al., 2008). These studies suggest that AC inhibition could be a broadly effective strategy for cancers exhibiting sphingolipid dysregulation, particularly acid ceramidase upregulation.

AC INHIBITORS

Several classes of AC inhibitors exist. B13 was identified as a moderate AC inhibitor and several derivates have increased inhibitory effects on AC (Bai et al., 2014; Bielawska et al., 1992). Structurally distinct inhibitors such as ARN14988 also effectively target AC (Realini et al., 2016). The common therapeutics tamoxifen (Morad et al., 2013) and fluorouracil (5-FU) were also identified as acid ceramidase inhibitors, and derivatives have been developed to improve specificity (Realini et al., 2013).

Multiple AC inhibitors are currently being utilized to restore cell death pathways in cancer cells. AC inhibition with ceramide analogs SABRAC and RBM1-12 induced ceramide accumulation, followed by induction of cell death in metastatic prostate cancer cells (Camacho et al., 2013). Another recent AC inhibitor was discovered as a potent treatment for stage II melanoma. ARN14899 induces ceramide accumulation and decreases AC activity. Alone, the compound is only mildly toxic at micromolar concentrations, but viability of proliferative melanoma cells is drastically reduced when combined with chemotherapeutics (Realini et al., 2016).

AC IN AML

AC was recently identified as a novel therapeutic target for AML (Tan et al., 2016). In a study by our lab, AC inhibitor LCL-204 decreased AC activity, inducing apoptosis of AML cells mediated by ceramide and Mcl-1. AC knockdown reduced viability of AML cells, revealing an important role for AC in AML blast survival. Importantly, treatment with LCL-204 also significantly extended the life of AML engrafted mice. However, LCL-204 causes lysosome rupturing making it impractical for clinical trials. Because of these off-target effects, further exploration of AC inhibitors is essential.

AC also promotes drug resistance in AML, mediated by P-glycoprotein (P-gp) and NF-kB (Tan et al., 2019). In this study, resistant cell lines exhibited higher levels of both AC and P-gp protein relative to parental cell lines. Further, AC knockdown in resistant cell lines attenuated P-gp expression and resistance to chemotherapeutics. These studies demonstrate that AC is critical for the survival of AML cells, revealing a promising therapeutic target.

1.2.4 APOPTOTIC PATHWAYS

AC inhibition and ceramide accumulation have been shown to induce apoptosis as the predominant mechanism of cell death (Haimovitz-Friedman et al., 1997; Mullen and Obeid, 2012; Roh et al., 2016; Tan et al., 2016). These pathways can involve several key players like kinases and phosphatases, ceramide channels and Bcl-2 family proteins, all contributors of mitochondrial dysfunction (Colombini, 2017; Ruvolo, 2003; Zhang and Saghatelian, 2013).

BCL-2 FAMILY PROTEINS

Here, we focus on dysregulation of Bcl-2 family proteins, specifically Mcl-1. Bcl-2 family proteins can contain up to four Bcl-2 homology (BH) domains, including the critical BH3 domain that is essential for apoptotic activity (Kelekar and Thompson, 1998; Chittenden, 2002). Anti-apoptotic Bcl-2 family members (Mcl-1, Bcl-2, Bcl-xL) sequester pro-apoptotic BH3-only proteins (Bim, Bid, PUMA) in order to maintain homeostasis (Hata et al., 2015). When signals cue the release of BH3-only proteins, this facilitates activation and oligomerization of Bax and Bak, pro-apoptotic Bcl-2 family proteins. These proteins can then permeabilize the mitochondria, causing depolarization. Upon depolarization, pro-apoptotic effectors like caspases are released from the mitochondria (Lomonosova and Chinnadurai, 2008). Ceramide accumulation has been shown to impact Bcl-2 family protein expression and activation: increased ceramide promotes activation of Bax and Bak and decreases levels of anti-apoptotic proteins in the outer membrane of the mitochondria (Ueda, 2015).

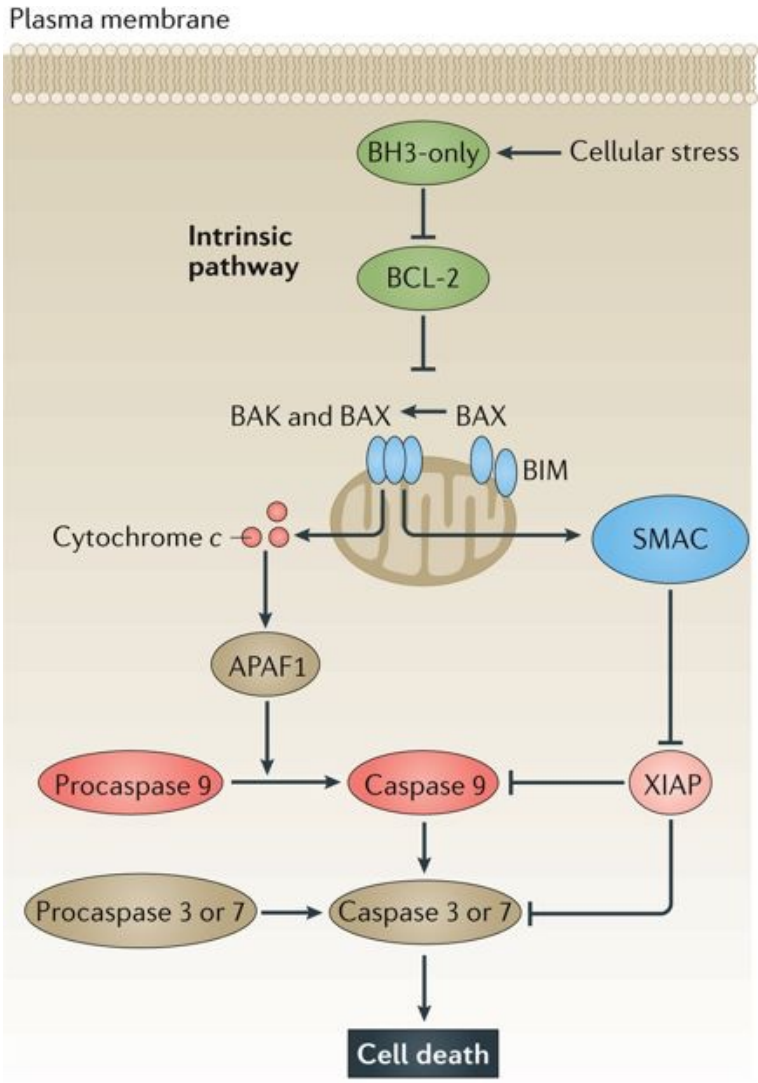

Figure 1.5: The intrinsic apoptosis pathway

Following activation of the intrinsic pathway by cellular stress, pro-apoptotic BH3-only proteins inhibit anti-apoptotic Bcl-2 family proteins. Bax and Bak oligomerize, releasing pro-apoptotic factors and activating a caspase cascade (Ashkenazi et al., 2017).

ALTERNATIVE SPLICING

Other factors can contribute to change of function in Bcl-2 family proteins, including alternative splicing. Both Mcl-1 and Bcl-x can be alternatively splicing to generate shorter isoforms Mcl-1S and Bcl-xS. These isoforms retain their BH3 domains but lose their ability to sequester pro-apoptotic signals. In turn, these proteins switch from anti-apoptotic to pro-apoptotic (**Figure 1.5**) (Bae et al., 2000; Wu et al., 2016).

There are several therapeutic implications for targeting splicing to induce apoptosis. Targeting splicing modulation in leukemia stem cells stalls their proliferation, preventing relapse in patients (Crews et al., 2016). Inhibition of splicing factor 3b subunit 1 (SF3B1) in chronic lymphocytic leukemia induces apoptosis through altering Mcl-1 levels (Larrayoz et al., 2016; Ten Hacken et al., 2018). Interestingly, these inhibitors decrease Mcl-1 dependence and increase Bcl-2 dependence, making combination therapies particularly beneficial.

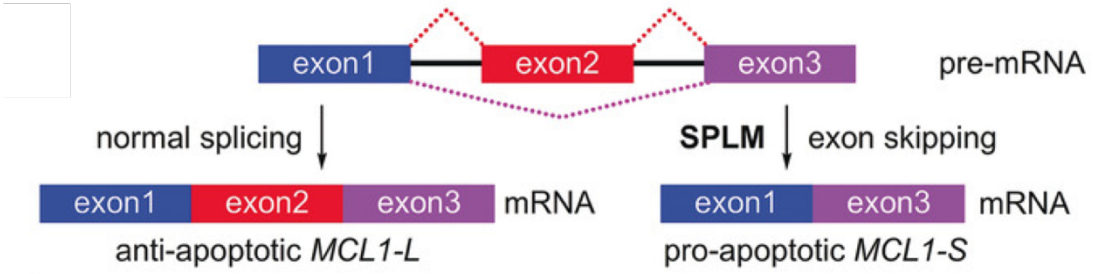

Figure 1.6: Alternative splicing of Mcl-1

Anti-apoptotic Mcl-1L can be alternatively spliced to pro-apoptotic MCL-1S, which does not contain exon 2, when spliceosome assembly is disrupted (León et al., 2017).

2 CHARACTERIZING NOVEL AC INHIBITOR SACLAC

ABSTRACT

Acute myeloid leukemia (AML) is a disease characterized by uncontrolled proliferation of immature myeloid cells in the blood and bone marrow. The five-year survival rate is approximately 25% and recent therapeutic developments have yielded little survival benefit. Therefore, there is an urgent need to identify novel therapeutic targets. We previously demonstrated that acid ceramidase (AC) is upregulated in AML and high AC activity correlates with poor patient survival. Here, we characterized a novel AC inhibitor, SACLAC, that significantly reduced viability of AML cells with an EC_{50} of approximately 3 μM across 30 human AML cell lines. Treatment of AML cell lines with SACLAC effectively blocked AC activity, induced a decrease of sphingosine 1-phosphate and a 2.5-fold increase in total ceramide levels. In the first mechanistic characterization of this compound, we showed that SACLAC induced apoptosis and alternative Mcl-1 mRNA splicing to yield pro-apoptotic Mcl-1S in AML cells. Further, we demonstrated that SACLAC treatment leads to a 37 to 75% reduction in leukemic burden in two human AML xenograft mouse models. These data further emphasize AC as a therapeutic target in AML and define SACLAC as a potent inhibitor that presents promise for future clinical development.

2.1 INTRODUCTION

Acute myeloid leukemia (AML) is a malignancy of the blood and bone marrow, characterized by uncontrolled proliferation of immature myeloid blasts. The current prognosis for most patients is poor, with 5-year survival at only 27% (Noone et al.). AML is more common in older populations, with a median age of 68 at diagnosis. Unfortunately, older patients have even worse prognoses, with only 7% of patients over the age of 65 surviving 5 years past diagnosis (Dombret and Gardin, 2016; Klepin and Balducci, 2009; Noone et al.). Patients generally receive a combination of general chemotherapeutics cytarabine (7 days) and daunorubicin (3 days) by continuous infusion. While new therapies have been approved recently, there is little change in overall survival. Some targeted therapies are available for patients with genetic mutations such as FLT3 and JAK2 (Hatzimichael et al., 2013), but AML is an extremely heterogeneous disease where the most recurrent genetic abnormality only exists in about 30% of patients (Cancer Genome Atlas Research Network et al., 2013; Martelli et al., 2013; Tyner et al., 2018). As an example, treatment with FLT3 inhibitor quizartinib achieved about 50% composite complete remission for FLT3-ITD-positive patients, but only about 5% of patients achieved complete remission (Cortes et al., 2018).

There is an urgent need for novel therapeutics in AML due to the limitations of current treatment options and poor patient survival (Hong and Medeiros, 2011; Wiese and Daver, 2018), especially in the aging population that cannot tolerate intensive therapy (Klepin and Balducci, 2009; Papaemmanuil et al., 2016). There are several hurdles involved in AML treatment, including therapy-related toxicity (Buckley et al., 2015), genetic heterogeneity, *de novo* drug resistance and relapse (Burrell and Swanton, 2014). Identification of therapeutics that address

these issues could greatly influence the future of AML treatment and improve patient prognosis.

An emerging area of study in cancer therapy involves manipulating sphingolipid metabolism in cancer cells to control cell fate (Ryland et al., 2011). While sphingolipids are generally perceived as structural components of cellular membranes, there are two key bioactive sphingolipids at the center of this pathway. Ceramide is a known second messenger in cell death while sphingosine 1-phosphate (S1P) is pro-survival (Takabe and Spiegel, 2014). Enzymes that mediate the conversion of ceramide to S1P are tightly regulated to maintain the balance between the integrity of healthy cells and the destruction of damaged cells. However, dysregulation of the enzymes regulating this pathway can contribute to many diseases including cancer (Mao and Obeid, 2008; Morad and Cabot, 2013; Ryland et al., 2011). Acid ceramidase (ASAH1, referred to as AC) plays an important role in balancing these two lipids (Mao and Obeid, 2008). AC is part of a family of lipid hydrolases that cleave ceramide to form sphingosine, which can be subsequently phosphorylated to produce S1P. AC is upregulated in several cancers (Camacho et al., 2013; Flowers et al., 2012; Leclerc et al., 2019; Nguyen et al., 2018). We recently established that it is the highest expressed and most upregulated ceramidase in AML and mediates survival of AML cells (Tan et al., 2016). We further demonstrated that elevated AC activity contributes to increased P-glycoprotein (P-gp) expression and a drug resistance phenotype in AML (Tan et al., 2019). Importantly, AC upregulation was observed in most AML patient samples, indicating that AC is a promising therapeutic target that may be applicable to a large percentage of AML patients.

We previously demonstrated that AC inhibition with LCL204 coincided with a loss of pro-survival Mcl-1 protein, leading to apoptosis (Tan et al., 2016). This finding is particularly relevant given the known importance of Bcl-2 family members in AML pathogenesis and response to therapy (Glaser et al., 2012). For example, upregulation of Mcl-1 is an established mechanism of resistance to the promising Bcl-2 inhibitor venetoclax, which is currently approved for use in elderly AML in combination with hypomethylating agents or low dose cytarabine (Aldoss et al., 2018; Luedtke et al., 2017; Teh et al., 2018). The full-length pro-survival Mcl-1 protein can also be referred to as Mcl-1L. Mcl-1 function can also be altered through alternative mRNA splicing (Gao and Koide, 2013; Morciano et al., 2016). When splicing is disrupted, exclusion of exon 2 results in formation of Mcl-1S. This step is regulated by SF3B1, a critical component of spliceosome assembly (Gao and Koide, 2013). Importantly, this alternative splicing event results in a dramatic change of function—Mcl-1L is pro-survival while Mcl-1S is pro-apoptotic (Bae et al., 2000). Mcl-1S retains the functional BH3 domain, which is critical for mitochondria-mediated induction of apoptosis (Bae et al., 2000; Chittenden, 2002). Previous studies have demonstrated that modulation of mRNA splicing can induce apoptosis of cancer cells (Gao and Koide, 2013; Lee and Abdel-Wahab, 2016).

Here, we utilize AC inhibition to increase ceramide levels and induce selective toxicity of AML cells. Further, we characterize a novel AC inhibitor to determine its clinical potential. By targeting AC, we aim to exploit a common biochemical dependence in AML cells that may represent a therapeutic approach that is broadly applicable to the diverse population of AML patients.

2.2 MATERIALS AND METHODS

CELL LINES

Kasumi-1, Kasumi-3, Kasumi-6, ME-1, SET2 and SKM-1 cells were cultured in RPMI-1640 (Corning #10-040) with 20% FBS (VWR #97068-085). OCI-AML3 cells were cultured in RPMI-1640 with 15% FBS. OCI-AML4 cells were cultured in α-MEM (ThemoFisher #12571063) with 20% FBS and supplemented with 100 ng/ml hGM-CSF (Milltenyi Biotec #130-095-372). All KG1 derivative cells and OCI-M2 cells were cultured in IMDM (ThermoFisher #12440) with 20% FBS. All other cell lines were cultured in RPMI-1640 media supplemented with 10% FBS.

HL-60/VCR (McGrath et al., 1989) cells were maintained in the presence of 1 μg/ml vincristine sulfate (Cayman #11764). HL-60/ABTR (Doi et al., 2014) cells were maintained in the presence of 5 μM ABT-737 (Cayman #11501). KG1/ABTR and KG1a/ABTR (Doi et al., 2014) cells were maintained in the presence of 1 μM ABT-737. Kasumi-6 and SNKO1 cells were supplemented with 10 ng/ml hGM-CSF. TF-1 cells were supplemented with 2 ng/ml hGM-CSF.

OCI-M2, SKNO1 and SKM-1 cell lines were obtained from DSMZ. All other cell lines were obtained from ATCC or kindly gifted according to the appendix. All cells were grown at 37°C and 5% CO_2 in a humidified incubator. Cell lines were authenticated by short tandem repeat DNA profiling (Genetica DNA laboratories) and tested for mycoplasma contamination routinely using the MycoAlert PLUS detection kit (Lonza #LT07-710). Experiments were performed within 6 weeks of thawing.

HL-60/VCR, OCI-AML2 and THP-1 cell lines were chosen for characterization studies based on prevalence in literature and ease of maintenance. KG1a cells were chosen for siRNA studies based on transfection efficiency with published electroporation parameters.

AML PATIENT SAMPLES

Samples were prepared from peripheral blood collected from newly diagnosed and untreated AML patients. Mononuclear cells were isolated by Ficoll-Paque (GE Healthcare Life Sciences) density gradient centrifugation. Cells were cultured in the serum-free medium StemSpan SFEM™ (referred to as SFEM) purchased from Stem Cell Technologies and supplemented with recombinant human stem cell factor (SCF, 100 ng/ml), interleukin-3 (IL-3, 20 ng/ml), FMS-like tyrosine kinase ligand (FLT3L, 100 ng/ml), granulocyte colony-stimulating factor (G-CSF, 20 ng/ml) and granulocyte-macrophage colony-stimulating factor (GM-CSF, 20 ng/ml) (Shenandoah Biotechnology). All cultures were incubated at 37°C with 5% CO_2. Informed consent was obtained from all patients under Penn State College of Medicine Institutional Review Board-approved protocol according to the Declaration of Helsinki.

HEALTHY DONOR SAMPLES

PBMCs from healthy donors were obtained from Virginia Blood Services and enriched using the Ficoll-Paque gradient separation method. $CD34^+$ PBMCs mobilized with G-CSF were obtained from the University of Virginia Health System Blood Bank. $CD34^+$ cells were isolated from PBMCs with a Human CD34 MicroBead Kit (Miltenyi Biotec #130-046) using the autoMACS Pro Separator (Milltenyi Biotec #130-092-545).

COMPOUNDS

SACLAC *N*-[(2*S*,3*R*)-1,3-dihydroxyoctadecan-2-yl]2-chloroacetamide was synthesized as previously described (IQAC-CSIC) (Ordóñez et al., 2019). The structure was validated using mass spectrometry. 2-hydroxypropyl β-cyclodextrin was obtained from Acros Organics (#297561000). ABT-737 and ceramides mixture were obtained from Cayman Chemicals (#11501 and #22853, respectively). The ceramide mixture contained trace amount of C16 ceramide and varying amounts of longer chain and 2-hydroxy ceramides with C24 species being most abundant. C16 was purchased from Avanti Polar Lipids (#860516). All ceramides were dissolved in methanol with 2% dodecane. LCL204 was synthesized according to previously published methods (Bai et al., 2009). RBM14C12 substrate for AC activity assays was provided by Gemma Fabrias and Antonio Delgado (IQAC-CSIC).

ACID CERAMIDASE ACTIVITY ASSAY

Cells were seeded at 2 x 10^4 cells per well in 50 µl. Acid ceramidase activity was measured at 24 hours using the RBM14C12 fluorogenic substrate as previously described (Gouazé-Andersson et al., 2011; Tan et al., 2016).

SPHINGOLIPID ANALYSIS

Lipid extraction and analysis was done using liquid chromatography-electrospray ionization-tandem mass spectrometry (LC-ESI-MS/MS) as previously described (Tan et al., 2016). Cells were plated at 5 million cells per 6 ml and treated with SACLAC or DMSO for 24 hours. Lipids were extracted from cell pellets using an azeotrophic mix of isopropanol:water:ethyl acetate (3:1:6; v:v:v). Internal standards (50 pmol of d17 long-chain bases and C12 acylated sphingolipids) were added to samples at the onset of the extraction

procedure. Extracts were separated on a Waters I-class Acquity UPLC chromatography system. Mobile phases were (A) 60:40 water:acetonitrile and (B) 90:10 isopropanol:methanol with both mobile phases containing 5 mM ammonium formate and 0.1% formic acid. A Waters C18 CSH 2.1 mm ID × 10 cm column maintained at 65°C was used for the separation of the sphingoid bases, 1-phosphates, and acylated sphingolipids. The eluate was analyzed with an inline Waters TQ-S mass spectrometer using multiple reaction monitoring. All data reported are based on monoisotopic mass and are represented as pmol/mg protein.

CELL VIABILITY ASSAY

For cell viability, cell lines were plated at 2.5 x 10^4 cells per well in a 96-well plate and treated with SACLAC or DMSO vehicle (0.4% of total volume) for the indicated time points and doses. At the experiment end point, 3-(4,5-Dimethylthiazol-2-yl)-5-(3-carboxymethoxyphenyl)-2-(4-sulfophenyl)-2H-tetrazolium (MTS) Cell Proliferation Colorimetric Assay Kit (BioVision # K300-5000) reagent was added and incubated for 2 hours. Conversion of MTS to formazan product was measured by absorbance at 490 nm using a BioTek Cytation 3 plate reader. Absorbance was normalized to DMSO control, which was defined as 100% viability. Due to limited cell numbers, patient samples and normal samples were plated at 5x10^3 cells per well in a 384-well plate with SACLAC or DMSO control for the indicated time points and doses. At the experiment end point, CellTiter-Glo Luminescent reagent (Promega #G7572) was added. After 15 minutes, luminescence was read on a BioTek Cytation 3 plate reader. Absorbance was normalized to DMSO control, which was defined as 100% viability.

COLONY FORMING ASSAY

Cryopreserved human AML patient samples were thawed and washed twice with RPMI-1640 supplemented with 2% heat inactivated fetal bovine serum (FBS). After washes, cells were cultured in triplicate in 12-well plates at a density of 0.1 to 2 x 10^5 cells per well in Human Methylcellulose Complete Media (R&D Systems, #HSC003). Plating densities were selected for each case to yield colony outgrowth of 20-100 colonies per well. The desired cell number and dose of SACLAC or DMSO was added to the culture media and dispensed to multi-well plates. Colonies were propagated for 10-14 days and blast colonies (>20 cells) were counted in a blinded manner under the light microscope.

FLOW CYTOMETRY

Apoptosis in cell lines was assessed after treating 2.5 x 10^5 cells per ml with drug or vehicle in a 48-well plate for the indicated time points and doses. Primary human AML cells were pre-incubated with SFEM for 48 hours before plating 2 x 10^5 cells in 24-well plates for the indicated times point and doses. Samples were stained using the Muse Annexin V & Dead Cell Kit (Millipore #MCH100105). Change in mitochondrial membrane potential in cell lines was measured with the Muse MitoPotential Kit (Millipore #MCH100110). Caspase activation was measured using the Muse Caspase 3/7 Assay Kit (Millipore # MCH100108). For rescue experiments, cells were diluted 1:2 in a 6-well plate 24 hours after electroporation. Cells were treated with DMSO or SACLAC for 48 hours and apoptosis was detected as stated above. All kits were used according to manufacturer's protocol. Cells were then analyzed using the Muse Cell Analyzer (Daniele et al., 2014; Ru et al., 2018). Experiments included positive and negative controls for proper analysis.

WESTERN BLOTTING

Cells were plated at 2.5 x 10^5 cells per ml in 6-well plates and treated with drug, vehicle or siRNA at the indicated doses and time points. Cells were harvested, washed with PBS, then lysed with RIPA buffer (Sigma #R0278) containing phosphatase inhibitor cocktails 2 and 3 (Sigma #P5726, #P0044) and protease inhibitor cocktail (Sigma #P8340). Protein was quantified using a bicinchoninic acid (BCA) protein assay kit (Pierce #23225). Samples were resolved on a Bolt 4-12% SDS-PAGE gel (ThermoFisher #NW00082) and transferred to PVDF membrane (Bio-Rad #170-4274). Antibodies were obtained from Cell Signaling Technology unless indicated otherwise. Primary antibodies used were: Mcl-1 (#5453), SF3B1 (#14434), β-actin (#3700) and AC (BD Biosciences #612302). Secondary antibodies used were HRP-linked goat anti-mouse (#7076) or goat anti-rabbit IgG (#7074). Clarity Max Western ECL Substrate (Bio-Rad #1705062) was added to visualize relative protein expression by chemiluminescence using the Bio-Rad ChemiDoc MP imaging system. Quantification was done using Bio-Rad ImageLab 6.0.1 software. For quantification, bands were normalized to β-actin as a loading control.

TRANSFECTION WITH SIRNA BY ELECTROPORATION

KG1a cells were electroporated with non-targeting scrambled siRNA (Dharmacon #D-001810-10-20), siRNA targeting *ASAH1* (Dharmacon #L-005228-03-0010) or *MCL-1S* (Dharmacon #CTM-481502) using the Neon Transfection System (Invitrogen) according to the manufacturer's protocol with the following parameters: 3 x 10^7 cells per ml, 1700 pulse voltage, and 20 ms pulse width for a single pulse. AC knockdown cells were harvested 48 hours after transfection for analysis by western blot. Mcl-1S knockdown cells were re-plated to 2.5 x 10^5 cells per ml and treated with SACLAC 24 hours after

electroporation. Control- and SACLAC-treated cells were harvested 48 hours after SACLAC treatment, corresponding to 72 hours after electroporation.

QUANTITATIVE REVERSE TRANSCRIPTION PCR

Cells were seeded at 2.5 x 10^5 cells per ml in 6-well plates and treated with DMSO or SACLAC for six hours. Cells were harvested and resuspended in TRIzol reagent (Invitrogen #15596026). RNA was isolated using Direct-zol RNA Miniprep Plus (Zymo Research #R2072) according to the manufacturer's protocol. RNA was quantified using the Take3 microplate and the pre-programmed RNA quantification protocol on the Gen5 software for the Cytation 3 plate reader (BioTek). DNase treatment and reverse transcription were done using the iScript gDNA Clear cDNA Synthesis Kit (Bio-Rad #1725035) in accordance with the manufacturer's protocol. The qPCR reaction contained iTaq Universal SYBR Green (Bio-Rad #1725122), 140 ng cDNA and primers specific for *HPRT* (Bio-Rad #100-25636), *B2M* (Bio-Rad #100-25636) and *MCL-1S* (Eurofins; forward, 5'-GAGGAGGACGAGTTGTACCG-3' and reverse, 5'-ACTCCACAAACCCATCCTTG-3') (Crews et al., 2016). C_T values were normalized using *B2M* and *HPRT* housekeeping genes and transformed to $2^{-\Delta CT}$ and the DMSO control was set to 1.

***IN VIVO* AML XENOGRAFT MODEL**

Maximum tolerated dose of SACLAC was determined in NOD-*scid* IL2Rgamma^{null} (NSG) mice (*n*=5; Jackson Laboratories). Mice were injected with SACLAC reconstituted in β-HPCD (IV) daily for 5 days at a dose of 5 mg/kg body weight. For pharmacokinetics studies, Swiss Webster mice (*n*=3; Charles River Laboratories) were injected with SACLAC dissolved in DMSO (40 mg/kg body weight, intraperitoneally) or dissolved in β-HPCD (5 mg/kg

body weight, via tail-vein injection). Mice were euthanized and blood was harvested at time points ranging from 0 to 48 hours. Serum concentration of SACLAC was measured by mass spectrometry quantification relative to SACLAC standard using the method referenced above.

To assess the efficacy of SACLAC in a transplantable human AML model, two cell line models were used. For the MV4-11 model, 2.5 x 10^6 luciferase and yellow fluorescent protein (YFP)-expressing MV4-11 cells in HBSS were introduced into 6- to 8-week-old female NSG mice via tail-vein injections. After 10-12 days, engraftment was confirmed using bioluminescence imaging with the IVIS Lumina LT Series III imaging system (Perkin Elmer). Mice were equally randomized into two groups of three mice and treated with vehicle or SACLAC at 5 mg/kg/day five times per week for 18 total injections. At the end of the treatment, animals were euthanized and peripheral blood was collected for flow cytometry analysis.

For the U937 model, 1 x 10^4 luciferase and tdTomato-expressing U937 cells in HBSS were introduced into 6- to 8-week-old female NSG mice via tail-vein injections. After six days, engraftment was confirmed as stated above. Mice were equally randomized into two groups of five mice and treated with vehicle or SACLAC at 5 mg/kg/day five times per week for 15 total injections. Animals were euthanized and bone marrow was collected for flow cytometry analysis.

Red blood cells (RBC) were lysed with RBC Lysis Buffer (BioLegend #420301) followed by cell surface staining with anti-human CD45 antibodies (BioLegend #304014, clone HI30) and 7AAD (BioLegend #420404) to detect viable human white blood cells (WBC) using an LSR II flow cytometer and BD FACS Diva software at the Penn State College of Medicine Flow Cytometry Core. Viable

cells were identified by gating on 7AAD-negative cells gated from singlets (SSC-A and FSC-W scales), after excluding the debris (SSC-A and FSC-A scales). Percentage of YFP, tdTomato or hCD45 positive cells was determined in FlowJo software (Becton Dickinson). All animal studies were performed with IACUC approval (PRAMS201246746).

STATISTICAL ANALYSIS

Significance between two treatment groups was determined by the two-tailed unpaired *t*-test using the GraphPad Prism 7.0 software. Cell line studies were repeated for three independent experiments, each with three or more technical replicates, unless otherwise stated. One representative experiment is shown with error bars representing standard error of the mean (SEM).

2.3 RESULTS

Previously published literature validated AC as a therapeutic target in AML while utilizing the small molecule inhibitor LCL204, which is clinically limited by lysosomal toxicity (Tan et al., 2016). To further investigate the potential of AC inhibitors for AML treatment, we tested a novel inhibitor that binds irreversibly to AC.

SACLAC INHIBITS AC AND SHIFTS LIPID LEVELS TOWARD A PRO-DEATH PHENOTYPE

SACLAC is an α-chloroamide ceramide analog (**Figure 2.1A**) that binds irreversibly to AC by transferring a covalent adduct to the enzyme catalytic site (Ordóñez et al., 2019). We expected that inhibition of AC with SACLAC would cause accumulation of ceramides by blocking the breakdown of ceramide to sphingosine and further conversion to S1P. Three human AML cell lines were selected to evaluate SACLAC inhibition of AC activity in AML. The multidrug resistant HL-60/VCR cell line, which overexpresses P-gp (Tan et al., 2019) was treated with SACLAC (2.5 μM) alongside THP-1 and OCI-AML2 cell lines. AC activity of these cell lines was reduced by 98%, 71% and 100%, respectively, with 24-hour treatment (**Figure 2.1B**). This is superior to LCL204, which requires a four-fold higher dose to achieve similar effects (**Figure 2.2**). We measured changes in S1P and ceramides under the same conditions. SACLAC reduced S1P content by 87% in HL-60/VCR and reduced S1P levels to below the limit of detection in THP-1 and OCI-AML2 cell lines (**Figure 2.1C**). Further, these conditions led to a 2- to 3-fold increase in total ceramide production (**Figure 2.1D**). Most individual ceramide species increased upon SACLAC treatment, with the most pronounced changes being C16, C18, C22:1 and C24:2 (**Figure 2.3**). Together these data indicate that SACLAC robustly inhibits AC activity and shifts lipid levels in the expected manner, increasing pro-death ceramides and decreasing pro-survival S1P.

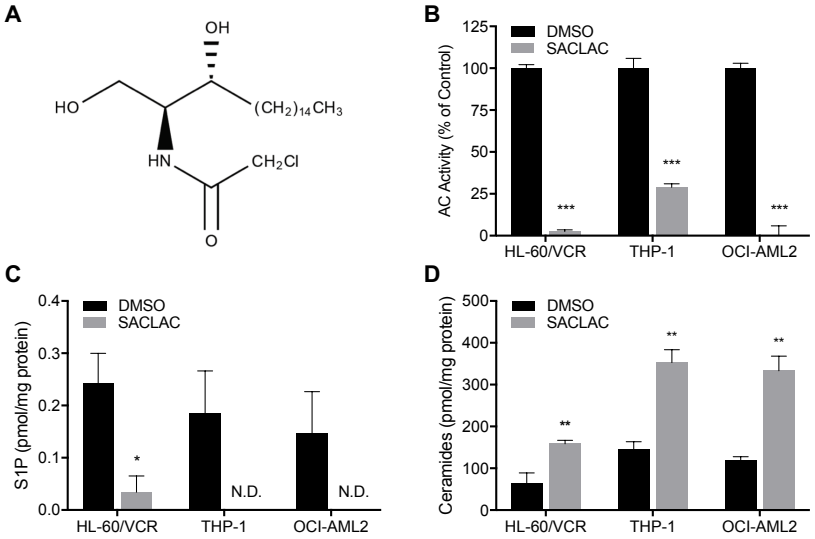

Figure 2.1: SACLAC inhibits AC and shifts lipid levels toward a pro-death phenotype

A) SACLAC is an α-chloroamide ceramide analog. **B)** Acid ceramidase activity levels were measured by fluorogenic substrate conversion to determine AC inhibition after SACLAC (2.5 μM) treatment of HL-60/VCR, THP-1 and OCI-AML2 human AML cell lines for 24 hours (n=2-3). **C)** Sphingosine 1-phosphate and **D)** total ceramide levels were measured by mass spectrometry and normalized to total protein to determine sphingolipid changes in response to SACLAC (2.5 μM) treatment of human AML cell lines for 24 hours (n=1). * $p < 0.05$, ** $p < 0.01$, *** $p < 0.001$ relative to DMSO control. N.D. indicates values were below the limit of detection. Number of experimental replicates is indicated by n.

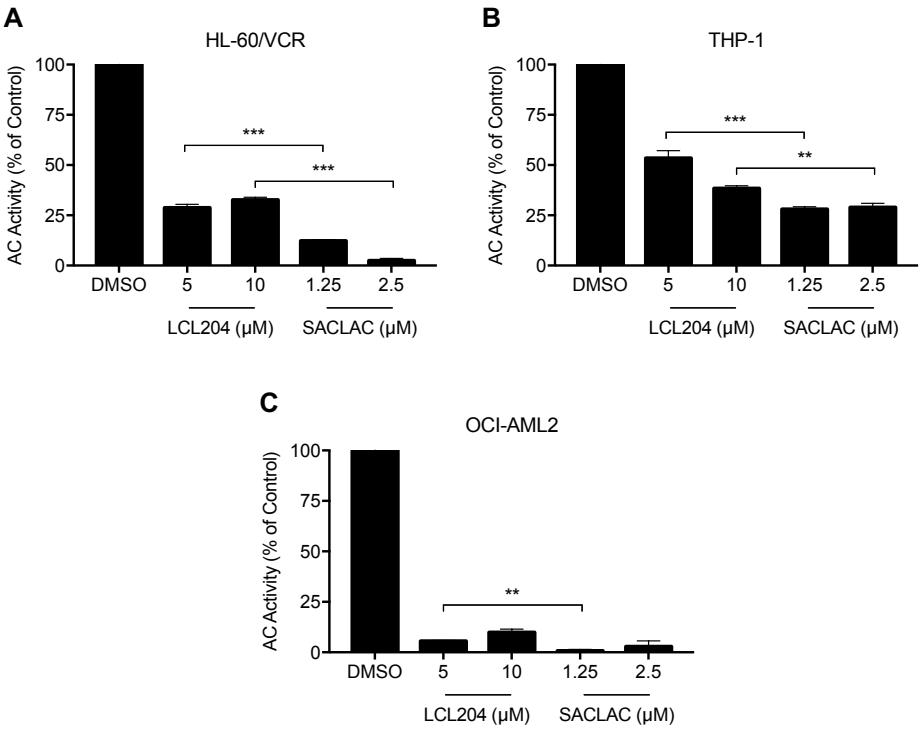

Figure 2.2: SACLAC reduces AC activity at lower doses than LCL204

A fluorogenic substrate was used to measure AC activity after treatment with DMSO vehicle, LCL204 (5 or 10 μM) or SACLAC (1.25 or 2.5 μM) in **A)** HL-60/VCR, **B)** THP-1 and **C)** OCI-AML2 cell lines (n=2). ** $p < 0.01$, *** $p < 0.001$. Number of experimental replicates is indicated by n.

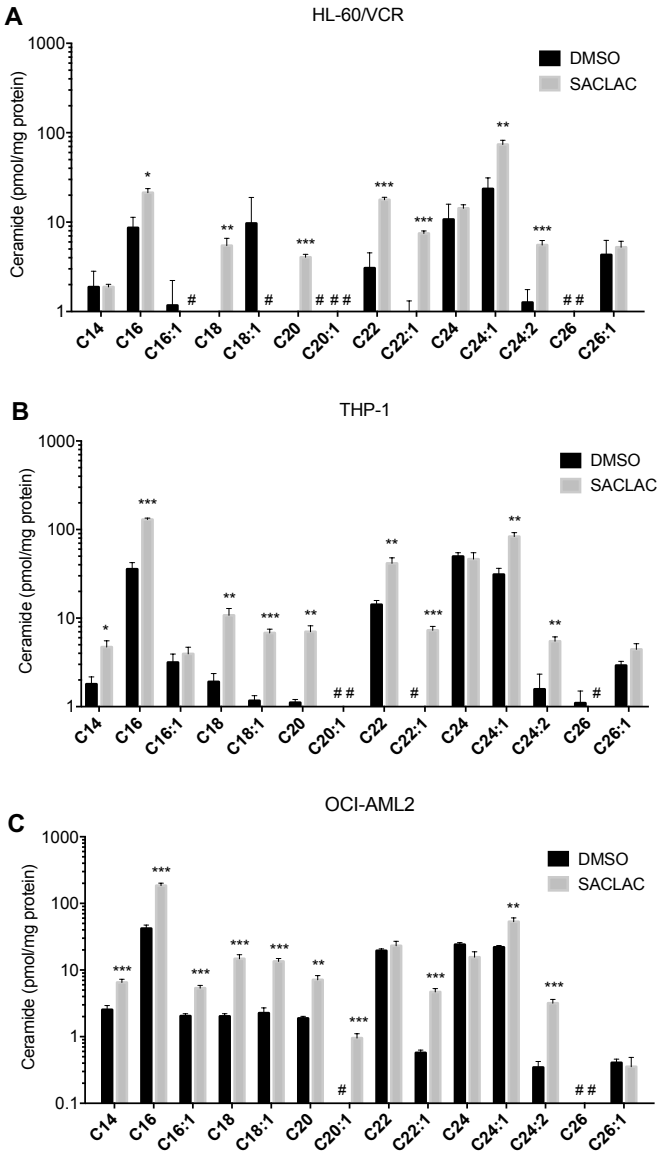

Figure 2.3: SACLAC treatment increases production of multiple ceramide species in human AML cell lines

Mass spectrometry was used to measure ceramide content after treatment with DMSO vehicle or SACLAC (2.5 μM) for 24 hours in **A)** HL-60/VCR, **B)** THP-1 and **C)** OCI-AML2 cell lines. The y-axis shown is $\log_{10}$ to accommodate all species on an unbroken axis. Each bar represents the mean ± SEM of 5 technical replicates (n=1). * $p < 0.05$, ** $p < 0.01$, *** $p < 0.001$. Number of experimental replicates is indicated by n. # indicates that bar value falls below lower axis limit.

SACLAC REDUCES VIABILITY AND COLONY FORMATION

Next, we determined if these shifts in lipid content were functionally significant and universally observed in human AML cell lines and patient samples. The same three representative cell lines were treated with SACLAC and cell viability was determined by MTS assay. HL-60/VCR, THP-1 and OCI-AML2, had EC_{50} values in the low-micromolar range (3.3, 2.6 and 1.8 μM, respectively) with 24-hour treatment (**Figure 2.4A**). To determine if this effect translated to AML patient cells, colony formation was analyzed in a panel of six primary patient samples. These six primary patient samples showed a reduced ability to form colonies in the presence of increasing doses of SACLAC. On average, colony formation decreased 32% with 5 μM treatment and 69% with 20 μM treatment (**Figure 2.4B**). Since AML is a heterogeneous disease, we assayed 30 human AML cell lines by MTS assay at 24 and 48-hour time points. Remarkably, 25 of 30 cell lines had EC_{50} values below 5 μM, with an average EC_{50} of 3.2 μM (**Figure 2.4C**). The outlier cell line OCI-M2 could be an interesting cell line to investigate further in the context of sphingolipid metabolism, AC and mechanisms of SACLAC action and/or resistance. SACLAC treatment for 24 hours slightly reduced normal cell viability. PBMCs had an average EC_{50} of 7.4 μM (n=6) while $CD34^+$ cells averaged 4.0 μM (n=4; data not shown). These data show that, although there is variability in sensitivity, SACLAC is broadly toxic to AML cells with lesser toxicity in normal cells.

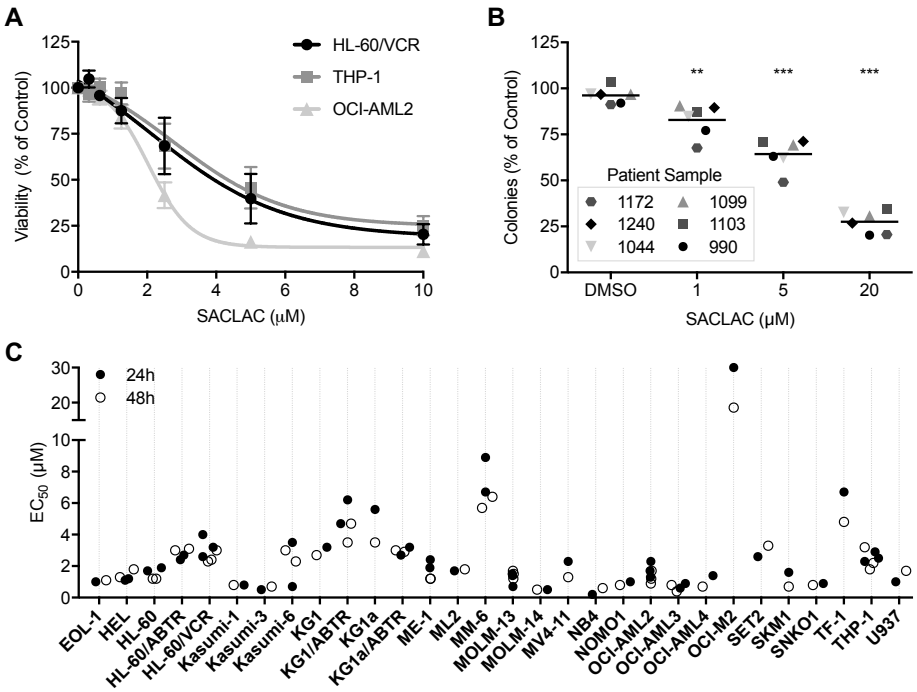

Figure 2.4: SACLAC reduces cell viability and colony formation

A) Viability of three human AML cell lines was measured by MTS assay after 24-hour treatment with the indicated dose of SACLAC. **B)** Colony formation assay was used to measure clonogenic potential in a panel of six primary AML patient samples with increasing doses of SACLAC. **C)** The concentration of SACLAC required to achieve a 50% reduction in cell viability (EC_{50}) in 30 different human AML cell lines was measured by MTS at 24 and 48 hours. Each dot represents one MTS assay (n=2-6). ** $p < 0.01$, *** $p < 0.001$. Number of experimental replicates is indicated by n.

SACLAC INDUCES APOPTOSIS AND LOSS OF MITOCHONDRIAL MEMBRANE POTENTIAL

After confirming that SACLAC treatment reduced cell viability, the mechanism of cell death was examined. First, apoptosis induction was evaluated over time in OCI-AML2 cells treated with SACLAC (5 μM; **Figure 2.5A**). Apoptosis was induced as early as 12 hours (79% apoptosis) with nearly all cells undergoing apoptosis at 24 hours. Loss of mitochondrial membrane potential (**Figure 2.5B**) occurred in parallel with positive staining for the apoptosis marker annexin V (**Figure 2.5A**). These patterns were also observed in an additional cell line, THP-1 (**Figure 2.6A-B**). Three human AML cell lines exhibited dose-dependent apoptosis induction with 48-hour SACLAC treatment, albeit with varying sensitivity (**Figure 2.5C**). AML patient samples exhibited similar results with more than half the samples reaching 80% apoptosis or greater with SACLAC treatment (**Figure 2.5D**). These data suggest that apoptosis is the predominant mechanism for SACLAC-induced cell death in AML cells.

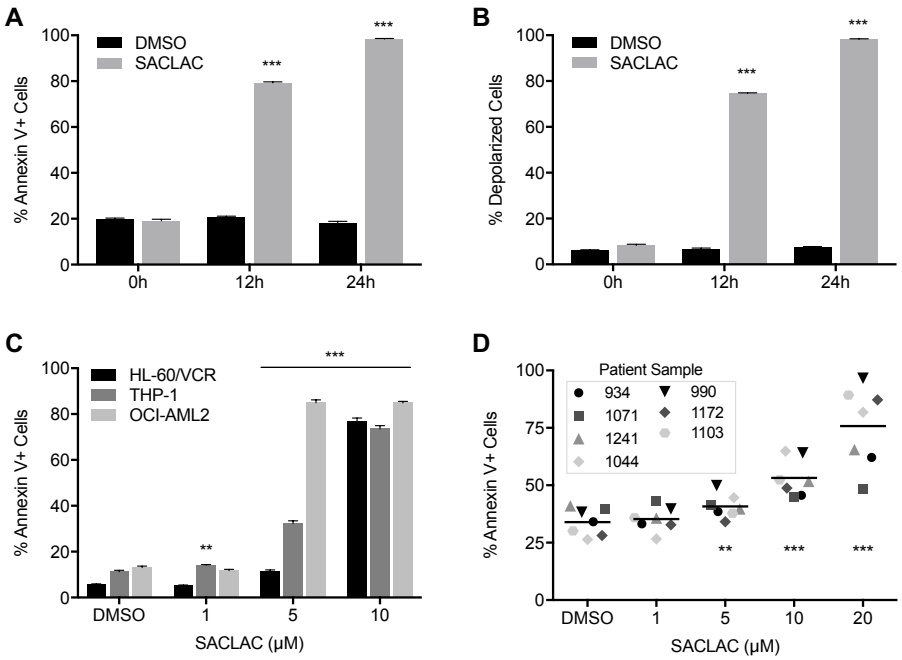

Figure 2.5: SACLAC induces apoptosis and loss of mitochondrial membrane potential

OCI-AML2 cells were treated with DMSO or SACLAC (5 μM) and evaluated for **A)** apoptosis and **B)** mitochondrial membrane depolarization at the indicated time (*n*=2). Dose-dependent apoptosis was measured in **C)** human AML cell lines and **D)** primary patient samples with 48-hour SACLAC treatment. All values under the bar in panel C are statistically significant when compared to DMSO. Studies of patient samples were performed once with a panel of seven patient samples and the line represents the group mean. * $p < 0.05$, ** $p < 0.01$, *** $p < 0.001$. Number of experimental replicates is indicated by *n*.

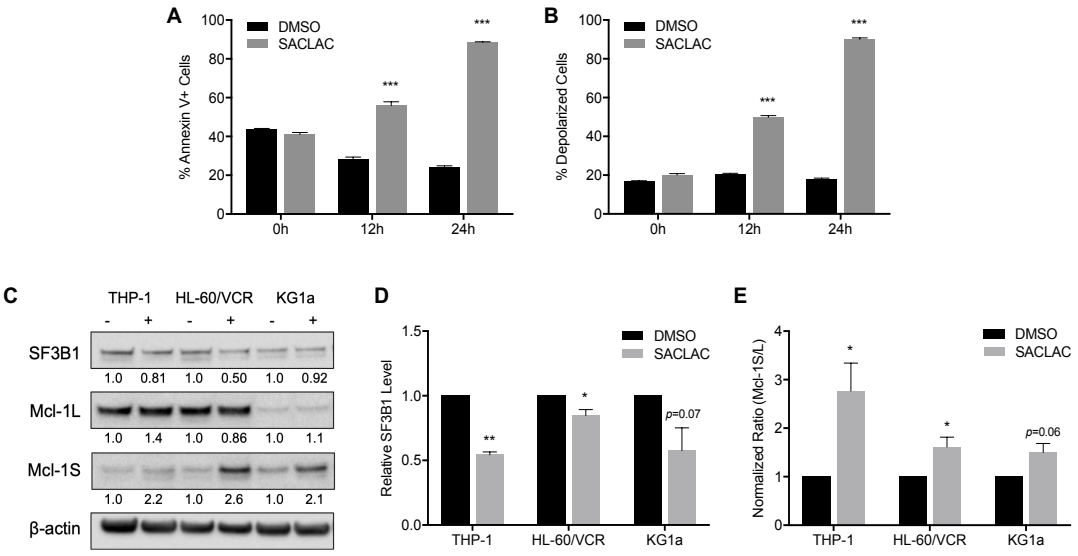

Figure 2.6: SACLAC mechanism of action is consistent in multiple human AML cell lines

THP-1 cells were treated with DMSO or SACLAC (10 μM) for 0 to 24 hours and evaluated for **A)** apoptosis and **B)** mitochondrial membrane depolarization. Data presented is from one of two independent experiments with equivalent results. **C)** THP-1, HL-60/VCR, and KG1a cells were treated with DMSO (-) or 20 μM SACLAC (+) for 48 hours and assayed for protein levels via western blotting. A representative blot is shown with fold change relative to DMSO listed below. **D)** SF3B1 level and **E)** Mcl-1S/L ratio from three independent experiments were quantified by normalizing to β-actin loading and compared to DMSO control. * $p < 0.05$, ** $p < 0.01$, *** $p < 0.001$.

SACLAC ALTERS THE RATIO OF PRO-SURVIVAL TO PRO-APOPTOTIC MCL-1 ISOFORMS

Next, we investigated mechanisms that mediate apoptosis induction in SACLAC-treated OCI-AML2 cells after 24-hour exposure to increasing doses of SACLAC. Since Mcl-1 has been implicated in AML pathogenesis and specifically in response to sphingolipid modulation (Tan et al., 2016), changes in Mcl-1 with SACLAC treatment were examined. Most notably, SACLAC induced a 10-fold upregulation of the Mcl-1S isoform, which translated to a 3-fold increase in the ratio of pro-apoptotic Mcl-1S to pro-survival Mcl-1L (**Figure 2.7A,C**). Since changes in Mcl-1S were observed, splicing factors known to regulate Mcl-1 were also examined. SACLAC treatment reduced SF3B1 protein expression (**Figure 2.7A-B**), suggesting that spliceosome assembly and exon inclusion may be disrupted (Dolatshad et al., 2015). Another splicing factor SRSF1 was not affected (data not shown). Because Mcl-1 can also be cleaved by caspases to generate a smaller protein fragment, ABT-737-treated cells were used as a positive control for Mcl-1 cleavage (Ryu et al., 2014). Mcl-1 cleavage resulted in the expected smaller fragment with the largest being around 22 kDa. However, SACLAC treatment led to the appearance of the larger Mcl-1S at about 32 kDa, which is the result of alternative mRNA splicing (**Figure 2.7D**). Mcl-1 exon 2 exclusion was confirmed using RT-qPCR with primers specific for the Mcl-1S isoform. We observed increased MCL-1S transcript in OCI-AML2 cells treated with 5 μM SACLAC (**Figure 2.7E**). Additionally, dose-dependent caspase activation was observed in about 50% of cells at the highest dose of 7.5 μM (**Figure 2.7F**). In order to determine if this mechanism is conserved across different AML cell lines, we examined changes in protein signaling after treating THP-1, HL60-VCR and KG1a cell lines with SACLAC for 48 hours. SACLAC reduced SF3B1 levels and increased the pro-apoptotic ratio of Mcl-1S/L in all three cell lines (**Figure 2.6C-E**). These observations reinforced the involvement of SF3B1 and Mcl-1S in SACLAC-mediated intrinsic apoptosis.

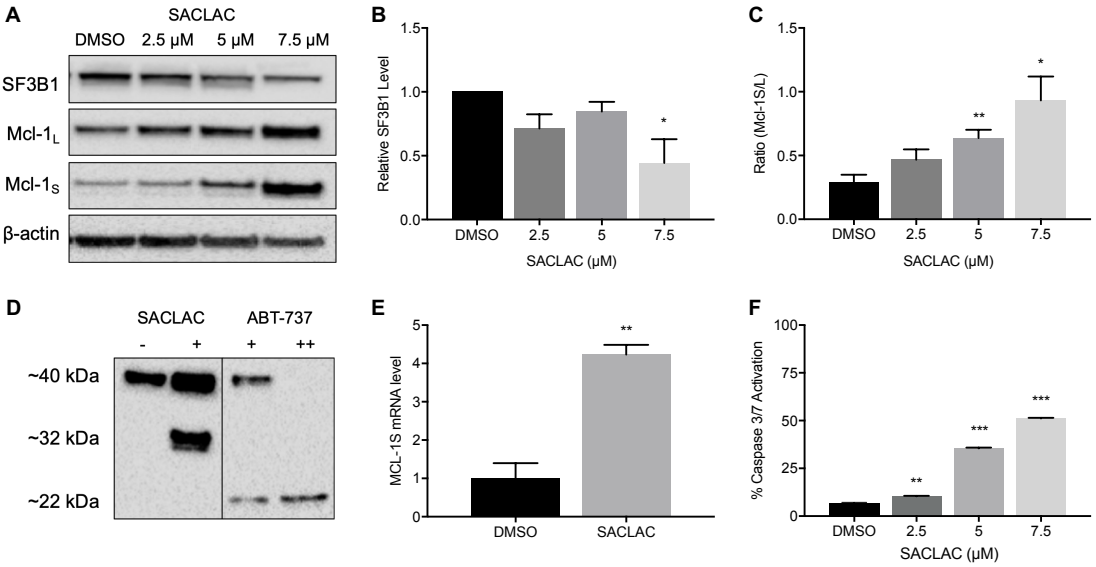

Figure 2.7: SACLAC reduces expression of SF3B1 and increases pro-apoptotic Mcl-1S

A) SF3B1, Mcl-1S and Mcl-1L protein expression was measured by western blot. **B)** SF3B1 and **C)** Mcl-1S/L ratio were quantified relative to β-actin loading control and compared to DMSO vehicle control. **D)** Alternative splicing of Mcl-1 in OCI-AML2 cells treated for 24 hours with 5 μM SACLAC (+) was distinguished from proteolytic cleavage of Mcl-1 induced by 100 nM (+) or 250 nM (++) ABT-737 as a positive control (n=1). All samples were run on the same blot, with the break excluding alternative controls. **E)** *MCL-1S* transcript levels after 6-hour treatment with 5 μM SACLAC were measured using RT-qPCR (n=2). **F)** Caspase 3/7 activation was determined in OCI-AML2 cells treated with increasing doses of SACLAC for 24 hours. * $p < 0.05$, ** $p < 0.01$, *** $p < 0.001$. Number of experimental replicates is indicated by n.

C16 CERAMIDE TREATMENT AND AC KNOCKDOWN REDUCE SF3B1 AND ALTER MCL-1 RATIO

In order to determine if ceramide is upstream of this mechanistic observation, three human AML cell lines were treated with a 100 μg/ml (~150 μM) mixture of ceramides, predominantly C18 species and longer. The ceramide mixture induced 60% apoptosis with 48-hour treatment (**Figure 2.8A**). Treatment with C16 ceramide (20 μM) induced similar effects, indicating a potential role for C16 in SACLAC-mediated cell death (**Figure 2.8B**). Further, treatment with C16 ceramide induced similar mechanistic effects as SACLAC, with a reduction in SF3B1 and an increase in the ratio of Mcl-1S to Mcl-1L (**Figure 2.9A-C**). These data demonstrate that exogenous supplementation with ceramides, specifically those that were shown to increase in response to SACLAC treatment (**Figure 2.3**) is sufficient to induce apoptosis and alternative Mcl-1 splicing in AML. To determine if SACLAC effects on AML cells are dependent on AC, we knocked down AC protein using siRNA. Treatment of KG1a cells with siRNA targeting AC reduced AC protein by 76% at 48 hours post-transfection (**Figure 2.9D**). At this time point, SF3B1 was reduced 37% (**Figure 2.9E**). Levels of Mcl-1L decreased while Mcl-1S remained constant, increasing the ratio of Mcl-1S to Mcl-1L (**Figure 2.9F**).

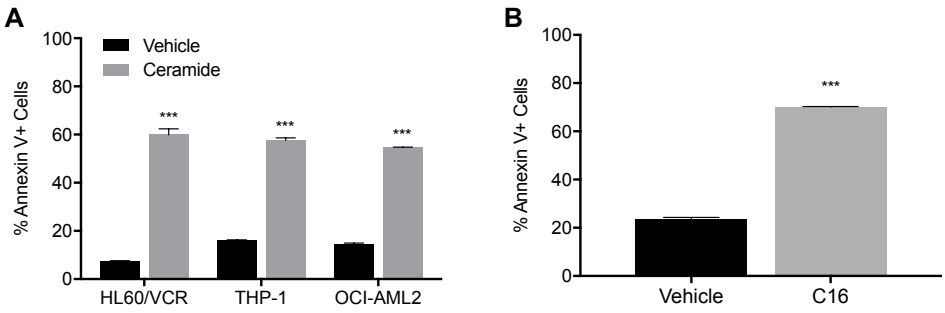

Figure 2.8: Exogenous ceramides induce apoptosis in human AML cell lines

A) HL-60/VCR, THP-1 and OCI-AML2 human AML cell lines were treated with long-chain ceramide mixture (100 μg/ml) and assayed for apoptosis at 48 hours. **B)** OCI-AML2 cells were treated with DMSO or C16 ceramide (20 μM) for 48 hours and assayed for apoptosis. *** $p < 0.001$.

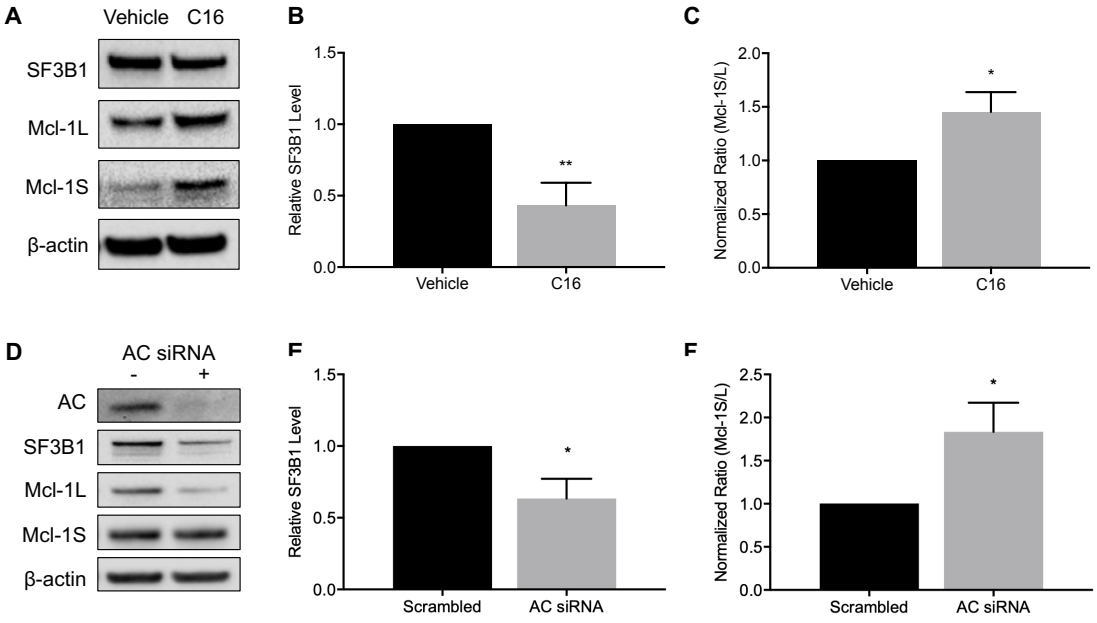

Figure 2.9: C16 ceramide treatment and AC knockdown reduce SF3B1 and alter Mcl-1S to L ratio

A) SF3B1, Mcl-1L and Mcl-1S protein expression was measured by western blot after treatment with 20 μM C16 ceramide for 48 hours in OCI-AML2 human AML cells. **B)** SF3B1 and **C)** Mcl-1S/L ratio were quantified relative to β-actin loading control and compared to DMSO vehicle control. **D)** KG1a cells were electroporated with siRNA (50 nM) targeting AC and harvested 48 hours later. Knockdown was confirmed and changes in protein levels were evaluated using western blotting. Change in **E)** SF3B1 level and **F)** Mcl-1S/L ratio were quantified relative to scrambled siRNA as the control. * $p < 0.05$, ** $p < 0.01$.

MCL-1S KNOCKDOWN ATTENUATES THE EFFECTS OF SACLAC TREATMENT

Next, we investigated the importance of Mcl-1S in the mechanism of SACLAC-mediated cell death. A custom siRNA was designed to target the junction of exons 1 and 3, which is present only in the MCL-1S transcript. KG1a cells were electroporated with this siRNA and treated with DMSO or SACLAC. Presence of short isoform-specific siRNA attenuated the induction of Mcl-1S protein expression upon SACLAC treatment (**Figure 2.10A)**. Further, apoptosis induction was reduced by 36% in SACLAC-treated Mcl-1S knockdown cells (**Figure 2.10B**). In summary, SACLAC treatment inhibits AC which leads to increased ceramide and decreased SF3B1. As ceramide accumulates, alternative splicing of Mcl-1 results in Mcl-1S accumulation that facilitates mitochondrial membrane depolarization. With loss of mitochondrial membrane potential ($\Delta\Psi m$), pro-apoptotic signals are released to activate caspases and induce apoptosis (**Figure 2.10C**).

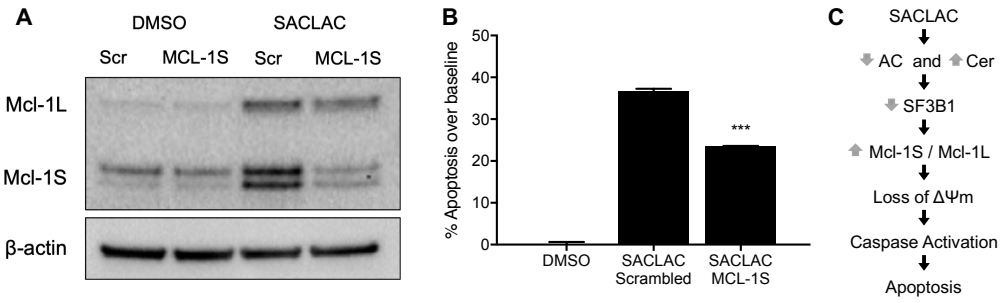

Figure 2.10: Mcl-1S knockdown attenuates the effects of SACLAC treatment

A) KG1a cells were electroporated with custom siRNA (100 nM) targeting the *MCL-1S* transcript. After 24 hours, cells were treated with 15 μM SACLAC and analyzed by western blot for Mcl-1S protein expression 48 hours later (n=2). **B)** The ability of Mcl-1S knockdown to rescue cells from SACLAC mediated cell death was measured by comparing apoptosis induction over baseline (DMSO) for each condition (n=2). **C)** A mechanistic summary incorporates changes in AC, ceramide, SF3B1 and Mcl-1S leading to SACLAC-mediated apoptosis of AML cells. *** $p < 0.01$. Number of experimental replicates is indicated by n.

SACLAC REDUCES LEUKEMIC BURDEN IN NSG MOUSE MODELS OF AML

Ultimately, we wanted to determine if SACLAC treatment provides therapeutic benefit. We first confirmed that our maximum deliverable dose did not exceed a tolerable dose for the animals (data not shown). Then, NOD-*scid* IL2Rgamma^{null} (NSG) immunodeficient mice were engrafted with human MV4-11 AML cells and then treated with 5 mg/kg SACLAC (**Figure 2.11A**). Because the half-life of SACLAC in the blood is short (**Figure 2.12**), animals were treated five times per week by tail-vein injection. After 18 injections, circulating leukemic cells in the blood were counted using flow cytometry. SACLAC treatment resulted in a significant (~75%) decrease in leukemic burden (**Figure 2.11B-C**). A second, more aggressive model using U937 AML cells (**Figure 2.11D**) exhibited up to 37% reduction in leukemic cells in the bone marrow of SACLAC-treated mice (**Figure 2.11E-F**). These data in two preclinical human AML xenograft models highlight the potential therapeutic efficacy of SACLAC in AML.

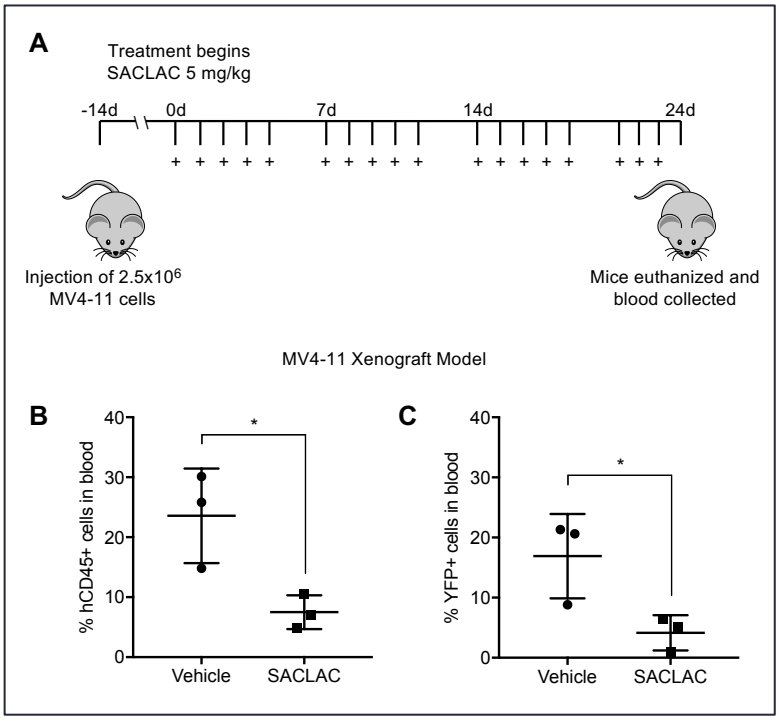
A
Treatment begins
SACLAC 5 mg/kg
-14d
0d
7d
14d
24d
Injection of 2.5x10^6
MV4-11 cells
Mice euthanized and
blood collected
MV4-11 Xenograft Model
B
% hCD45+ cells in blood
Vehicle
SACLAC
C
% YFP+ cells in blood
Vehicle
SACLAC

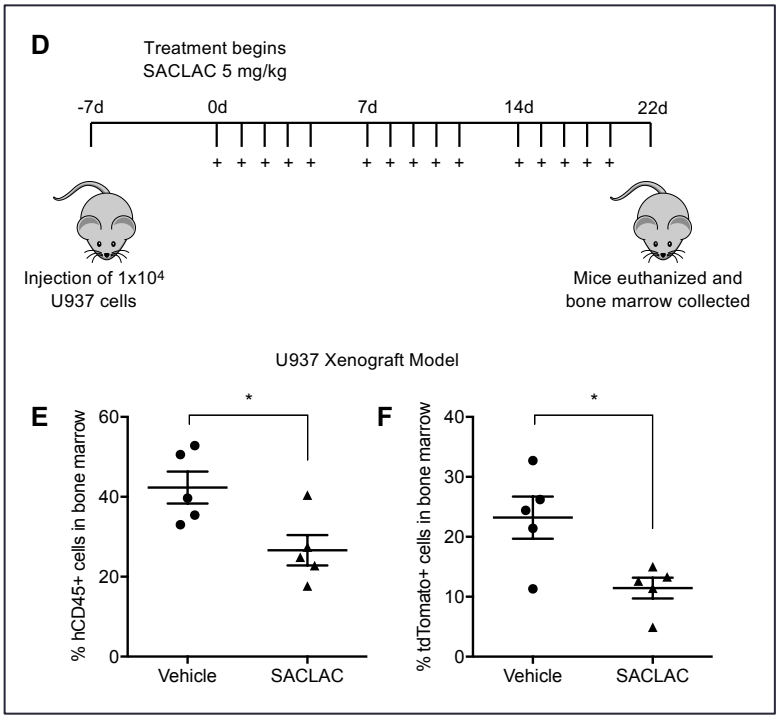
D
Treatment begins
SACLAC 5 mg/kg
-7d
0d
7d
14d
22d
Injection of 1x10^4
U937 cells
Mice euthanized and
bone marrow collected
U937 Xenograft Model
E
% hCD45+ cells in bone marrow
Vehicle
SACLAC
F
% tdTomato+ cells in bone marrow
Vehicle
SACLAC

Figure 2.11: SACLAC reduces leukemic burden in NSG mouse models of AML

A) NOD-*scid* IL2Rgamma^{null} (NSG) mice (*n*=3 per group) were injected with 2.5x10^6 human MV4-11 cells labeled with YFP-Luc, and engraftment was confirmed by bioluminescence imaging after two weeks. Each animal received five tail-vein injections per week of SACLAC (5 mg/kg SACLAC in 45% w/v 2-hydroxypropyl-β-cyclodextrin in PBS) or vehicle control. After 18 injections, leukemic burden was measured in blood by flow cytometry staining for **B)** hCD45 and **C)** YFP markers to identify MV4-11 cells. **D)** NSG mice (*n*=5 per group) were injected with 1x10^4 human U937 cells labeled with tdTomato-Luc, and engraftment was confirmed by bioluminescence imaging after one week. Each animal received five tail-vein injections per week of SACLAC (5 mg/kg SACLAC in 45% w/v 2-hydroxypropyl-β-cyclodextrin in PBS) or vehicle control. After 15 injections, leukemic burden was measured by flow cytometry staining for **E)** hCD45 and **F)** tdTomato markers to identify U937 cells in bone marrow. * $p < 0.05$.

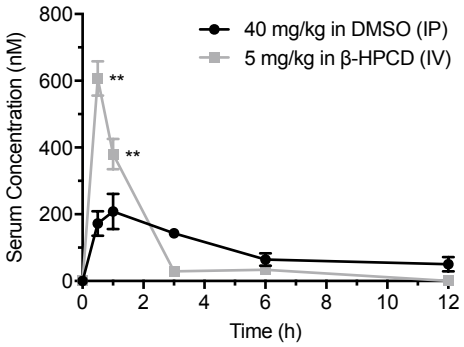

Figure 2.12: Delivery of SACLAC is improved with intravenous relative to intraperitoneal administration

SACLAC was administered to three Swiss Webster mice intraperitoneally in DMSO (40 mg/kg) or intravenously in β-HPCD (5 mg/kg). Animals were killed at the indicated time points and concentration of SACLAC in the blood was measured by mass spectrometry. ** $p < 0.01$.

2.4 DISCUSSION

Here we determined that the AC inhibitor SACLAC kills cells via intrinsic apoptosis mediated by ceramide and Mcl-1S. We showed that SACLAC is a promising therapeutic because it is broadly cytotoxic across AML cell lines and patient samples. Importantly, SACLAC treatment reduces leukemic burden in mice, even at nanomolar serum concentrations.

Our findings build upon previous reports that AC is an emerging therapeutic target that regulates the crucial balance between pro-survival S1P and pro-death ceramides (Coant et al., 2017; Morad and Cabot, 2013; Ryland et al., 2011; Tan et al., 2017). However, current studies targeting AC in AML are limited. Those that exist utilized inhibitors that have overt off-target effects (Tan et al., 2016) or require large doses for cytotoxicity (Morad et al., 2015). In contrast, SACLAC binds directly to the catalytic site of AC and does not appear to have phenotype-inducing off-target effects. Moreover, it does not require large doses for therapeutic effects in mice. Although normal cells were somewhat sensitive to SACLAC *in vitro,* the *in vivo* models affirm that SACLAC is non-toxic at the administered therapeutic dose.

Our studies identify a novel association between AC inhibition and alternative splicing in AML. Mcl-1 protein is clearly associated with survival of AML cells (Glaser et al., 2012). Mcl-1 and sphingolipids have been linked by previous work connecting Mcl-1 with AC (Tan et al., 2016), S1P (Powell et al., 2017), and ceramide signaling (Lin et al., 2016). However, these "traditional" relationships focused on changes in the full length Mcl-1 protein (Mcl-1L). In contrast, our studies highlight a unique mechanism whereby altered splicing leads to a pro-apoptotic Mcl-1 ratio. Importantly, this key role for Mcl-1S in SACLAC-

mediated cell death is reinforced by a partial rescue of viability with knockdown of Mcl-1S (**Figure 6B**). This suggests that alternative splicing of Mcl-1 cooperates with other major apoptotic contributors, such as ceramide accumulation and S1P depletion, to induce SACLAC-mediated cell death.

The relationship between SF3B1 and Mcl-1 has been established (Gao and Koide, 2013), but the upstream connection between ceramides and SF3B1 is unclear. Ceramides may regulate SF3B1 expression through activation of protein phosphatase 1 (PP1) which is known to bind the RNA recognition motif of several splicing factors (Massiello and Chalfant, 2006).

Reduced SF3B1 levels and increased Mcl-1S/L ratios were observed consistently upon AC knockdown, SACLAC treatment and ceramide supplementation (**Figures 4-5**). The AC knockdown results differed slightly in that loss of Mcl-1L was the major factor in the 2-fold increase of Mcl-1S to Mcl-1L (**Figure 5D**) as opposed to primarily an increase in Mcl-1S in the other models. This difference is likely associated with variation in temporal dynamics and sphingolipid subcellular distribution associated with different types of manipulation. Another likely contributor is the abundance of Mcl-1S and L isoforms in KG1a cells relative to other AML cell lines (**Figure S3C**). Expanding our understanding of temporal and spatial relationships when utilizing sphingolipid modulators or sphingolipids themselves will enhance future therapeutic targeting of sphingolipid metabolism.

The observed changes in SF3B1 and Mcl-1 are particularly interesting since a subset of the common somatic mutations in AML involve genes that regulate RNA binding and spliceosome assembly (Makishima et al., 2012). Interestingly, myelodysplastic syndrome (MDS), which sometimes precedes AML, exhibits

spliceosome mutations in about 50% of cases and responds noticeably well to spliceosomal inhibition (Lee and Abdel-Wahab, 2016). Additional clinical relevance of our studies is highlighted by Mcl-1's known role in resistance to Bcl-2 inhibitor venetoclax (ABT-199) (Luedtke et al., 2017; Wang et al., 2019). Venetoclax was recently granted breakthrough status for the treatment of newly diagnosed AML in combination with hypomethylating agents or low dose cytarabine (DiNardo et al., 2019; Wei et al., 2018). Because of its ability to transition Mcl-1 from pro-survival to pro-apoptotic isoforms, SACLAC combination may further enhance the efficacy of venetoclax in AML patients and other cancers. SACLAC may also be more beneficial than Mcl-1 specific inhibitors in combination therapies due to its pro-apoptotic conversion of sphingolipid levels. Ongoing studies in our lab are exploring the relative efficacy of SACLAC combinatorial treatments.

The primary limitation for *in vivo* studies was the solubility and uptake of SACLAC. We were able to improve delivery of SACLAC by changing administration route and vehicle (**Figure S5**), but only achieved peak serum SACLAC levels of less than 1 μM. The control and SACLAC-treated mice were of similar health at the end of the study, which suggests limited toxicity at this given dose. Nonetheless, we observed significant differences in leukemic burden at the cellular level. Identifying improved solvents, alternative formulations or structural derivatives of SACLAC may improve therapeutic efficacy.

Our findings are especially important because of AML patient heterogeneity (Martelli et al., 2013). While mutation-targeted therapeutics are best suited for specific patient subpopulations, SACLAC appears to exploit a common biochemical dependence across the vast majority of AML cell lines and patient

samples. While AC upregulation and ceramide mediated apoptosis have been established previously (Tan et al., 2016), we have advanced this field by characterizing a novel inhibitor with a unique mechanism of action (**Figure 4**) and *in vivo* efficacy (**Figure 7**). Additionally, our screen of 30 AML cell lines represents the largest panel of AC inhibitor efficacy studies in AML to date. Further, these studies elucidate the mechanism of SACLAC cytotoxicity in AML cells and inform future efforts to design combination therapies or combat potential resistance.

Together, our studies demonstrate that ceramide accumulation leading to SF3B1 reduction and Mcl-1S induction is a primary mechanism of action for novel inhibitor SACLAC. Our findings highlight the role of AC and sphingolipids in AML and identify SACLAC as a novel and promising therapeutic strategy.

3 NANOLIPOSOMAL STRATEGIES FOR ALTERING SPHINGOLIPID METABOLISM

ABSTRACT

Sphingolipid metabolism is dysregulated in several cancers. These disease states create an imbalance of pro-survival sphingosine 1-phosphate and pro-death ceramides. *In vitro* studies have highlighted the benefit of using ceramide analogs to inhibit the breakdown of endogenous ceramides, leaving them available to signal cell death in cancerous cells. However, lipid-based therapies are particularly difficult to use *in vivo* due to poor solubility in safe vehicles. These studies present and optimize a nanoformulation of ceramide analog SACLAC in the context of acute myeloid leukemia. We utilize viability assays, pharmacokinetics and an immunocompromised mouse model to observe the impact of changes in nanoliposome formulations. Incorporating cholesterol into liposomes increases sensitivity to nanoSACLAC *in vitro*. Bioavailability of nanoSACLAC approaches 100%, a remarkable improvement over free SACLAC. This improved formulation facilitates safe delivery of SACLAC *in vivo*. While drug loading is still limited, nanoSACLAC reduces leukemic burden by 50% even at a low dose of 3.3 mg/kg. Further optimization of nanoliposome formulation and loading may reveal increased preclinical potential for SACLAC.

3.1 INTRODUCTION

Sphingolipids are generally perceived as structural components of cell membranes, but can also serve important biological functions. Ceramide and sphingosine 1-phosphate (S1P) are at the forefront of cancer research due to their bioactivity. Ceramide is a well-established second messenger in cell death that promotes apoptosis upon accumulation. On the other hand, S1P promotes cell survival via both autocrine and paracrine signaling (Ryland et al., 2011).

The conversion of ceramide to S1P is carefully controlled in order to maintain homeostasis in normal cells. Ceramide is hydrolyzed by ceramidase to create sphingosine, which can be subsequently phosphorylated by sphingosine kinase to produce S1P. Multiple studies have shown that targeting this conversion can kill cancer cells (Powell et al., 2017; Tan et al., 2016). Acute myeloid leukemia (AML) is of particular interest due to the challenge of genetic heterogeneity and established dysregulated sphingolipid metabolism (Tan et al., 2016).

Recently, SACLAC was identified as an inhibitor of acid ceramidase (AC), one of the enzymes that initiates breakdown of ceramides (Ordóñez et al., 2019). SACLAC is a potent and specific inhibitor of AC that exhibits therapeutic potential in AML. This is supported by widespread efficacy in a panel of 30 human AML cell lines and reduced leukemic burden in two mouse models of AML (Chapter 2). However, SACLAC has a short half-life in the blood and is poorly soluble in vehicles that are safe for intravenous delivery.

Solubility and delivery are persistent concerns when using lipid-based therapies with traditional vehicles. However, using lipids themselves as the

vehicle has revolutionized the ability to deliver otherwise insoluble compounds *in vivo* (Yingchoncharoen et al., 2016). Lipid-based drug delivery systems like nanoliposomes are similar in structure to the cell membrane, containing a bilayer with hydrophobic interiors and hydrophilic exteriors (**Figure** 3.1). This juxtaposition allows nanoliposomes to solubilize both hydrophobic and hydrophilic compounds. Hydrophobic compounds like SACLAC readily localize between the membrane where similar residues are present.

Nanoliposomes are composed of a variety of phospho- and sphingolipids, predominantly phosphatidylcholine (PC), a major component of biological membranes (Vemuri and Rhodes, 1995). Additional molecules such as cholesterol can be added to improve the stability of nanoliposomes in fluids like blood and serum (Damen et al., 1981). Although nanoliposomes are not a new discovery, continuing efforts aim to optimize membrane composition and synthesis methods to improve encapsulation efficiency and bioavailability.

One of the most promising nanotherapies is sphingolipid-based, the C6 ceramide nanoliposomes (CNL). C6-ceramide is a synthetic short-chain ceramide that induces cell death in multiple cancers (Flowers et al., 2012; Zhu et al., 2011). This is even more pronounced when C6-ceramide is administered via nanoliposomes (Li et al., 2018; Liu et al., 2010; Watters et al., 2013). CNL is a potent therapy currently in clinical trials for advanced solid tumors (Kester et al., 2015; Keystone Nano, Inc, 2019), highlighting the potential for nanoliposomes to safely advance lipid-based compounds to clinical stages.

As vehicles, nanoliposomes are very efficient due to their ability to readily interact with cell membranes. When like residues between nanoliposomes and

cell membranes intermingle, the nanoliposome can fuse with the cell to release the compound directly into the cell. Because of these properties, we chose to encapsulate SACLAC into nanoliposomes in order to determine if we could improve solubility and delivery of SACLAC to the blood. Ultimately, this could provide clarity of SACLAC's therapeutic potential in AML.

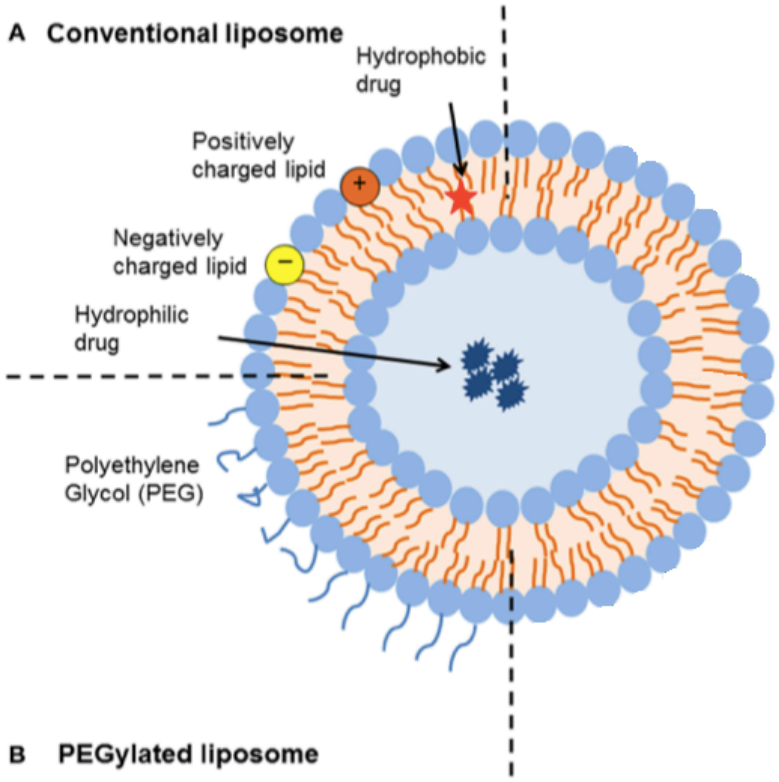

Figure 3.1: Nanoliposomes contain hydrophobic and hydrophilic regions to improve drug solubility

Nanoliposomes are useful vehicles for compounds with poor solubility due to their cell membrane-like composition and presence of both hydrophobic and hydrophilic regions. Liposomal components can be optimized several ways, including **A)** altering proportion of charged lipids and **B)** adding polyethylene glycol (PEG) for stability (Sercombe et al., 2015).

3.2 MATERIALS AND METHODS

AML CELL LINES AND PATIENT SAMPLES

HL-60/VCR (McGrath et al., 1989), OCI-AML2, THP-1, and MM-6 cell lines were maintained in RPMI-1640 (Corning #10-040) with 10% FBS (VWR #97068-085). HL60/VCR cells were supplemented with 1 μg/ml vincristine sulfate (Cayman #11764). These cell lines were obtained from ATCC unless otherwise specified. Primary patient sample 990 was prepared from peripheral blood collected from a newly diagnosed and untreated AML patient. Mononuclear cells were isolated by Ficoll-Paque (GE Healthcare Life Sciences) density gradient centrifugation. Cells were cultured in the serum-free medium StemSpan SFEM™ (referred to as SFEM) purchased from Stem Cell Technologies and supplemented with recombinant human stem cell factor (SCF, 100 ng/ml), interleukin-3 (IL-3, 20 ng/ml), FMS-like tyrosine kinase ligand (FLT3L, 100 ng/ml), granulocyte colony-stimulating factor (G-CSF, 20 ng/ml) and granulocyte-macrophage colony-stimulating factor (GM-CSF, 20 ng/ml) (Shenandoah Biotechnology). All cultures were incubated at 37°C with 5% CO_2. Informed consent was obtained from all patients under Penn State College of Medicine Institutional Review Board-approved protocol according to the Declaration of Helsinki.

COMPOUNDS

SACLAC *N*-[(2*S*,3*R*)-1,3-dihydroxyoctadecan-2-yl]2-chloroacetamide was synthesized as previously described (IQAC-CSIC) (Ordóñez et al., 2019). The structure was validated using mass spectrometry. Ceramides and lipid components were obtained from Avanti Polar Lipids.

NANOLIPOSOMES

Lipids dissolved in chloroform were mixed in a ratio of [1,2-dioleoyl-sn-glycero-3-phosphocholine (DSPC)/1,2-dioleoyl-sn-glycero-3

phosphoethanolamine (DOPE)/1,2-distearoyl-sn-glycero-3-phosphoethanolamine-N-[methoxy PEG(2000)/cholesterol] 4.5:2:1:2 with or without 8.4mg of SACLAC in a glass vial and dried under nitrogen gas. The dried lipid film was rehydrated in 1X PBS at 60C with periodic vortexing for 3 hours. The hydrated lipid mixture was then sonicated until clear and passed through a 100nm pore polycarbonate membrane using an Avanti Mini Extruder (Avanti Polar Lipids) to size the particles. Excess SACLAC was removed by size exclusion chromatography utilizing a CL-4B column. SACLAC encapsulation was confirmed by RP-HPLC.

CELL VIABILITY ASSAY

For cell viability, cell lines were plated at 2.5 x 10^4 cells per well in a 96-well plate and treated with SACLAC, nanoSACLAC, ghost nanoliposome or DMSO vehicle (0.4% of total volume) for the indicated time points and doses. At the experiment end point, 3-(4,5-Dimethylthiazol-2-yl)-5-(3-carboxymethoxyphenyl)-2-(4-sulfophenyl)-2H-tetrazolium (MTS) Cell Proliferation Colorimetric Assay Kit (BioVision # K300-5000) reagent was added and incubated for 2 hours. Conversion of MTS to formazan product was measured by absorbance at 490 nm using a BioTek Cytation 3 plate reader. Absorbance was normalized to DMSO control, which was defined as 100% viability.

FLOW CYTOMETRY

Primary human AML cells were pre-incubated with cytokines (listed previously) and SFEM or SFEM with 10% FBS for 48 hours before plating 2 x 10^5 cells in 24-well plates for the indicated times point and doses. Samples were stained using the Muse Annexin V & Dead Cell Kit (Millipore #MCH100105). Cells were treated with SACLAC, nanoSACLAC or ghost nanoliposome for 48 hours and apoptosis was detected as stated above. All kits were used according

to manufacturer's protocol. Cells were then analyzed using the Muse Cell Analyzer (Daniele et al., 2014; Ru et al., 2018). Experiments included positive and negative controls for proper analysis.

IN VIVO AML XENOGRAFT MODEL

Maximum tolerated dose of SACLAC was determined in NOD-*scid* IL2Rgamma^{null} (NSG) mice (*n*=5; Jackson Laboratories). Mice were injected with nanoSACLAC (IV) daily for 5 days at a dose of 3.3 mg/kg body weight, respectively. For pharmacokinetics studies, Swiss Webster mice (*n*=3; Charles River Laboratories) were injected with SACLAC dissolved in DMSO (40 mg/kg body weight, intraperitoneally) or nanoSACLAC (3.3 mg/kg body weight, via tail-vein injection). Mice were euthanized and blood was harvested at time points ranging from 0 to 48 hours. Serum concentration of SACLAC was measured by mass spectrometry quantification relative to SACLAC standard using the method referenced in Chapter 2.

To assess the efficacy of SACLAC in a transplantable human AML model, a cell line model was used. Injections of 1 x 10^4 luciferase and dTomato-expressing U937 cells in HBSS were introduced into 6- to 8-week-old female NSG mice via tail-vein injections. After six days, engraftment was confirmed as stated above. Mice were equally randomized into two groups of five mice and treated with vehicle or nanoSACLAC at 3.3 mg/kg/day multiple times per week for 12 total injections. Animals were euthanized and blood was collected for flow cytometry analysis.

Red blood cells (RBC) were lysed with RBC Lysis Buffer (BioLegend #420301) followed by cell surface staining with anti-human CD45 antibodies (BioLegend #304014, clone HI30) and 7AAD (BioLegend #420404) to detect viable human white blood cells (WBC) using an LSR II flow cytometer and BD FACS Diva

software at the Penn State College of Medicine Flow Cytometry Core. Viable cells were identified by gating on 7AAD-negative cells gated from singlets (SSC-A and FSC-W scales), after excluding the debris (SSC-A and FSC-A scales). Percentage of dTomato or hCD45 positive cells was determined in FlowJo software (Becton Dickinson). All animal studies were performed with IACUC approval (PRAMS201246746).

STATISTICAL ANALYSIS

Significance between two treatment groups was determined by the two-tailed unpaired *t*-test using the GraphPad Prism 7.0 software. Each experiment contained three or more technical replicates. Graphs depict mean and standard error of the mean (SEM) from a single experiment.

3.3 RESULTS

Previous studies revealed that SACLAC is a promising therapeutic for AML. However, solubility and bioavailability in the blood were suboptimal, which limited interpretation of clinical potential.

NANOSACLAC IS NOT AS EFFECTIVE *IN VITRO* AS FREE SACLAC

SACLAC was incorporated into nanoliposomes using a proprietary mix of membrane lipids. To determine whether SACLAC and nanoSACLAC were comparable *in vitro,* HL60/VCR, OCI-AML2 and MM-6 cell lines were treated with increasing doses of nanoSACLAC, free SACLAC and ghost nanoliposome for 24 or 48 hours (**Figure 3.2**). SACLAC killed cells at lower doses than nanoSACLAC in all three cell lines. In OCI-AML2 cells (**Figure 3.2B**), SACLAC killed about 85% of cells at 2.5 μM, while nanoSACLAC only killed 25% of cells, which was similar to the ghost nanoliposome. In HL60/VCR (**Figure 3.2A**) and

THP-1 cells (**Figure 3.2C**), nanoSACLAC killed less than 25% of cells even at the highest dose of 10 μM. Toxicity was not significantly improved by extending exposure time to these formulations (**Figure 3.2D-F**). These results indicate that the nanoliposomal structure or synthesis process impedes the ability of SACLAC to act on cells.

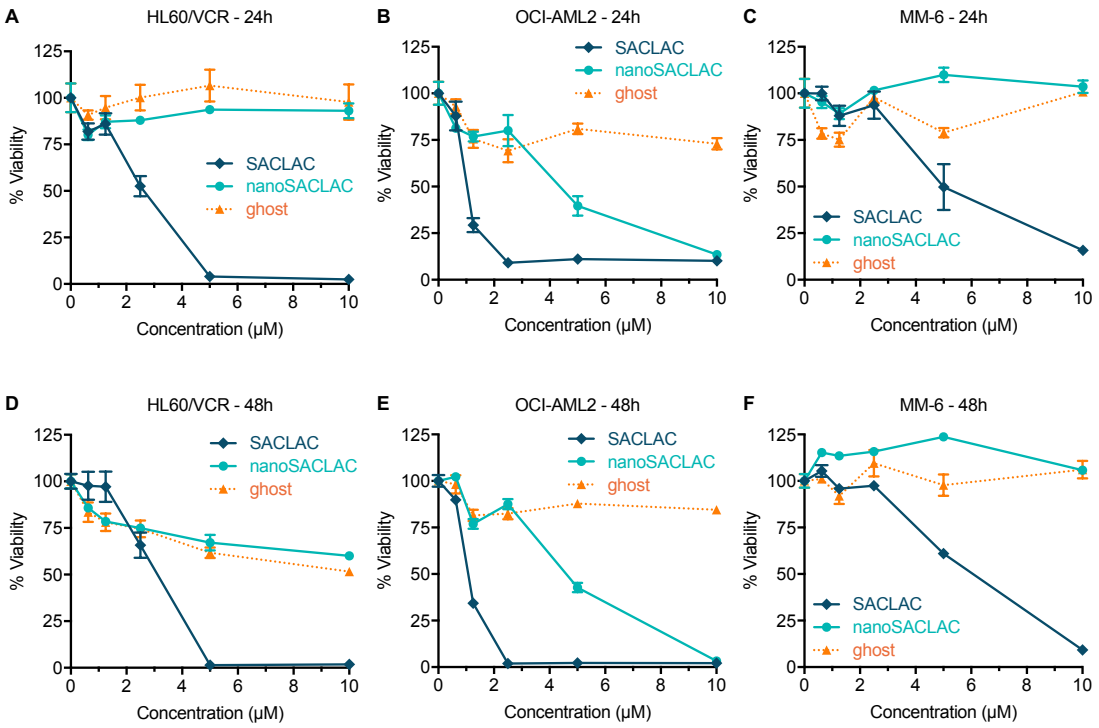

Figure 3.2: nanoSACLAC is not as effective *in vitro* as free SACLAC

A) HL60/VCR, **B)** OCI-AML2 and **C)** MM-6 cell lines were assayed for change in viability upon treatment with increasing dose of ghost nanoliposome, SACLAC or nanoSACLAC for **(A-C)** 24 or **(D-F)** 48 hours using MTS assay. DMSO represents SACLAC vehicle and ghost represents nanoSACLAC vehicle. DMSO was set to 100% to examine relative differences in toxicity. Error bars represent mean +/- SEM from three or more technical replicates. Nanoliposomes were generated by Tye Deering (University of Virginia).

ADDITION OF CHOLESTEROL IMPROVES TOXICITY OF NANOSACLAC

To encourage release of SACLAC from nanoliposomes in culture, cholesterol was incorporated at either 10% or 20% of membrane lipids. To determine if this formulation improved toxicity, OCI-AML2 and THP-1 AML cell lines were treated with free SACLAC and nanoSACLAC containing either 10% or 20% cholesterol for 24 hours. In OCI-AML2 cells (**Figure 3.3A**), both concentrations of cholesterol restored nanoSACLAC toxicity to the same level as free SACLAC. In THP-1 cells (**Figure 3.3B**), nanoSACLAC was more effective with 10% cholesterol than with 20% cholesterol with EC_{50} values only differing by about 1.5 μM. Together, this suggests that addition of cholesterol to the nanoliposome formulation allows improved release of SACLAC available to act on cultured cells.

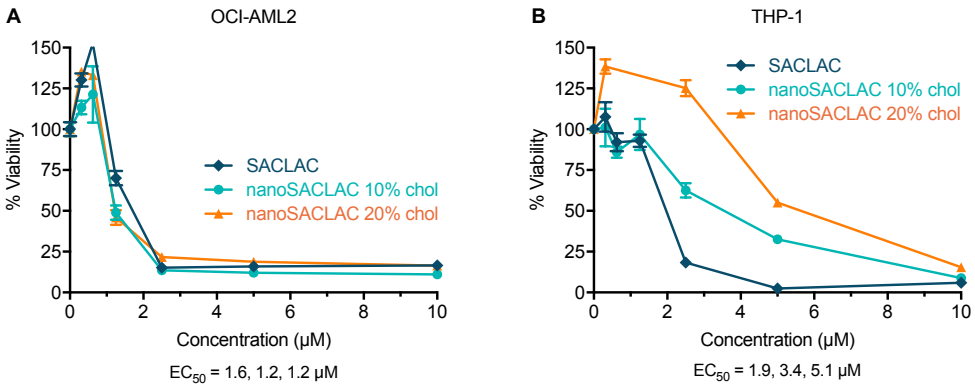

Figure 3.3: Addition of cholesterol improves toxicity of nanoSACLAC

A) OCI-AML2 and **B)** THP-1 cells were treated with increasing dose of SACLAC or nanoSACLAC containing either 10% or 20% membrane cholesterol for 24 hours using MTS assay. DMSO was set to 100% viability and ghost nanoliposome (no effect) is not shown. Error bars represent mean +/- SEM from three or more technical replicates. Nanoliposomes were generated by Tye Deering (University of Virginia).

ADDITION OF CHOLESTEROL DOES NOT IMPROVE SYNERGY WITH CNL

Many sphingolipid targeting therapies can be improved by combining them with CNL. To determine if combining two nanoliposomal therapies was more efficacious, we treated cells with free SACLAC and nanoSACLAC containing cholesterol and examined changes in cell viability. There was no improvement in toxicity in combination treatment when exchanging free SACLAC for nanoSACLAC in OCI-AML2 (**Figure 3.4A**) or THP-1 cells (**Figure 3.4B**). These data support use of freeSACLAC rather than nanoSACLAC in combination therapies with CNL.

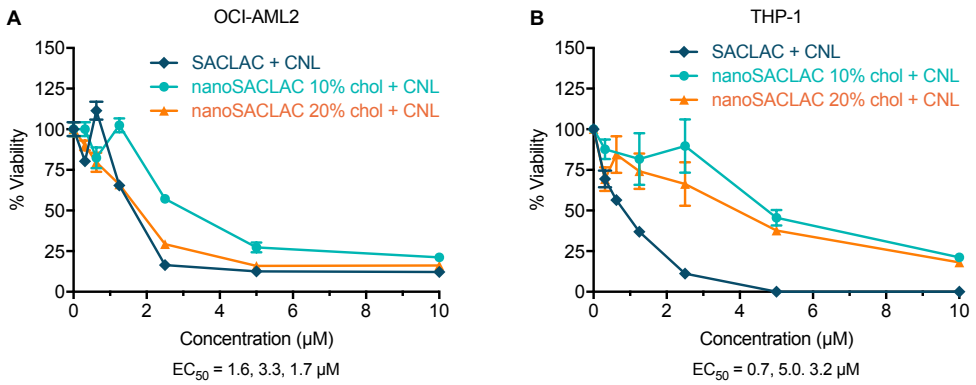

Figure 3.4: Addition of cholesterol does not improve synergy with CNL

A) OCI-AML2 and **B)** THP-1 cells were treated with increasing dose of SACLAC or nanoSACLAC containing either 10% or 20% membrane cholesterol combined with C6 ceramide nanoliposome (CNL) for 24 hours using MTS assay. DMSO was set to 100% viability and ghost nanoliposome (no effect) is not shown. Error bars represent mean +/- SEM from three or more technical replicates. Nanoliposomes were generated by Tye Deering (University of Virginia).

PATIENT CELLS IN SERUM-FREE MEDIA ARE MORE RESPONSIVE TO SACLAC

To determine if the separation between effect of free SACLAC and nanoSACLAC was due to liposomal interaction with serum, one primary patient sample was cultured in media supplemented with cytokines with and without serum. In serum-free media, about 45% more cells underwent apoptosis with nanoSACLAC versus free SACLAC treatment at the highest dose (**Figure 3.5A**). nanoSACLAC-treated cells also reduced viability more drastically than SACLAC-treated cells in serum-free media (**Figure 3.5C**). This pattern did not occur in the presence of 10% FBS (**Figure 3.5B,D**), similar to what was observed in cell lines. These results suggest that nanoliposomal components interact with serum to reduce sensitivity to nanoSACLAC.

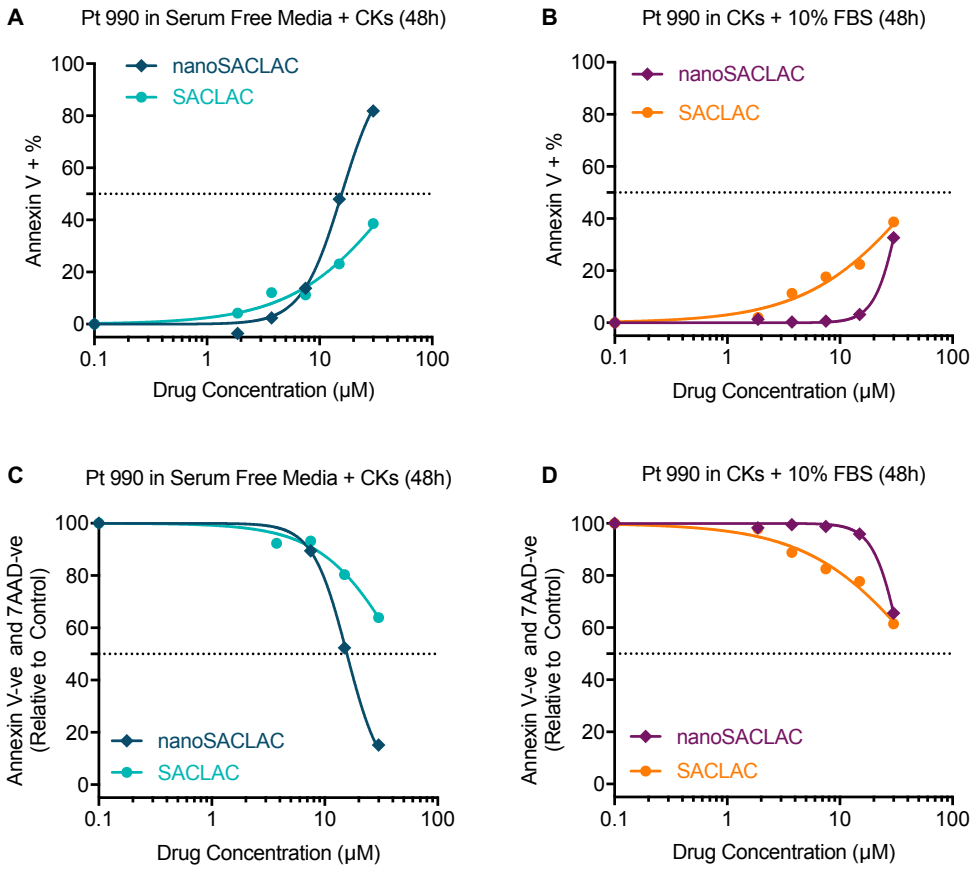

Figure 3.5: Patient cells in serum free media are more responsive to SACLAC

A) Primary patient cells were cultured in SFEM with cytokines (CKs) for 48 hours, treated with SACLAC or nanoSACLAC, and evaluated for apoptosis using Annexin V staining by flow cytometry. **C)** In the same assay, cell viability was evaluated by plotting Annexin V and 7AAD negative cells relative to DMSO control. The same patient cells were treated in the presence of cytokines and 10% fetal bovine serum (FBS) and analyzed for **B)** apoptosis and **D)** viability. DMSO control was set to 100%. This experiment was done by Arati Sharma and Charyguly Annageldiyev (Penn State Hershey). Nanoliposomes were generated by Tye Deering (University of Virginia).

CELL LINES IN REDUCED SERUM ARE MORE SENSITIVE TO NANOSACLAC

In order to see if the results observed in a primary patient sample were consistent with one of the cell lines previously tested, serum concentration was incrementally decreased and viability was measured. With 10% FBS (**Figure 3.6A**), 5 μM nanoSACLAC did not reduce viability while SACLAC killed 75% of HL60/VCR cells. With 5% FBS (**Figure 3.6B**), the difference in toxicity was also around 75%. With 1% FBS (**Figure 3.6C**), nanoSACLAC killed about 60% of cells with 5 μM treatment, a marked improvement from higher serum conditions. Notably, free SACLAC toxicity also improved with lower serum levels, with EC_{50} values decreasing from 3.8 μM with 10% FBS to 0.8 μM with 1% FBS. These results confirm that sensitivity to nanoSACLAC varies in cell lines as well.

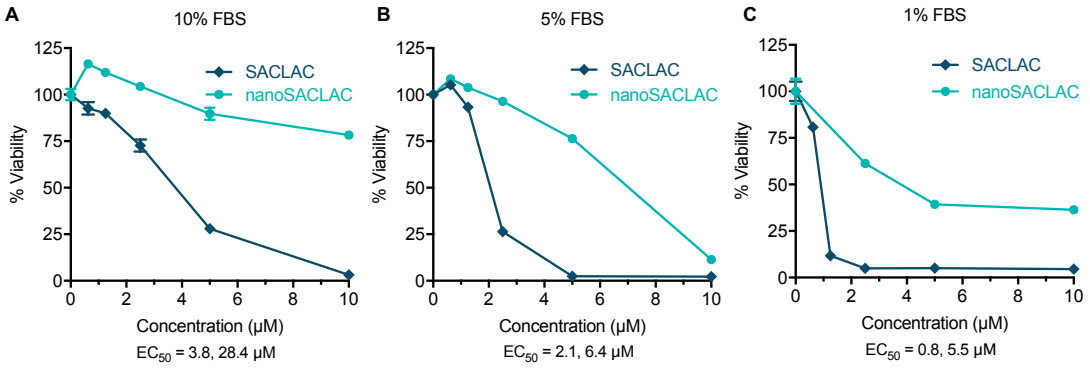

Figure 3.6: Cell lines in reduced serum are more sensitive to nanoSACLAC

A) HL60/VCR cells were treated with SACLAC or nanoSACLAC in RPMI-1640 media with 10%, **B)** 5% or **C)** 1% FBS. Changes in toxicity were measured using MTS assay after 24 hours. DMSO was set to 100% and ghost nanoliposome did not affect viability significantly. Error bars represent mean +/- SEM from three or more technical replicates. Nanoliposomes were generated by Tye Deering (University of Virginia).

SACLAC IS DELIVERED TO BLOOD MORE EFFECTIVELY WHEN USING NANOLIPOSOMES

In order to examine the effects of nanoSACLAC *in vivo*, we first compared the levels of SACLAC in the blood with free SACLAC versus nanoSACLAC (**Figure 3.7**). Free SACLAC delivered intraperitoneally (IP) at 40 mg/kg in DMSO only reached a peak concentration of around 200 nM at 30 minutes after injection. For nanoSACLAC, the dose administered to mice was limited by volume due to low encapsulation efficiency. Regardless, intravenous (IV) injection of 3.3 mg/kg nanoSACLAC led to 1100 nM SACLAC in the blood. The direct administration of nanoSACLAC to the blood and, theoretically, the composition of the nanoliposome improved delivery to the blood 5-fold (200 v. 1100 nM), even with one-tenth the dose administered (40 v. 3.3 mg/kg). DMSO is not a safe vehicle for IV administration, so this condition could not be used for comparison. These data support the use of nanoliposomes for improved bioavailability of poorly soluble compounds.

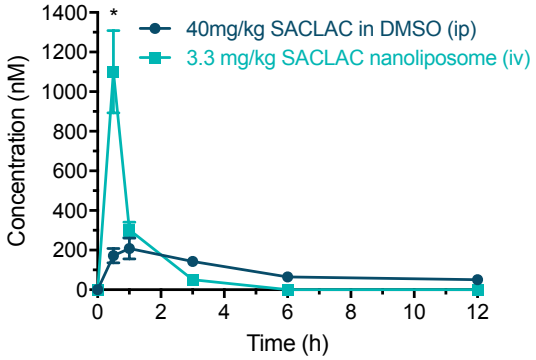

Figure 3.7: SACLAC is delivered to blood more efficiently when using nanoliposomes

SACLAC was administered to three Swiss Webster mice intraperitoneally in DMSO (40 mg/kg) or intravenously in nanoliposomes (3.3 mg/kg). Animals were euthanized at the indicated time points and concentration of SACLAC in the blood was measured by mass spectrometry. Error bars represent mean +/- SEM from three or more technical replicates. This experiment was done by Arati Sharma and Charyguly Annageldiyev (Penn State Hershey) and quantified by Todd Fox (University of Virginia). * $p < 0.05$.

NANOSACLAC REDUCES LEUKEMIC BURDEN IN U937-ENGRAFTED NSG MICE

Although the peak serum concentration of SACLAC in the blood was just above 1 μM when nanoSACLAC was administered, we wanted to determine whether this had an impact on leukemic burden. Immunocompromised mice were engrafted with an aggressively-growing AML cell line and injected with nanoSACLAC or ghost nanoliposome multiple times per week for a total of 12 injections (**Figure 3.8A**). At this point, animals were euthanized due to sickness in both control and treatment groups. However, leukemic burden was decreased about 50% at the cellular level (**Figure 3.8B-C**), indicating that nanoSACLAC may be even more beneficial *in vivo* when conditions are optimized.

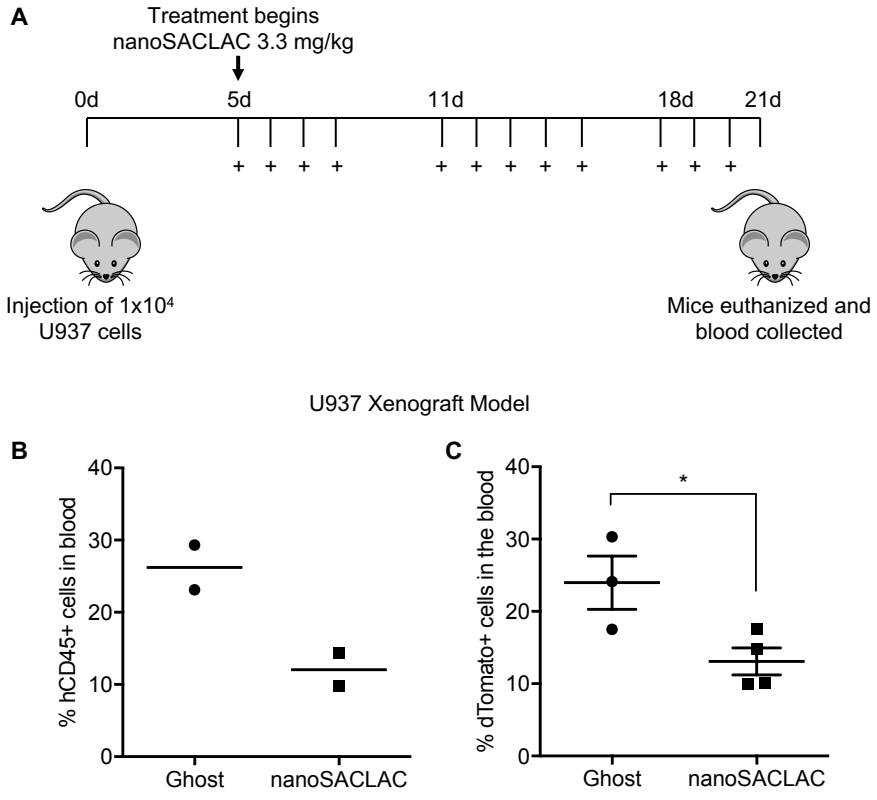

Figure 3.8: nanoSACLAC reduces leukemic burden in U937-engrafted NSG mice

A) NOD-*scid* IL2Rgamma^{null} (NSG) mice (n=5 per group) were injected with 1x10^4 human U937 cells labeled with dTomato-Luc, and engraftment was confirmed by bioluminescence imaging after five days. Each animal received multiple tail-vein injections per week of nanoSACLAC (3.3 mg/kg) or ghost nanoliposome vehicle control. After 12 injections, leukemic burden was measured in blood by flow cytometry staining for **B)** hCD45 and **C)** dTomato markers to identify U937 cells. This experiment was done by Arati Sharma, Charyguly Annageldiyev and Viola Devine (Penn State Hershey). n per group represents number of samples withdrawn from blood with enough volume to measure indicated markers. * $p < 0.05$.

3.4 DISCUSSION

The major contribution of these studies was identification of a nanoliposome formulation that allows safe delivery of SACLAC to mice intravenously. Importantly, optimizing the formulation to include cholesterol reduced serum interactions and restored sensitivity to nanoSACLAC *in vitro* to a level that was comparable to free SACLAC (**Figure 3.3**). Further, we saw that nanoSACLAC delivered SACLAC directly to the blood more efficiently than previous administration routes (Chapter 2, **Figure 3.7**). We observed a 50% decrease in leukemic burden of mice with only 3.3 mg/kg nanoSACLAC administered to mice (**Figure 3.8**).

These studies are limited by poor encapsulation efficiency of SACLAC into nanoliposomes. Maximum concentration of nanoSACLAC achieved in formulation attempts was around 1 μM. This could be attempted by titrating SACLAC input, changing proportion of charged lipids, or altering loading technique (Akbarzadeh et al., 2013; Sercombe et al., 2015).

Interestingly, cell lines differed in the gap between sensitivity to SACLAC and nanoSACLAC (**Figure 3.2**). Sensitivity was improved when cholesterol was added to the nanoliposome, but level of restoration still varied between cell lines (**Figure 3.3**). This suggests that nanoSACLAC efficacy varies in cell lines. This could be affected by how readily different cell lines fuse with other membranes like the nanoliposome. This characteristic could control the amount of SACLAC available to the cell versus SACLAC still encapsulated by nanoliposomes.

Pharmacokinetic studies (**Figure 3.7**) indicate that about 100% of drug injected in nanoliposomes can be delivered to the blood. Although encapsulation efficiency at this stage was low, this method is clearly advantageous over free SACLAC injection with either DMSO or β-HPCD, which had bioavailabilites around 0.05% and 40%, respectively (Chapter 2). The reduction in leukemic burden with nanoSACLAC treatment is modest in terms of remission status, but remarkable with the amount of SACLAC delivered to the animals in the study (~ 1 μM).

While these studies do not completely clarify the clinical potential of SACLAC, we have advanced our knowledge of nanoSACLAC interactions with serum—an essential understanding when target cells are in the blood and bone marrow. Further, we have identified and began optimizing a method of SACLAC *in vivo* delivery that is almost 100% bioavailable. These findings are crucial to moving forward with SACLAC as a potential AML therapeutic.

4 INVESTIGATING SYNERGISM OF THERAPEUTICS TARGETING AC AND BCL-2

ABSTRACT

Acute myeloid leukemia (AML) is the most common adult leukemia with 20,000 new cases and 10,000 deaths each year. Recent treatment advancements have yet to significantly improve survival time for patients. However, ABT-199 (venetoclax) was recently granted breakthrough approval by the FDA as part of a combination treatment for treatment of older adults who are otherwise ineligible for therapy. ABT-199 has also demonstrated preclinical potential in other patient populations. ABT-199 directly inhibits Bcl-2, a known regulator of AML progression and treatment response. As a therapeutic, ABT-199 has several advantages including target specificity, a substantial therapeutic window and oral bioavailability. However, mechanisms of Mcl-1 mediated resistance have already been established. We utilized viability assays, synergy analysis and an *in vivo* mouse model to determine the potential for combination of ABT-199 with ceramide analog SACLAC. While ABT-199 inhibits Bcl-2, SACLAC induces ceramide accumulation and shifts Mcl-1 ratio from anti- to pro-apoptotic. We found that combination treatment is synergistic *in vitro* in cells that require higher doses of ABT-199 (referred to as ABT-199 resistant cells). While *in vivo* studies require further optimization, these studies highlight the potential for SACLAC to combat resistance to ABT-199.

4.1 INTRODUCTION

Acute myeloid leukemia is the most common form of adult leukemia, and over 20,000 new cases are diagnosed each year (Noone et al.). Patients with AML present with fever, fatigue and frequent infections as a result of immature myeloid cells overpopulating the blood and bone marrow. Standard induction therapy (see Chapter 2, Section 1) facilitates remission in a substantial percentage of patients, but the majority of patients relapse (Döhner et al., 2017). Unfortunately, 5-year survival for AML patients is around 27% (Noone et al.). Several emerging treatment strategies have been developed, but as of yet these therapies have not significantly increased survival.

One of the most promising therapeutics recently approved for treatment of AML is ABT-199 (venetoclax). ABT-199 (**Figure 4.1**) is a selective Bcl-2 inhibitor that was first characterized in 2013 with mention in over 700 publications since then (Souers et al., 2013). Importantly, ABT-199 spares normal cells, making it an extremely attractive therapeutic. Additionally, efficacy has been demonstrated in a wide variety of cancer cell types including leukemia, lymphoma, breast cancer and nasopharyngeal carcinoma (Žigart and Časar, 2019). The first FDA approval came in 2016 for chronic lymphocytic leukemia (Cang et al., 2015). ABT-199 was recently granted breakthrough approval for use in elderly AML patients in combination with hypomethylating agents or low dose cytarabine (Aldoss et al., 2018; Luedtke et al., 2017; Teh et al., 2018). This treatment strategy provides a treatment opportunity for older adults who may not be eligible for intensive chemotherapy.

Bcl-2 is the namesake of the Bcl-2 family of proteins which is composed of several important regulators of apoptosis. The expression of these pro- and

anti-apoptotic proteins mediates the delicate balance between cell survival and cell death. In a healthy cell, pro-apoptotic family members (Bim, Bid, Bax, Bak, etc.) are sequestered by anti-apoptotic family members (Mcl-1, Bcl-2, etc.). All of these proteins contain a critical BH3 (Bcl-2 homology 3) domain that allows recognition between proteins and plays a key role in cell death. When any of these proteins is dysregulated, homeostasis is disrupted and unhealthy cells can evade cell death. ABT-199 is a BH3 mimetic that binds to Bcl-2, preventing it from sequestering pro-apoptotic effectors. This allows BH3-only proteins to bind to pro-apoptotic Bax and Bak, leading to mitochondrial depolarization and cell death (Ashkenazi et al., 2017; Kale et al., 2018).

Bcl-2 family proteins have been implicated in leukemia for decades (Kusenda, 1998), and increased expression of Bcl-2 in AML cells is associated with resistance to chemotherapy (Campos et al., 1993). Mcl-1 is also a key regulator of AML cell growth and treatment response (Glaser et al., 2012; Gores and Kaufmann, 2012). Importantly, Mcl-1 can be upregulated as a resistance mechanism in response to Bcl-2 inhibitors like ABT-199. This resistance occurs due to stabilization of Mcl-1 through increased association with Bim when Bcl-2 is competitively inhibited. (Luedtke et al., 2017; Wang et al., 2019).

Bcl-2 family members also cooperate with lipid shifts in the cells to induce apoptosis (Zhang and Saghatelian, 2013; Zhang et al., 2015). Ceramide analog SACLAC (Chapter 2) increases ceramide levels and induces alternative splicing that shifts Mcl-1 from anti- to pro-apoptotic. Given that Bcl-2 cooperates with ceramide changes to induce apoptosis and Bcl-2 inhibitors can develop Mcl-1 mediated resistance, we hypothesized that SACLAC co-treatment with ABT-199 would address these challenges and reveal a promising therapeutic strategy.

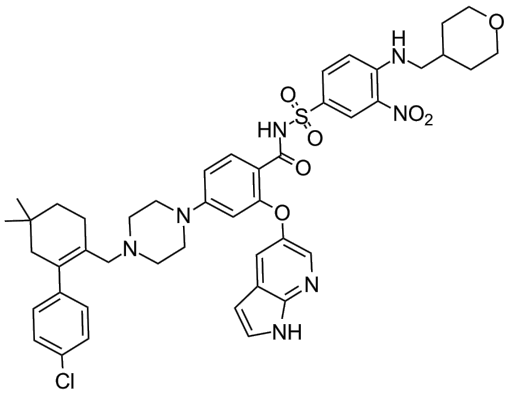

Figure 4.1: Structure of Bcl-2 inhibitor ABT-199

ABT-199 is a novel and specific inhibitor of Bcl-2 maintaining a sub-nanomolar affinity towards Bcl-2 and over three orders of magnitude less affinity towards Bcl-xL (ApexBio Technology).

4.2 MATERIALS AND METHODS

CELL LINES

HL-60/VCR (McGrath et al., 1989), THP-1, MOLM-13, MV4-11 and MM-6 cell lines were maintained in RPMI-1640 (Corning #10-040) with 10% FBS (VWR #97068-085). HL60/VCR cells were supplemented with 1 μg/ml vincristine sulfate (Cayman #11764). These cell lines were obtained from ATCC unless otherwise specified.

COMPOUNDS

SACLAC *N*-[(2*S*,3*R*)-1,3-dihydroxyoctadecan-2-yl]2-chloroacetamide was synthesized as previously described (IQAC-CSIC) (Ordóñez et al., 2019). The structure was validated using mass spectrometry. 2-hydroxypropyl β-cyclodextrin (β-HPCD) was obtained from Acros Organics (#297561000). ABT-199 was obtained from Selleckchem (#S8048).

CELL VIABILITY ASSAY

For cell viability, cell lines were plated at 2.5 x 10^4 cells per well in a 96-well plate and treated with ABT-199, SACLAC, combination or DMSO vehicle (0.4% of total volume) for the indicated time points and doses. At the experiment end point, 3-(4,5-Dimethylthiazol-2-yl)-5-(3-carboxymethoxyphenyl)-2-(4-sulfophenyl)-2H-tetrazolium (MTS) Cell Proliferation Colorimetric Assay Kit (BioVision #K300-5000) reagent was added and incubated for 2 hours. Conversion of MTS to formazan product was measured by absorbance at 490 nm using a BioTek Cytation 3 plate reader. Absorbance was normalized to DMSO control, which was defined as 100% viability.

WESTERN BLOTTING

Cells were plated at 1 x 10^6 cells per ml in 6-well plates and treated with drug, vehicle or siRNA at the indicated doses and time points. Cells were harvested, washed with PBS, then lysed with RIPA buffer (Sigma #R0278) containing phosphatase inhibitor cocktails 2 and 3 (Sigma #P5726, #P0044) and protease inhibitor cocktail (Sigma #P8340). Protein was quantified using a bicinchoninic acid (BCA) protein assay kit (Pierce #23225). Samples were resolved on a Bolt 4-12% SDS-PAGE gel (ThermoFisher #NW00082) and transferred to PVDF membrane (Bio-Rad #170-4274). Antibodies were obtained from Cell Signaling Technology unless indicated otherwise. Primary antibodies used were: Mcl-1 (#5453), β-actin (#3700) and AC (BD Biosciences #612302). Secondary antibodies used were HRP-linked goat anti-mouse (#7076) or goat anti-rabbit IgG (#7074). Clarity Max Western ECL Substrate (Bio-Rad #1705062) was added to visualize relative protein expression by chemiluminescence using the Bio-Rad ChemiDoc MP imaging system. Quantification was done using Bio-Rad ImageLab 6.0.1 software. For quantification, bands were normalized to β-actin as a loading control.

TRANSFECTION WITH SIRNA BY ELECTROPORATION

KG1a cells were electroporated with non-targeting scrambled siRNA (Dharmacon #D-001810-10-20), siRNA targeting *ASAH1* (AC) (Dharmacon #L-005228-03-0010) using the Neon Transfection System (Invitrogen) according to the manufacturer's protocol with the following parameters: 3 x 10^7 cells per ml, 1700 pulse voltage, and 20 ms pulse width for a single pulse. AC knockdown cells were harvested 48 hours after transfection for analysis by western blot. To assess viability, 24 hours after electroporation AC knockdown cells were diluted 1:2 in fresh media then treated with ABT-199 then plated for viability assay as described previously. Control- and ABT-199-treated cells were harvested 48 hours after treatment, corresponding to 72 hours after electroporation.

LENTIVIRAL TRANSDUCTION OF CDNA CLONES

AC-expressing plasmid pLOC-ASAH1 was purchased from Open Biosystems (Thermo Scientific) and pLKO.1-ASAH1 containing AC shRNA and pLKO.1-GFP control were purchased from Mission (SigmaAldrich). Plasmids were transfected into HEK293 T/17 cells with lentiviral packaging plasmids (Invitrogen). Viral supernatant was collected after 48 and 72 hours and filtered using a 0.45 μm-filter syringe. Cells were transduced with viral supernatant plus 6 μg/ml polybrene every 12 hours for three days. Transduced cells with pLOC-ASAH1 were selected with 6 μg/ml Blasticidin S for 12 days. Lysates were harvested 72 hours post-transduction for AC knockdown and 72 hours after stable selection for AC overexpression.

***IN VIVO* AML XENOGRAFT MODEL**

Maximum tolerated dose of SACLAC was determined in NOD-*scid* IL2Rgamma^{null} (NSG) mice (*n*=5; Jackson Laboratories). Mice were injected

with SACLAC reconstituted in β-HPCD (IV) or ABT-199 (PO) daily for 5 days at a dose of 5 mg/kg or 100 mg/kg body weight, respectively.

To assess the efficacy of ABT-199 and SACLAC combination in a transplantable human AML model, 1 x 10^4 luciferase and tdTomato-expressing U937 cells in HBSS were introduced into 6- to 8-week-old female NSG mice via tail-vein injections. After six days, engraftment was confirmed as stated above. Mice were equally randomized into two groups of five mice and treated with control, ABT-199 (100 mg/kg), SACLAC (5 mg/kg) or both five times per week for 15 total injections. Animals were euthanized and bone marrow was collected for flow cytometry analysis.

Red blood cells (RBC) were lysed with RBC Lysis Buffer (BioLegend #420301) followed by cell surface staining with anti-human CD45 antibodies (BioLegend #304014, clone HI30) and 7-AAD (BioLegend #420404) to detect viable human white blood cells (WBC) using an LSR II flow cytometer and BD FACS Diva software at the Penn State College of Medicine Flow Cytometry Core. Viable cells were identified by gating on 7-AAD-negative cells gated from singlets (SSC-A and FSC-W scales), after excluding the debris (SSC-A and FSC-A scales). Percentage of tdTomato positive cells was determined in FlowJo software (Becton Dickinson). All animal studies were performed with IACUC approval (PRAMS201246746).

STATISTICAL ANALYSIS

Significance between two treatment groups from a single experiment was determined by the two-tailed unpaired *t*-test using the GraphPad Prism 7.0 software. Error bars represent standard error of the mean (SEM) from three or more technical replicates.

4.3 RESULTS

AC KNOCKDOWN INCREASES SENSITIVITY TO ABT-199 TREATMENT

In order to determine if AC level is related to ABT-199 sensitivity, AC was knocked down using siRNA in KG1a cells. Knockdown was efficient, with a 77% reduction in AC protein (**Figure 4.2A**). Mcl-1 levels were not affected. Cells treated with scrambled siRNA or AC siRNA were treated with increasing doses of ABT-199 for comparison. AC knockdown cells were more sensitive to ABT-199 treatment by about 20% (**Figure 4.2B**). This suggests that reduced AC levels make AML cells more vulnerable to ABT-199 treatment.

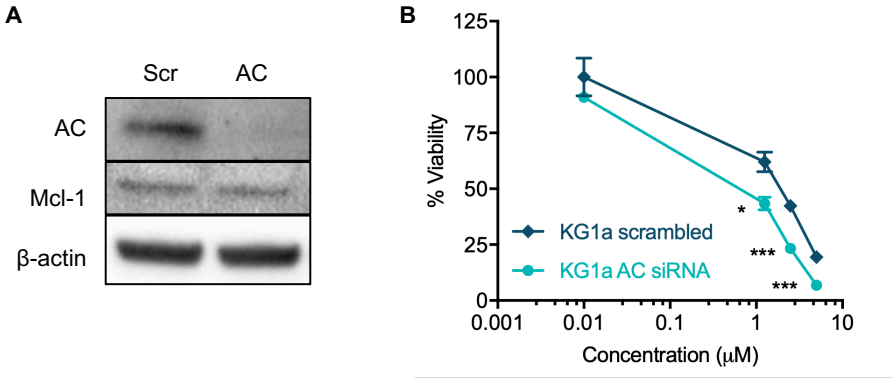

Figure 4.2: AC knockdown increases sensitivity to ABT-199 treatment

A) KG1a human AML cells were electroporated with 50 nM scrambled siRNA or siRNA targeting ASAH1/AC and harvested after 48 hours. Levels of AC and Mcl-1 were determined by western blot with β-actin as the loading control. **B)** AC knockdown cells were treated with increasing doses of ABT-199 for 24 hours and change in viability was observed using MTS assay. * $p < 0.05$, *** $p < 0.001$.

AC OVEREXPRESSION REDUCES SENSITIVITY TO ABT-199

To reinforce the hypothesis that AC level plays a role in ABT-199 sensitivity, THP-1 cells were generated that overexpress AC or RFP control. Increase in AC protein was verified by western blot (**Figure 4.3A**). Mcl-1 protein also increased about 2-fold. Combined, these protein changes led to a 25% decrease in sensitivity to ABT-199 (**Figure 4.3B**). These data suggest that increased AC and corresponding increase in Mcl-1 contribute to resistance to ABT-199 treatment.

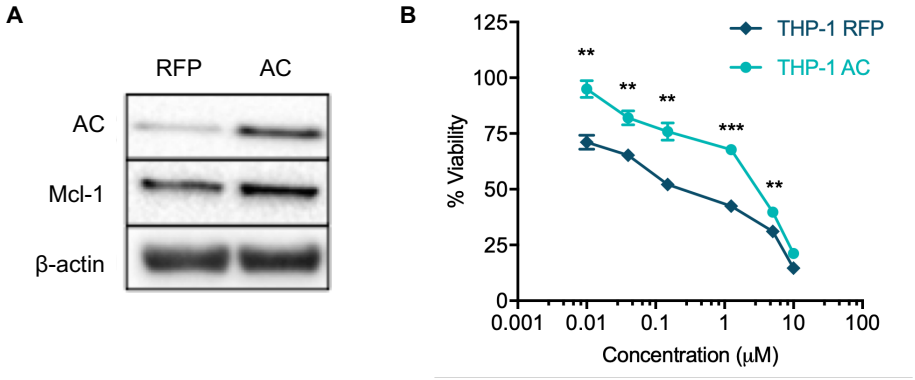

Figure 4.3: AC overexpression reduces sensitivity to ABT-199

A) THP-1 human AML cells were transduced with lentivirus containing RFP or AC ORFs and harvested after 72 hours. Levels of AC and Mcl-1 were determined by western blot with β-actin as the loading control. **B)** AC knockdown cells were treated with increasing doses of ABT-199 for 24 hours and change in viability was observed using MTS assay. ** $p < 0.01$, *** $p < 0.001$. Su-Fern Tan (University of Virginia) generated the AC overexpression cell line and the western blot.

AML CELL LINES CAN BE STRATIFIED AS ABT-199 SENSITIVE OR RESISTANT

Next, we investigated the baseline sensitivity of four AML cell lines to determine the proper dose range of ABT-199 for subsequent studies. We found that these cell lines could be separated into two groups—sensitive or "resistant"—based on the dose required for cytotoxicity. MOLM-13 and MV4-11 cells only required nanomolar doses of ABT-199 to reduce viability at 24 and 48 hours post-treatment (**Figure 4.4A,B**). On the other hand, ABT-199 had no effect on HL60/VCR and MM-6 cells at nanomolar doses but instead required micromolar doses for toxicity at 24 and 48 hours post-treatment (**Figure 4.4C,D**). Strikingly, the difference in sensitivity of sensitive versus "resistant" cell lines was 100-fold. It is important to note that "resistant" is used as a comparative term which describes this large fold change between groups and does not indicate that cells are not responsive to ABT-199 at all.

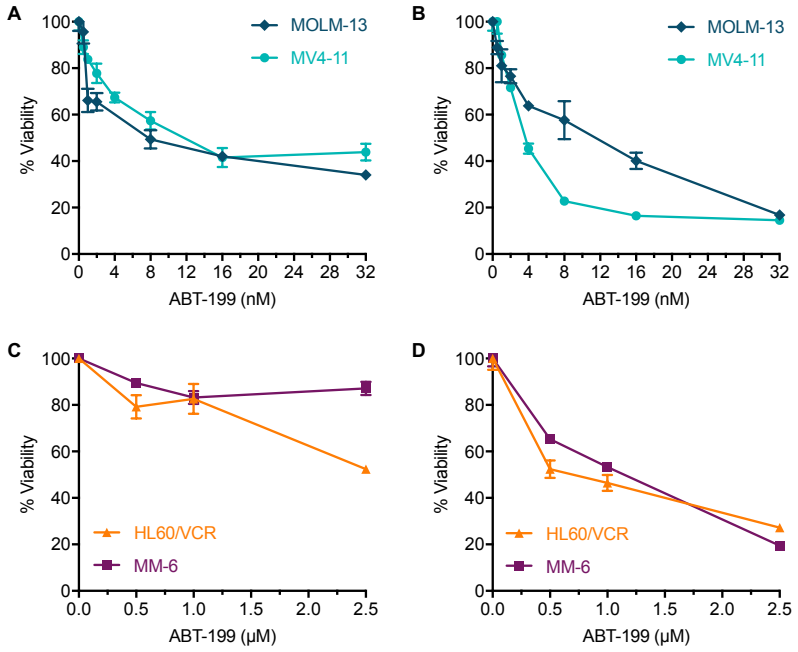

Figure 4.4: AML cell lines can be stratified as ABT-199 sensitive or resistant

MOLM-13 and MV4-11 human AML cell lines were treated with increasing nanomolar doses of ABT-199 for **A)** 24 or **B)** 48 hours. HL60/VCR and MM-6 human AML cell lines were treated with increasing micromolar doses of ABT-199 for **C)** 24 or **D)** 48 hours. Sensitivity of cell lines to ABT-199 treatment was determined using MTS assay with viability as the readout. Assays with HL60/VCR and MM-6 were performed by Bhavishya Ramamoothy and Irene Lee (University of Virginia).

SACLAC SENSITIZES RESISTANT CELL LINES TO ABT-199

Since it has been established that SACLAC inhibits AC and alters Mcl-1 ratio (Chapter 2), we examined the effects of combination treatment with SACLAC and ABT-199. In sensitive cell lines MOLM-13 (**Figure 4.5A**) and MV4-11 (**Figure 4.5B**), viability was not significantly reduced with combination treatment over individual treatment with either drug. However, there was a pronounced increase in cell death with SACLAC and ABT-199 combination in resistant cell lines HL60/VCR (**Figure 4.5C**) and MM-6 (**Figure 4.5D**). This suggests that SACLAC is beneficial for sensitizing resistant cells to ABT-199 treatment.

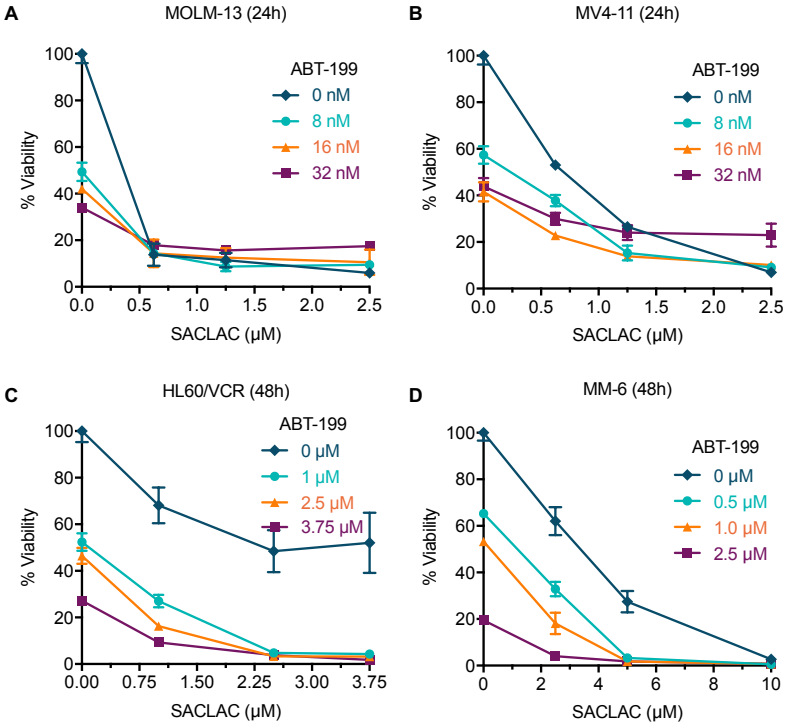

Figure 4.5: SACLAC sensitizes resistant cell lines to ABT-199

A) MOLM-13 and **B)** MV4-11 human AML cell lines were treated with a combination of SACLAC and ABT-199 over 24 hours. **C)** HL60/VCR and **D)** MM-6 were treated with a combination of SACLAC and ABT-199 over 48 hours. Viability was analyzed using MTS assay. Combination treatments for HL60/VCR and MM-6 were performed by Bhavishya Ramamoothy and Irene Lee (University of Virginia).

SACLAC IS SYNERGISTIC WITH ABT-199 IN RESISTANT CELL LINES

In order to determine if SACLAC and ABT-199 combination treatment is additive or synergistic, synergy analysis was done using CompuSyn Software (ComboSyn, Inc). For sensitive cell lines MOLM-13 (**Figure 4.6A**) and MV4-11 (**Figure 4.6B**), the average combination index (CI) was around 1, indicating additivity. The resistant cell line HL60/VCR (**Figure 4.6C**) had an average CI value below 0.25, indicating strong synergism and MM-6 had an average of 0.6, indicating synergism (**Figure 4.6D**). These data encourage the use of SACLAC to improve toxicity of ABT-199 in resistant cell lines.

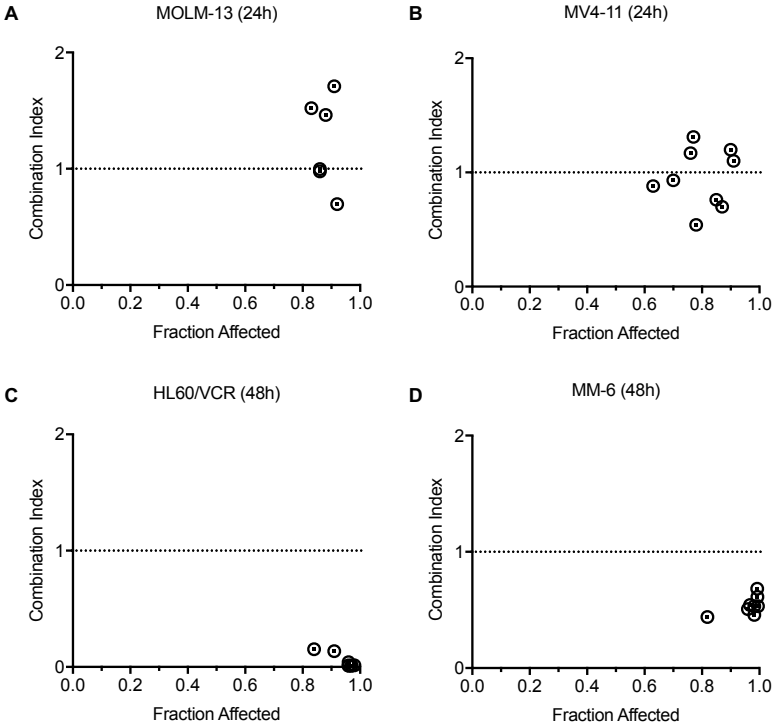

Figure 4.6: SACLAC is synergistic with ABT-199 in resistant cell lines

Synergy analysis of SACLAC and ABT-199 combination treatments was performed using CompuSyn software. Combination Index (CI) < 1 indicates synergy. CI = 1 indicates additivity, and CI > 1 indicates antagonism. Each data point represents the CI of one condition. **A)** MOLM-13 and **B)** MV4-11 analysis was done on 24-hour combination treatments while **C)** HL60/VCR and **D)** MM-6 analysis was done at 48 hours post-treatment.

COMBINATION OF SACLAC AND ABT-199 DOES NOT IMPROVE EFFICACY IN U937-ENGRAFTED NSG MICE

Ultimately, we wanted to determine if combination treatment provides therapeutic benefit. We first confirmed that our maximum deliverable dose did not exceed a tolerable dose for the animals (data not shown). Then, NOD-*scid* IL2Rgamma^{null} (NSG) immunodeficient mice were engrafted with human U937 AML cells and then treated daily with 5 mg/kg SACLAC, 100 mg/kg ABT-199 or both (**Figure 4.7A**). Luciferase signal was tracked over time to visualize leukemic cell expansion. Margin of error was high and there were no significant radiance changes between control and treatment groups (**Figure 4.7B**). At termination of the study, circulating leukemic cells in the blood were counted using flow cytometry. SACLAC and ABT-199 treatment both resulted in a significant decrease in leukemic burden, about 50% and 70% respectively. However, combination treatment did not reduce leukemic burden beyond the level that individual treatments achieved (**Figure 4.7C**).

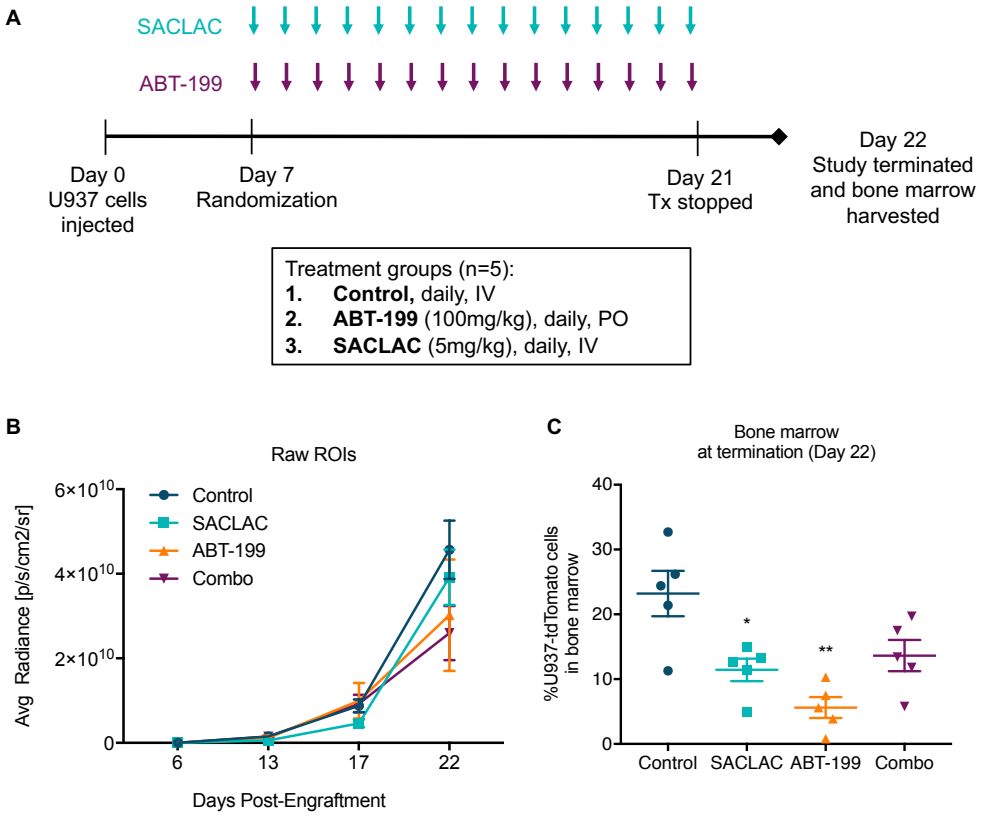

Figure 4.7: Combination of SACLAC and ABT-199 does not improve efficacy in U937-engrafted NSG mice

A) NOD-*scid* IL2Rgamma^{null} (NSG) mice (n=5 per group) were injected with 1x10^4 human U937 cells labeled with tdTomato-Luc, and engraftment was confirmed by bioluminescence imaging after one week. Each animal received SACLAC via tail-vein injection (5 mg/kg SACLAC in 45% w/v 2-hydroxypropyl-β-cyclodextrin in PBS), ABT-199 orally (100 mg/kg), both, or vehicle control five times per week. **B)** *In vivo* imaging was used to measure change in radiance (overall disease burden) throughout the treatment period. After 15 injections, leukemic burden was measured by flow cytometry staining for C**)** tdTomato markers to identify U937 cells in bone marrow. * $p < 0.05$, ** $p < 0.01$. Mouse studies were performed by Arati Sharma, Charyguly Annageldiyev and Viola Devine (Penn State Hershey).

4.4 DISCUSSION

Our studies identified a potential combination therapy for use in AML that combats known mechanisms of resistance. We first established that sensitivity to ABT-199 may be impacted by AC levels (**Figure 4.2, Figure 4.3**). This creates a therapeutic vulnerability that we strategically targeted with AC inhibitor SACLAC (Chapter 2). Importantly, the combination of ABT-199 and SACLAC worked particularly well *in vitro* in cells that were not as sensitive to ABT-199 alone (**Figure 4.6**), suggesting that combination with SACLAC may facilitate a broader response to ABT-199.

In order to determine the full extent of AC involvement in ABT-199 sensitivity, further experiments would include measuring AC activity in cell lines with ABT-199 and combination treatment with SACLAC. Further investigation of protein changes would highlight Mcl-1 change in response to ABT-199 and any attenuation of this signal with SACLAC combination treatment. It would be particularly interesting to examine these protein changes in both ABT-sensitive and -"resistant" cell lines. This may reveal the mechanism behind lack of synergy in cell lines that are already generally sensitive to ABT-199.

Additionally, it would be interesting to ask these questions in a set of patient samples. This could reveal patient characteristics that contribute to ABT-199 resistance and clarify whether AC levels play a role in this resistance. In a large patient cohort, these studies could also predict percentage of patients that would respond to ABT-199 and/or combination treatment.

While we did find that combination treatment was efficacious *in vitro* in cell lines that were less sensitive to ABT-199, we did not see an improvement in any

parameters measures in the *in vivo* combination group. The first potential explanation for this is the cell line model used. The U937 cell line has been studied by other groups and falls into the category of ABT-199 resistant cells. Our sample size for ABT-199 resistant cell lines was small (n=2), so the synergy of SACLAC and ABT-199 in resistant cell lines may not be universal. Expanding combination treatment to more cell line, both sensitive and resistant, would help strengthen our studies. More likely, the doses administered in the *in vivo* studies could be unrealistic when trying to resolve synergy between two compounds. It was not surprising that ABT-199 was slightly more efficacious than SACLAC, especially considering that 20-times more ABT-199 was administered to the mice. With the current formulation of SACLAC, a lower dose of ABT-199 (potentially 10 or 20 mg/kg) may reveal synergy, but ultimately reformulation of SACLAC is necessary to fully understand the *in vivo* impact of this combination.

Since ABT-199 is safe and orally bioavailable and SACLAC is poorly soluble, this combination approach may alleviate the need to drastically increase SACLAC solubility for *in vivo* delivery. Even though reformulation is necessary to determine if the combination can be synergistic *in vivo*, combination therapies generally require lower doses of individual drugs. Even a 2-fold increase in SACLAC dose may clarify this relationship since low micromolar doses were synergistic in *in vitro* studies (**Figure 4.5**).

Overall, our studies present a promising correlation between AC protein levels and ABT-199 sensitivity. Most importantly, cell lines that are resistant to ABT-199 become sensitized when SACLAC is added. Expansion of these studies may present a novel prognostic factor for ABT-199 treated patients and a strategy to combat resistance.

5 CONCLUSION

5.1 CONCLUSION

The limitations of current and emerging treatment strategies for acute myeloid leukemia (AML) is a major concern, and characterization of potential therapeutics is critical to informing therapeutic design. These studies present several contributions to the field by characterizing a novel compound, optimizing delivery methods and initiating informed combination studies.

In Chapter 2, a novel AC inhibitor SACLAC was characterized. We found that SACLAC effectively inhibits AC and increases ceramide levels. These changes are complemented by SACLAC-induced alternative splicing of Mcl-1. This splicing event shifts Mcl-1 from an anti-apoptotic to a pro-apoptotic ratio. Further, SACLAC treatment reduced leukemic burden in two *in vivo* mouse models. These findings advance the field by characterizing a novel AC inhibitor that alters mRNA splicing in AML cells.

In Chapter 3, we initiated optimization of nanoliposomes for delivery of SACLAC and dramatically improved bioavailability. We found that the original nanoSACLAC formulation interacts with serum, diminishing its potency. Addition of cholesterol to the nanoliposome improved potency *in vitro*, indicating that this interaction can be attenuated with exchange of liposome components. These findings reveal strategies for improved delivery of lipid-based therapeutics.

Finally, Chapter 4 describes investigating synergy between the recently approved Bcl-2 inhibitor ABT-199 and SACLAC. We demonstrated that AML cell lines can be stratified as sensitive or resistant to ABT-199, and ABT-199 sensitivity may be related to acid ceramidase (AC) expression. Importantly,

SACLAC can sensitize ABT-199 resistant cells. These findings highlight the potential for SACLAC to inform strategies for combatting ABT-199 resistance.

5.2 LIMITATIONS

Although these findings are novel and interesting, there are several limitations to consider when evaluating these data and conclusions. The primary limitations of these studies are the inherently difficult properties of SACLAC: low solubility and short half-life. Because SACLAC has a long carbon chain, it is poorly soluble in common *in vivo* vehicles. We identified a vehicle safe for *in vivo* delivery, but were still only able to administer 5 mg/kg SACLAC to mice. However, we had to administer SACLAC daily via tail-vein injection which is cannot be humanely sustained long-term. For these reasons, our *in vivo* data with SACLAC does not fully elucidate the potential for SACLAC as a therapeutic.

Another limitation of these studies is different doses required to induce apoptosis in some cell lines and patient samples. While some of this concern can be alleviated by considering variability between cell lines and patient culture conditions, we had hoped that response to SACLAC would be more "universal" than many existing targeted therapeutics. It is also possible that the effects seen with higher SACLAC doses are off-target. This could indicate that AC inhibition sensitizes these cells to ceramide and alternative splicing rather than being the upstream initiator.

There are several limitations in the process of reformulating SACLAC. The most prevalent is the encapsulation efficiency of the existing method. Titration of increasing SACLAC mass with a fixed amount of lipids did not result in

linear increase in nanoSACLAC concentration. Instead, the maximum encapsulation translated to a concentration of about 1 μM. This is similar to the concentration achieved with SACLAC in β-HPCD used in Chapter 2. Surprisingly, these concentrations were still useful for *in vivo* studies, indicating that cells may be more sensitive to SACLAC *in vivo*, but there was no survival benefit in any of these studies.

Overall, SACLAC currently exists as a tool compound rather than a potential therapeutic unless these processes can be optimized for improved *in vivo* delivery.

5.3 FUTURE DIRECTIONS

In order to address these issues, there are several key experiments that could be done in the future. *In vitro*, the dosing discrepancy could be examined using current versus fresh batches of SACLAC from each source used throughout the course of these studies. This may reveal that SACLAC stability is altered over time and clarify higher doses used in later studies. Additionally, it may be interesting to investigate the mechanism of action of SACLAC analogs. This could be particularly useful if increased doses of SACLAC do not provide an appropriate therapeutic window for advancement.

Mechanistically, there are some interesting leads that could reveal more clinical relevance for SACLAC. Some AML patients have mutations in spliceosome machinery, so it would be valuable to study SACLAC treatment in patients cells with and without these mutations. For combination treatments with SACLAC and ABT-199, it would be useful to expand studies to more cell lines and even to patient samples. This could clarify the correlation between AC

levels and ABT-199 and also determine the prevalence of SACLAC sensitization in ABT-199 resistant cells.

For nanoSACLAC formulations, there are some methods that could be used to improve encapsulation. In addition to titrating SACLAC input, changing proportion of charged lipids and altering loading technique could be beneficial (Akbarzadeh et al., 2013; Sercombe et al., 2015). Alternatively, there is opportunity to pursue a collaboration with Virginia Tech to create and test SACLAC nanopolymers. These polymers can be fine-tuned to the structure of SACLAC in order to resolve issues with solubility.

Overall, we demonstrated that SACLAC is a novel AC inhibitor that increases ceramides and induces alternative splicing of Mcl-1 to kill AML cells. Additionally, *in vivo* delivery of nanoSACLAC can be improved with nanoliposomes. Finally, SACLAC sensitizes cells that are resistant to ABT-199, creating an opportunity to combat resistance to an emerging clinical therapeutic. This work contributes advanced understanding of a new AC-targeting therapeutic and the various implications for its preclinical potential.

6 REFERENCES

Akbarzadeh, A., Rezaei-Sadabady, R., Davaran, S., Joo, S.W., Zarghami, N., Hanifehpour, Y., Samiei, M., Kouhi, M., and Nejati-Koshki, K. (2013). Liposome: classification, preparation, and applications. Nanoscale Res Lett *8*, 102.

Aldoss, I., Yang, D., Aribi, A., Ali, H., Sandhu, K., Al Malki, M.M., Mei, M., Salhotra, A., Khaled, S., Nakamura, R., et al. (2018). Efficacy of the combination of venetoclax and hypomethylating agents in relapsed/refractory acute myeloid leukemia. Haematologica *103*, e404–e407.

American Cancer Society Acute Myeloid Leukemia (AML) Subtypes and Prognostic Factors.

Arber, D.A., Orazi, A., Hasserjian, R., Thiele, J., Borowitz, M.J., Beau, M.M.L., Bloomfield, C.D., Cazzola, M., and Vardiman, J.W. (2016). The 2016 revision to the World Health Organization classification of myeloid neoplasms and acute leukemia. Blood *127*, 2391–2405.

Ashkenazi, A., Fairbrother, W.J., Leverson, J.D., and Souers, A.J. (2017). From basic apoptosis discoveries to advanced selective BCL-2 family inhibitors. Nature Reviews Drug Discovery *16*, 273–284.

Bae, J., Leo, C.P., Hsu, S.Y., and Hsueh, A.J.W. (2000). MCL-1S, a Splicing Variant of the Antiapoptotic BCL-2 Family Member MCL-1, Encodes a Proapoptotic Protein Possessing Only the BH3 Domain. Journal of Biological Chemistry *275*, 25255–25261.

Bai, A., Szulc, Z.M., Bielawski, J., Mayroo, N., Liu, X., Norris, J., Hannun, Y.A., and Bielawska, A. (2009). Synthesis and bioevaluation of ω-N-amino analogs of B13. Bioorg Med Chem *17*, 1840–1848.

Bai, A., Szulc, Z.M., Bielawski, J., Pierce, J.S., Rembiesa, B., Terzieva, S., Mao, C., Xu, R., Wu, B., Clarke, C.J., et al. (2014). Targeting (cellular) lysosomal acid ceramidase by B13: design, synthesis and evaluation of novel DMG-B13 ester prodrugs. Bioorg. Med. Chem. *22*, 6933–6944.

Bielawska, A., Linardic, C.M., and Hannun, Y.A. (1992). Ceramide-mediated biology. Determination of structural and stereospecific requirements through the use of N-acyl-phenylaminoalcohol analogs. J. Biol. Chem. *267*, 18493–18497.

Brown, T.J., Garcia, A.M., Kissinger, L.N., Shanmugavel, S.S., Wang, X., Cabot, M.C., Kester, M., Claxton, D.F., and Barth, B.M. (2013). Therapeutic Combination of Nanoliposomal Safingol and Nanoliposomal Ceramide for Acute Myeloid Leukemia. p.

Buckley, S.A., Othus, M., Estey, E.H., and Walter, R.B. (2015). The treatment-related mortality score is associated with non-fatal adverse events following intensive AML induction chemotherapy. Blood Cancer J *5*, e276.

Burrell, R.A., and Swanton, C. (2014). Tumour heterogeneity and the evolution of polyclonal drug resistance. Molecular Oncology *8*, 1095–1111.

Camacho, L., Meca-Cortés, O., Abad, J.L., García, S., Rubio, N., Díaz, A., Celià-Terrassa, T., Cingolani, F., Bermudo, R., Fernández, P.L., et al. (2013). Acid ceramidase as a therapeutic target in metastatic prostate cancer. J. Lipid Res. *54*, 1207–1220.

Campos, L., Rouault, J.P., Sabido, O., Oriol, P., Roubi, N., Vasselon, C., Archimbaud, E., Magaud, J.P., and Guyotat, D. (1993). High expression of bcl-2 protein in acute myeloid leukemia cells is associated with poor response to chemotherapy. Blood *81*, 3091–3096.

Cancer Genome Atlas Research Network, Ley, T.J., Miller, C., Ding, L., Raphael, B.J., Mungall, A.J., Robertson, A.G., Hoadley, K., Triche, T.J., Laird, P.W., et al. (2013). Genomic and epigenomic landscapes of adult de novo acute myeloid leukemia. N. Engl. J. Med. *368*, 2059–2074.

Cang, S., Iragavarapu, C., Savooji, J., Song, Y., and Liu, D. (2015). ABT-199 (venetoclax) and BCL-2 inhibitors in clinical development. J Hematol Oncol *8*, 129.

Castelli, G., Pelosi, E., and Testa, U. (2018). Targeting histone methyltransferase and demethylase in acute myeloid leukemia therapy. Onco Targets Ther *11*, 131–155.

Chittenden, T. (2002). BH3 domains: intracellular death-ligands critical for initiating apoptosis. Cancer Cell *2*, 165–166.

Coant, N., Sakamoto, W., Mao, C., and Hannun, Y.A. (2017). Ceramidases, roles in sphingolipid metabolism and in health and disease. Adv Biol Regul *63*, 122–131.

Colombini, M. (2017). Ceramide channels and mitochondrial outer membrane permeability. J. Bioenerg. Biomembr. *49*, 57–64.

Cortes, J., Perl, A.E., Döhner, H., Kantarjian, H., Martinelli, G., Kovacsovics, T., Rousselot, P., Steffen, B., Dombret, H., Estey, E., et al. (2018). Quizartinib, an FLT3 inhibitor, as monotherapy in patients with relapsed or refractory acute myeloid leukaemia: an open-label, multicentre, single-arm, phase 2 trial. The Lancet Oncology *19*, 889–903.

Cortes, J.E., Heidel, F.H., Hellmann, A., Fiedler, W., Smith, B.D., Robak, T., Montesinos, P., Pollyea, D.A., DesJardins, P., Ottmann, O., et al. (2019). Randomized comparison of low dose cytarabine with or without glasdegib in patients with newly diagnosed acute myeloid leukemia or high-risk myelodysplastic syndrome. Leukemia *33*, 379–389.

Crews, L.A., Balaian, L., Delos Santos, N.P., Leu, H.S., Court, A.C., Lazzari, E., Sadarangani, A., Zipeto, M.A., La Clair, J.J., Villa, R., et al. (2016). RNA Splicing Modulation Selectively Impairs Leukemia Stem Cell Maintenance in Secondary Human AML. Cell Stem Cell *19*, 599–612.

Damen, J., Regts, J., and Scherphof, G. (1981). Transfer and exchange of phospholipid between small unilamellar liposomes and rat plasma high density lipoproteins Dependence on cholesterol content and phospholipid composition. Biochimica et Biophysica Acta (BBA) - Lipids and Lipid Metabolism *665*, 538–545.

Daniele, S., Taliani, S., Da Pozzo, E., Giacomelli, C., Costa, B., Trincavelli, M.L., Rossi, L., La Pietra, V., Barresi, E., Carotenuto, A., et al. (2014). Apoptosis Therapy in Cancer: The First Single-molecule Co-activating p53 and the Translocator Protein in Glioblastoma. Sci Rep *4*.

Dany, M., Gencer, S., Nganga, R., Thomas, R.J., Oleinik, N., Baron, K.D., Szulc, Z.M., Ruvolo, P., Kornblau, S., Andreeff, M., et al. (2016). Targeting FLT3-ITD signaling mediates ceramide-dependent mitophagy and attenuates drug resistance in AML. Blood *128*, 1944–1958.

De Kouchkovsky, I., and Abdul-Hay, M. (2016). Acute myeloid leukemia: a comprehensive review and 2016 update. Blood Cancer J *6*, e441.

Devillier, R., Mansat-De Mas, V., Gelsi-Boyer, V., Demur, C., Murati, A., Corre, J., Prebet, T., Bertoli, S., Brecqueville, M., Arnoulet, C., et al. (2015). Role of ASXL1 and TP53 mutations in the molecular classification and prognosis of acute myeloid leukemias with myelodysplasia-related changes. Oncotarget *6*, 8388–8396.

Dhillon, S. (2019). Gilteritinib: First Global Approval. Drugs *79*, 331–339.

DiNardo, C.D., Pratz, K., Pullarkat, V., Jonas, B.A., Arellano, M., Becker, P.S., Frankfurt, O., Konopleva, M., Wei, A.H., Kantarjian, H.M., et al. (2019). Venetoclax combined with decitabine or azacitidine in treatment-naive, elderly patients with acute myeloid leukemia. Blood *133*, 7–17.

Döhner, H., Estey, E., Grimwade, D., Amadori, S., Appelbaum, F.R., Büchner, T., Dombret, H., Ebert, B.L., Fenaux, P., Larson, R.A., et al. (2017). Diagnosis and management of AML in adults: 2017 ELN recommendations from an international expert panel. Blood *129*, 424–447.

Doi, K., Liu, Q., Gowda, K., Barth, B.M., Claxton, D., Amin, S., Loughran, T.P., and Wang, H.-G. (2014). Maritoclax induces apoptosis in acute myeloid leukemia cells with elevated Mcl-1 expression. Cancer Biol. Ther. *15*, 1077–1086.

Dolatshad, H., Pellagatti, A., Fernandez-Mercado, M., Yip, B.H., Malcovati, L., Attwood, M., Przychodzen, B., Sahgal, N., Kanapin, A.A., Lockstone, H., et al. (2015). Disruption of SF3B1 results in deregulated expression and splicing of key genes and pathways in myelodysplastic syndrome hematopoietic stem and progenitor cells. Leukemia *29*, 1798.

Dombret, H., and Gardin, C. (2016). An update of current treatments for adult acute myeloid leukemia. Blood *127*, 53–61.

Dulaney, J.T., Milunsky, A., Sidbury, J.B., Hobolth, N., and Moser, H.W. (1976). Diagnosis of lipogranulomatosis (Farber disease) by use of cultured fibroblasts. J. Pediatr. *89*, 59–61.

Dworski, S., Berger, A., Furlonger, C., Moreau, J.M., Yoshimitsu, M., Trentadue, J., Au, B.C.Y., Paige, C.J., and Medin, J.A. (2015). Markedly perturbed hematopoiesis in acid ceramidase deficient mice. Haematologica *100*, e162-165.

Ehlert, K., Frosch, M., Fehse, N., Zander, A., Roth, J., and Vormoor, J. (2007). Farber disease: clinical presentation, pathogenesis and a new approach to treatment. Pediatr Rheumatol Online J *5*, 15.

El-Refaei, M., and Qahtani, F.A. (2016). Adult Acute Myeloid Leukemia – A Possible Relation to Disease Invasion and the Impact of Independent Prognostic Markers Associated with Survival Outcome. New Aspects in Molecular and Cellular Mechanisms of Human Carcinogenesis.

Enzyvant (2019). Enzyvant's Investigational Farber Disease Enzyme Replacement Therapy, RVT-801, Receives FDA Fast Track and Rare Pediatric Disease Designations. BioSpace.

Ferlinz, K., Kopal, G., Bernardo, K., Linke, T., Bar, J., Breiden, B., Neumann, U., Lang, F., Schuchman, E.H., and Sandhoff, K. (2001). Human acid ceramidase: processing, glycosylation, and lysosomal targeting. J. Biol. Chem. *276*, 35352–35360.

Flowers, M., Fabriás, G., Delgado, A., Casas, J., Abad, J.L., and Cabot, M.C. (2012). C6-ceramide and targeted inhibition of acid ceramidase induce synergistic decreases in breast cancer cell growth. Breast Cancer Res. Treat. *133*, 447–458.

Gao, Y., and Koide, K. (2013). Chemical perturbation of Mcl-1 pre-mRNA splicing to induce apoptosis in cancer cells. ACS Chem. Biol. *8*, 895–900.

Gebai, A., Gorelik, A., Li, Z., Illes, K., and Nagar, B. (2018). Structural basis for the activation of acid ceramidase. Nat Commun *9*, 1621.

Gilliland, D.G., and Griffin, J.D. (2002). The roles of FLT3 in hematopoiesis and leukemia. Blood *100*, 1532–1542.

Glaser, S.P., Lee, E.F., Trounson, E., Bouillet, P., Wei, A., Fairlie, W.D., Izon, D.J., Zuber, J., Rappaport, A.R., Herold, M.J., et al. (2012). Anti-apoptotic Mcl-1 is essential for the development and sustained growth of acute myeloid leukemia. Genes Dev. *26*, 120–125.

Gores, G.J., and Kaufmann, S.H. (2012). Selectively targeting Mcl-1 for the treatment of acute myelogenous leukemia and solid tumors. Genes Dev. *26*, 305–311.

Gouazé-Andersson, V., Flowers, M., Karimi, R., Fabriàs, G., Delgado, A., Casas, J., and Cabot, M.C. (2011). Inhibition of acid ceramidase by a 2-substituted aminoethanol amide synergistically sensitizes prostate cancer cells to N-(4-hydroxyphenyl) retinam... - PubMed - NCBI. The Prostate *71*, 1064–1073.

Greenblatt, S.M., and Nimer, S.D. (2014). Chromatin modifiers and the promise of epigenetic therapy in acute leukemia. Leukemia *28*, 1396–1406.

Guryanova, O.A., Shank, K., Spitzer, B., Luciani, L., Koche, R.P., Garrett-Bakelman, F.E., Ganzel, C., Durham, B.H., Mohanty, A., Hoermann, G., et al. (2016). DNMT3A R882 mutations promote anthracycline resistance in acute myeloid leukemia through impaired nucleosome remodeling. Nat Med *22*, 1488–1495.

Haimovitz-Friedman, A., Kolesnick, R.N., and Fuks, Z. (1997). Ceramide signaling in apoptosis. Br. Med. Bull. *53*, 539–553.

Hannun, Y.A., and Obeid, L.M. (2018). Sphingolipids and their metabolism in physiology and disease. Nat. Rev. Mol. Cell Biol. *19*, 175–191.

Hata, A.N., Engelman, J.A., and Faber, A.C. (2015). The BCL-2 family: key mediators of the apoptotic response to targeted anti-cancer therapeutics. Cancer Discov *5*, 475–487.

Hatzimichael, E., Georgiou, G., Benetatos, L., and Briasoulis, E. (2013). Gene mutations and molecularly targeted therapies in acute myeloid leukemia. Am J Blood Res *3*, 29–51.

He, X., Dworski, S., Zhu, C., DeAngelis, V., Solyom, A., Medin, J.A., Simonaro, C.M., and Schuchman, E.H. (2017). Enzyme replacement therapy for Farber disease: Proof-of-concept studies in cells and mice. BBA Clinical *7*, 85–96.

Heath, E.M., Chan, S.M., Minden, M.D., Murphy, T., Shlush, L.I., and Schimmer, A.D. (2017). Biological and clinical consequences of NPM1 mutations in AML. Leukemia *31*, 798–807.

Heuser, M., Thol, F., and Ganser, A. (2016). Clonal Hematopoiesis of Indeterminate Potential. Dtsch Arztebl Int *113*, 317–322.

Hong, W.-J., and Medeiros, B.C. (2011). Unfavorable-risk cytogenetics in acute myeloid leukemia. Expert Rev Hematol *4*, 173–184.

Inoue, D., Bradley, R.K., and Abdel-Wahab, O. (2016). Spliceosomal gene mutations in myelodysplasia: molecular links to clonal abnormalities of hematopoiesis. Genes Dev. *30*, 989–1001.

de Jonge, H.J.M., Valk, P.J.M., de Bont, E.S.J.M., Schuringa, J.J., Ossenkoppele, G., Vellenga, E., and Huls, G. (2011). Prognostic impact of white blood cell count in intermediate risk acute myeloid leukemia: relevance of mutated NPM1 and FLT3-ITD. Haematologica *96*, 1310–1317.

Kale, J., Osterlund, E.J., and Andrews, D.W. (2018). BCL-2 family proteins: changing partners in the dance towards death. Cell Death Differ *25*, 65–80.

Kang, Z.-J., Liu, Y.-F., Xu, L.-Z., Long, Z.-J., Huang, D., Yang, Y., Liu, B., Feng, J.-X., Pan, Y.-J., Yan, J.-S., et al. (2016). The Philadelphia chromosome in leukemogenesis. Chin J Cancer *35*.

Kelekar, A., and Thompson, C.B. (1998). Bcl-2-family proteins: the role of the BH3 domain in apoptosis. Trends Cell Biol. *8*, 324–330.

Kester, M., Bassler, J., Fox, T.E., Carter, C.J., Davidson, J.A., and Parette, M.R. (2015). Preclinical development of a C6-ceramide NanoLiposome, a novel sphingolipid therapeutic. Biol. Chem. *396*, 737–747.

Keystone Nano, Inc (2019). Ceramide NanoLiposome in Patients With Advanced Solid Tumors.

Klepin, H.D., and Balducci, L. (2009). Acute Myelogenous Leukemia in Older Adults. The Oncologist *14*, 222–232.

Kottaridis, P.D., Gale, R.E., Frew, M.E., Harrison, G., Langabeer, S.E., Belton, A.A., Walker, H., Wheatley, K., Bowen, D.T., Burnett, A.K., et al. (2001). The presence of a FLT3 internal tandem duplication in patients with acute myeloid leukemia (AML) adds important prognostic information to cytogenetic risk group and response to the first cycle of chemotherapy: analysis of 854 patients from the United Kingdom Medical Research Council AML 10 and 12 trials. Blood *98*, 1752–1759.

Kusenda, J. (1998). Bcl-2 family proteins and leukemia. Minireview. Neoplasma *45*, 117–122.

Lai, M., Realini, N., La Ferla, M., Passalacqua, I., Matteoli, G., Ganesan, A., Pistello, M., Mazzanti, C.M., and Piomelli, D. (2017). Complete Acid Ceramidase ablation prevents cancer-initiating cell formation in melanoma cells. Sci Rep *7*, 7411.

Larrayoz, M., Blakemore, S.J., Dobson, R.C., Blunt, M.D., Rose-Zerilli, M.J.J., Walewska, R., Duncombe, A., Oscier, D., Koide, K., Forconi, F., et al. (2016). The SF3B1 inhibitor spliceostatin A (SSA) elicits apoptosis in chronic lymphocytic leukaemia cells through downregulation of Mcl-1. Leukemia *30*, 351–360.

Leclerc, J., Garandeau, D., Pandiani, C., Gaudel, C., Bille, K., Nottet, N., Garcia, V., Colosetti, P., Pagnotta, S., Bahadoran, P., et al. (2019). Lysosomal acid

ceramidase ASAH1 controls the transition between invasive and proliferative phenotype in melanoma cells. Oncogene *38*.

Lee, S.C.-W., and Abdel-Wahab, O. (2016). Therapeutic targeting of splicing in cancer. Nat. Med. *22*, 976–986.

León, B., Kashyap, M.K., Chan, W.C., Krug, K.A., Castro, J.E., La Clair, J.J., and Burkart, M.D. (2017). A Challenging Pie to Splice: Drugging the Spliceosome. Angewandte Chemie International Edition *56*, 12052–12063.

Leone, G., Voso, M.T., Sica, S., Morosetti, R., and Pagano, L. (2001). Therapy related leukemias: susceptibility, prevention and treatment. Leuk. Lymphoma *41*, 255–276.

Li, F., and Zhang, N. (2015). Ceramide: Therapeutic Potential in Combination Therapy for Cancer Treatment. Curr. Drug Metab. *17*, 37–51.

Li, C.-M., Park, J.-H., Simonaro, C.M., He, X., Gordon, R.E., Friedman, A.-H., Ehleiter, D., Paris, F., Manova, K., Hepbildikler, S., et al. (2002). Insertional mutagenesis of the mouse acid ceramidase gene leads to early embryonic lethality in homozygotes and progressive lipid storage disease in heterozygotes. Genomics *79*, 218–224.

Li, G., Liu, D., Kimchi, E.T., Kaifi, J.T., Qi, X., Manjunath, Y., Liu, X., Deering, T., Avella, D.M., Fox, T., et al. (2018). Nanoliposome C6-Ceramide Increases the Anti-tumor Immune Response and Slows Growth of Liver Tumors in Mice. Gastroenterology *154*, 1024-1036.e9.

Lin, C.-F., Tsai, C.-C., Huang, W.-C., Wang, Y.-C., Tseng, P.-C., Tsai, T.-T., and Chen, C.-L. (2016). Glycogen Synthase Kinase-3β and Caspase-2 Mediate Ceramide- and Etoposide-Induced Apoptosis by Regulating the Lysosomal-Mitochondrial Axis. PLOS ONE *11*, e0145460.

Liu, X., Ryland, L., Yang, J., Liao, A., Aliaga, C., Watts, R., Tan, S.-F., Kaiser, J., Shanmugavelandy, S.S., Rogers, A., et al. (2010). Targeting of survivin by nanoliposomal ceramide induces complete remission in a rat model of NK-LGL leukemia. Blood *116*, 4192–4201.

Lomonosova, E., and Chinnadurai, G. (2008). BH3-only proteins in apoptosis and beyond: an overview. Oncogene *27*, S2-19.

Luedtke, D.A., Niu, X., Pan, Y., Zhao, J., Liu, S., Edwards, H., Chen, K., Lin, H., Taub, J.W., and Ge, Y. (2017). Inhibition of Mcl-1 enhances cell death induced

by the Bcl-2-selective inhibitor ABT-199 in acute myeloid leukemia cells. Signal Transduct Target Ther *2*, 17012.

Makishima, H., Visconte, V., Sakaguchi, H., Jankowska, A.M., Abu Kar, S., Jerez, A., Przychodzen, B., Bupathi, M., Guinta, K., Afable, M.G., et al. (2012). Mutations in the spliceosome machinery, a novel and ubiquitous pathway in leukemogenesis. Blood *119*, 3203–3210.

Mao, C., and Obeid, L.M. (2008). Ceramidases: regulators of cellular responses mediated by ceramide, sphingosine, and sphingosine-1-phosphate. Biochim. Biophys. Acta *1781*, 424–434.

Martelli, M.P., Sportoletti, P., Tiacci, E., Martelli, M.F., and Falini, B. (2013). Mutational landscape of AML with normal cytogenetics: biological and clinical implications. Blood Rev. *27*, 13–22.

Massiello, A., and Chalfant, C.E. (2006). SRp30a (ASF/SF2) regulates the alternative splicing of caspase-9 pre-mRNA and is required for ceramide-responsiveness. J. Lipid Res. *47*, 892–897.

Matera, A.G., and Wang, Z. (2014). A day in the life of the spliceosome. Nat. Rev. Mol. Cell Biol. *15*, 108–121.

McGrath, T., Latoud, C., Arnold, S.T., Safa, A.R., Felsted, R.L., and Center, M.S. (1989). Mechanisms of multidrug resistance in HL60 cells. Analysis of resistance associated membrane proteins and levels of mdr gene expression. Biochem. Pharmacol. *38*, 3611–3619.

Metzeler, K.H., Herold, T., Rothenberg-Thurley, M., Amler, S., Sauerland, M.C., Görlich, D., Schneider, S., Konstandin, N.P., Dufour, A., Bräundl, K., et al. (2016). Spectrum and prognostic relevance of driver gene mutations in acute myeloid leukemia. Blood *128*, 686–698.

Morad, S.A.F., and Cabot, M.C. (2013). Ceramide-orchestrated signalling in cancer cells. Nat. Rev. Cancer *13*, 51–65.

Morad, S.A.F., Levin, J.C., Tan, S.-F., Fox, T.E., Feith, D.J., and Cabot, M.C. (2013). Novel off-target effect of tamoxifen--inhibition of acid ceramidase activity in cancer cells. Biochim. Biophys. Acta *1831*, 1657–1664.

Morad, S.A.F., Tan, S.-F., Feith, D.J., Kester, M., Claxton, D.F., Loughran, T.P., Barth, B.M., Fox, T.E., and Cabot, M.C. (2015). Modification of sphingolipid metabolism by tamoxifen and N-desmethyltamoxifen in acute myelogenous

leukemia – Impact on enzyme activity and response to cytotoxics. Biochim Biophys Acta *1851*, 919–928.

Morciano, G., Giorgi, C., Balestra, D., Marchi, S., Perrone, D., Pinotti, M., and Pinton, P. (2016). Mcl-1 involvement in mitochondrial dynamics is associated with apoptotic cell death. Mol Biol Cell *27*, 20–34.

Mullen, T.D., and Obeid, L.M. (2012). Ceramide and apoptosis: exploring the enigmatic connections between sphingolipid metabolism and programmed cell death. Anticancer Agents Med Chem *12*, 340–363.

Musumarra, G., Barresi, V., Condorelli, D.F., and Scirè, S. (2003). A bioinformatic approach to the identification of candidate genes for the development of new cancer diagnostics. Biol. Chem. *384*, 321–327.

Nguyen, H., Awad, A., Shabani, S., Doan, N., Nguyen, H.S., Awad, A.J., Shabani, S., and Doan, N. (2018). Molecular Targeting of Acid Ceramidase in Glioblastoma: A Review of Its Role, Potential Treatment, and Challenges. Pharmaceutics *10*, 45.

Noone, A., Howlader, N., Krapcho, M., Miller, D., Brest, A., Yu, M., Ruhl, J., Tatalovich, Z., Mariotto, A., Lewis, D., et al. SEER Cancer Statistics Review, 1975-2015.

Norsworthy, K.J., By, K., Subramaniam, S., Zhuang, L., Del Valle, P.L., Przepiorka, D., Shen, Y.-L., Sheth, C.M., Liu, C., Leong, R., et al. (2019). FDA Approval Summary: Glasdegib for Newly Diagnosed Acute Myeloid Leukemia. Clin. Cancer Res.

Okuyama, N., Sperr, W.R., Kadar, K., Bakker, S., Szombath, G., Handa, H., Tamura, H., Kondo, A., Valent, P., Várkonyi, J., et al. (2013). Prognosis of acute myeloid leukemia transformed from myelodysplastic syndromes: a multicenter retrospective study. Leuk. Res. *37*, 862–867.

Ordóñez, Y.F., Abad, J.L., Asseri, M., Casas, J., Garcia, V., Casasampere, M., Schuchman, E.H., Levade, T., Delgado, A., Triola, G., et al. (2019). Activity-based imaging of acid ceramidase. Journal of the American Chemical Society.

Papaemmanuil, E., Gerstung, M., Bullinger, L., Gaidzik, V.I., Paschka, P., Roberts, N.D., Potter, N.E., Heuser, M., Thol, F., Bolli, N., et al. (2016). Genomic Classification and Prognosis in Acute Myeloid Leukemia. N. Engl. J. Med. *374*, 2209–2221.

Pollyea, D.A., Pratz, K.W., Jonas, B.A., Letai, A., Pullarkat, V.A., Wei, A., Konopleva, M.Y., Recher, C., Frankfurt, O., Rizzieri, D., et al. (2018). Venetoclax in Combination with Hypomethylating Agents Induces Rapid, Deep, and Durable Responses in Patients with AML Ineligible for Intensive Therapy. Blood *132*, 285–285.

Powell, J.A., Lewis, A.C., Zhu, W., Toubia, J., Pitman, M.R., Wallington-Beddoe, C.T., Moretti, P.A.B., Iarossi, D., Samaraweera, S.E., Cummings, N., et al. (2017). Targeting sphingosine kinase 1 induces MCL1-dependent cell death in acute myeloid leukemia. Blood *129*, 771–782.

Preudhomme, C., Sagot, C., Boissel, N., Cayuela, J.-M., Tigaud, I., Botton, S. de, Thomas, X., Raffoux, E., Lamandin, C., Castaigne, S., et al. (2002). Favorable prognostic significance of CEBPA mutations in patients with de novo acute myeloid leukemia: a study from the Acute Leukemia French Association (ALFA). Blood *100*, 2717–2723.

Quignon, F., Chen, Z., and de Thé, H. (1997). Retinoic acid and arsenic: towards oncogene-targeted treatments of acute promyelocytic leukaemia. Biochim. Biophys. Acta *1333*, M53-61.

Realini, N., Solorzano, C., Pagliuca, C., Pizzirani, D., Armirotti, A., Luciani, R., Costi, M.P., Bandiera, T., and Piomelli, D. (2013). Discovery of highly potent acid ceramidase inhibitors with in vitro tumor chemosensitizing activity. Sci Rep *3*.

Realini, N., Palese, F., Pizzirani, D., Pontis, S., Basit, A., Bach, A., Ganesan, A., and Piomelli, D. (2016). Acid Ceramidase in Melanoma: EXPRESSION, LOCALIZATION, AND EFFECTS OF PHARMACOLOGICAL INHIBITION. J. Biol. Chem. *291*, 2422–2434.

Roh, J.-L., Park, J.Y., Kim, E.H., and Jang, H.J. (2016). Targeting acid ceramidase sensitises head and neck cancer to cisplatin. Eur. J. Cancer *52*, 163–172.

Ru, Q., Li, W., Xiong, Q., Chen, L., Tian, X., and Li, C.-Y. (2018). Voltage-gated potassium channel blocker 4-aminopyridine induces glioma cell apoptosis by reducing expression of microRNA-10b-5p. Mol Biol Cell *29*, 1125–1136.

Ruvolo, P.P. (2003). Intracellular signal transduction pathways activated by ceramide and its metabolites. Pharmacol. Res. *47*, 383–392.

Ryland, L.K., Fox, T.E., Liu, X., Loughran, T.P., and Kester, M. (2011). Dysregulation of sphingolipid metabolism in cancer. Cancer Biology & Therapy *11*, 138–149.

Ryu, Y., Hall, C.P., Reynolds, C.P., and Kang, M.H. (2014). Caspase-dependent Mcl-1 cleavage and effect of Mcl-1 phosphorylation in ABT-737-induced apoptosis in human acute lymphoblastic leukemia cell lines. Exp. Biol. Med. (Maywood) *239*, 1390–1402.

Sercombe, L., Veerati, T., Moheimani, F., Wu, S.Y., Sood, A.K., and Hua, S. (2015). Advances and Challenges of Liposome Assisted Drug Delivery. Front Pharmacol *6*.

Shtraizent, N., Eliyahu, E., Park, J.-H., He, X., Shalgi, R., and Schuchman, E.H. (2008). Autoproteolytic cleavage and activation of human acid ceramidase. J. Biol. Chem. *283*, 11253–11259.

Souers, A.J., Leverson, J.D., Boghaert, E.R., Ackler, S.L., Catron, N.D., Chen, J., Dayton, B.D., Ding, H., Enschede, S.H., Fairbrother, W.J., et al. (2013). ABT-199, a potent and selective BCL-2 inhibitor, achieves antitumor activity while sparing platelets. Nat. Med. *19*, 202–208.

Stengel, A., Kern, W., Meggendorfer, M., Nadarajah, N., Perglerovà, K., Haferlach, T., and Haferlach, C. (2018). Number of RUNX1 mutations, wild-type allele loss and additional mutations impact on prognosis in adult RUNX1-mutated AML. Leukemia *32*, 295–302.

Stone, R.M., DeAngelo, D.J., Klimek, V., Galinsky, I., Estey, E., Nimer, S.D., Grandin, W., Lebwohl, D., Wang, Y., Cohen, P., et al. (2005). Patients with acute myeloid leukemia and an activating mutation in FLT3 respond to a small-molecule FLT3 tyrosine kinase inhibitor, PKC412. Blood *105*, 54–60.

Sud, M., Fahy, E., Cotter, D., Brown, A., Dennis, E., and Glass, C. (2006). LIPID MAPS Structure Database. Nucleic Acid Research *35*.

Sun, Y., Chen, B.-R., and Deshpande, A. (2018). Epigenetic Regulators in the Development, Maintenance, and Therapeutic Targeting of Acute Myeloid Leukemia. Front. Oncol. *8*.

Takabe, K., and Spiegel, S. (2014). Export of sphingosine-1-phosphate and cancer progression. Journal of Lipid Research *55*, 1839–1846.

Takahashi, S. (2011). Downstream molecular pathways of FLT3 in the pathogenesis of acute myeloid leukemia: biology and therapeutic implications. J Hematol Oncol *4*, 13.

Tan, S.-F., Liu, X., Fox, T.E., Barth, B.M., Sharma, A., Turner, S.D., Awwad, A., Dewey, A., Doi, K., Spitzer, B., et al. (2016). Acid ceramidase is upregulated in AML and represents a novel therapeutic target. Oncotarget *7*, 83208–83222.

Tan, S.F., Pearson, J.M., Feith, D.J., and Loughran, T.P. (2017). The emergence of acid ceramidase as a therapeutic target for acute myeloid leukemia. Expert Opinion on Therapeutic Targets *21*, 583–590.

Tan, S.-F., Dunton, W., Liu, X., Fox, T.E., Morad, S.A.F., Desai, D., Doi, K., Conaway, M.R., Amin, S., Claxton, D.F., et al. (2019). Acid ceramidase promotes drug resistance in acute myeloid leukemia through NF-kB-dependent P-glycoprotein upregulation. J. Lipid Res. *60*, 1078–1086.

Teh, T.-C., Nguyen, N.-Y., Moujalled, D.M., Segal, D., Pomilio, G., Rijal, S., Jabbour, A., Cummins, K., Lackovic, K., Blombery, P., et al. (2018). Enhancing venetoclax activity in acute myeloid leukemia by co-targeting MCL1. Leukemia *32*, 303–312.

Ten Hacken, E., Valentin, R., Regis, F.F.D., Sun, J., Yin, S., Werner, L., Deng, J., Gruber, M., Wong, J., Zheng, M., et al. (2018). Splicing modulation sensitizes chronic lymphocytic leukemia cells to venetoclax by remodeling mitochondrial apoptotic dependencies. JCI Insight *3*.

Tirodkar, T.S., and Voelkel-Johnson, C. (2012). Sphingolipids in apoptosis. Experimental Oncology *34*, 231–242.

Tussié-Luna, M.I., Rozo, L., and Roy, A.L. (2006). Pro-proliferative function of the long isoform of PML-RARalpha involved in acute promyelocytic leukemia. Oncogene *25*, 3375–3386.

Tyner, J.W., Tognon, C.E., Bottomly, D., Wilmot, B., Kurtz, S.E., Savage, S.L., Long, N., Schultz, A.R., Traer, E., Abel, M., et al. (2018). Functional genomic landscape of acute myeloid leukaemia. Nature *562*, 526–531.

Ueda, N. (2015). Ceramide-induced apoptosis in renal tubular cells: a role of mitochondria and sphingosine-1-phoshate. Int J Mol Sci *16*, 5076–5124.

Vemuri, S., and Rhodes, C.T. (1995). Preparation and characterization of liposomes as therapeutic delivery systems: a review. Pharm Acta Helv *70*, 95–111.

Vethakanraj, H.S., Babu, T.A., Sudarsanan, G.B., Duraisamy, P.K., and Ashok Kumar, S. (2015). Targeting ceramide metabolic pathway induces apoptosis in human breast cancer cell lines. Biochem. Biophys. Res. Commun. *464*, 833–839.

Wang, Q., Wan, J., Zhang, W., and Hao, S. (2019). MCL-1 or BCL-xL-dependent resistance to the BCL-2 antagonist (ABT-199) can be overcome by specific inhibitor as single agents and in combination with ABT-199 in acute myeloid leukemia cells. Leuk. Lymphoma 1–11.

Watters, R.J., Fox, T.E., Tan, S.-F., Shanmugavelandy, S., Choby, J.E., Broeg, K., Liao, J., Kester, M., Cabot, M.C., Loughran, T.P., et al. (2013). Targeting Glucosylceramide Synthase Synergizes with C6-Ceramide Nanoliposomes to Induce Apoptosis in NK Leukemia. Leuk Lymphoma *54*, 1288–1296.

Wei, A., Strickland, S.A., Hou, J.-Z., Fiedler, W., Lin, T.L., Walter, R.B., Enjeti, A.K., Hong, W.-J., Chyla, B., Popovic, R., et al. (2018). Venetoclax with Low-Dose Cytarabine Induces Rapid, Deep, and Durable Responses in Previously Untreated Older Adults with AML Ineligible for Intensive Chemotherapy. Blood *132*, 284–284.

Wiese, M., and Daver, N. (2018). Unmet clinical needs and economic burden of disease in the treatment landscape of acute myeloid leukemia. Am J Manag Care *24*, S347–S355.

Wu, L., Mao, C., and Ming, X. (2016). Modulation of Bcl-x Alternative Splicing Induces Apoptosis of Human Hepatic Stellate Cells. Biomed Res Int *2016*, 7478650.

Yingchoncharoen, P., Kalinowski, D.S., and Richardson, D.R. (2016). Lipid-Based Drug Delivery Systems in Cancer Therapy: What Is Available and What Is Yet to Come. Pharmacol. Rev. *68*, 701–787.

Zeidan, Y.H., Jenkins, R.W., Korman, J.B., Liu, X., Obeid, L.M., Norris, J.S., and Hannun, Y.A. (2008). Molecular targeting of acid ceramidase: implications to cancer therapy. Curr Drug Targets *9*, 653–661.

Zhang, T., and Saghatelian, A. (2013). Emerging roles of lipids in BCL-2 family-regulated apoptosis. Biochim. Biophys. Acta *1831*, 1542–1554.

Zhang, T., Barclay, L., Walensky, L.D., and Saghatelian, A. (2015). Regulation of mitochondrial ceramide distribution by members of the BCL-2 family. J. Lipid Res. *56*, 1501–1510.

Zhang, W., Konopleva, M., Shi, Y., McQueen, T., Harris, D., Ling, X., Estrov, Z., Quintás-Cardama, A., Small, D., Cortes, J., et al. (2008). Mutant FLT3: a direct target of sorafenib in acute myelogenous leukemia. J. Natl. Cancer Inst. *100*, 184–198.

Zhu, Q., Wang, Z., Ji, C., Cheng, L., Yang, Y., Ren, J., Jin, Y., Wang, Q., Gu, X., Bi, Z., et al. (2011). C6-ceramide synergistically potentiates the anti-tumor effects of histone deacetylase inhibitors via AKT dephosphorylation and α-tubulin hyperacetylation both in vitro and in vivo. Cell Death Dis *2*, e117.

Žigart, N., and Časar, Z. (2019). A literature review of the patent publications on venetoclax - a selective Bcl-2 inhibitor: discovering the therapeutic potential of a novel chemotherapeutic agent. Expert Opin Ther Pat *29*, 487–496.

7 APPENDICES

SUMMARY OF AC INHIBITORS TESTED

Compound	EC50 Range (MTS*)	Cell Lines
LCL-204	2-7 μM	HL60/VCR, OCI-AML2, THP-1
LCL-521	5-10 μM	THP-1, OCI-AML2, MV4-11
Carmofur	1-15 μM	HL60, HL60/VCR, OCI-AML2, OCI-AML3
Ceranib-1	15-20 μM (48h)	HL60/VCR
Ceranib-2	5 μM (48h)	HL60/VCR
5-FU hexylamine	1-15 μM	HL60, HL60/VCR, OCI-AML2, OCI-AML3, MOLM-14
5-FU octylamine	5-30 μM	HL60, HL60/VCR, OCI-AML2, OCI-AML3, MOLM-14
SACLAC	1-5 μM	HL60/VCR, OCI-AML2, THP-1
SABRAC	1-5 μM	HL60/VCR
SOBRAC	0.5-2 μM	HL60/VCR, OCI-AML2, THP-1
RBM1-12	8 μM	HL60/VCR
ZOBRAC	7 μM	HL60/VCR
SOCLAC	7 μM	HL60/VCR
SAFLOC	20 μM	HL60/VCR
N3-SOBRAC	1-2 μM	HL60/VCR, OCI-AML2, THP-1
A988 (ARN14988)	20 μM (48h)	HL60/VCR, OCI-AML2, THP-1
DV10 (ARN17640_Z_01)	8-15 μM	HL60/VCR, OCI-AML2
DV11 (ARN17641_Z_01)	8-20+ μM	HL60/VCR, OCI-AML2
DV12 (ARN17642_Z_01)	N/A	HL60/VCR, OCI-AML2
DV20 (ARN19724_Z_02)	N/A	HL60/VCR, OCI-AML2
DV21 (ARN19997_Z_01)	N/A	HL60/VCR, OCI-AML2
DV27 (ARN20018_Z_01)	N/A	HL60/VCR, OCI-AML2
DV29 (ARN20020_Z_01)	10-20 μM	HL60/VCR, OCI-AML2
DV30 (ARN20021_Z_01)	12-20+ μM	HL60/VCR, OCI-AML2
DV36 (ARN1335_Z_02)	N/A	HL60/VCR, OCI-AML2
DV55 (ARN19855_Z_01)	20-40 μM	HL60/VCR, OCI-AML2

*MTS assay was done at 24h unless noted otherwise. N/A indicates EC_{50} > 20 μM.

CELL LINE SOURCES

Many cell lines were generously provided for these studies and are attributed to the following: Dr. Jacqueline Cloos and Carolien van Alphen, VU Medical Center Amsterdam (EOL-1, HEL, Kasumi-3, Kasumi-6, ME-1, ML2, MM-6 and NB4); Dr. Mark Levis, Johns Hopkins Medical Institutions (MOLM-13 and MOLM-14); Dr. Douglas Graham, Emory University (NOMO1); Dr. Xiaorong Gu, Cleveland Clinic (OCI-AML2 and OCI-AML3); Dr. Harold L. Atkins, Ottawa Hospital Research Institute (OCI-AML4); Drs. Scott Kaufmann and Mithun Shah, Mayo Clinic (SET2); and Barbara Miller, Penn State Hershey (U937-Luc2-P2A-tdTomato).